University of Alberta

Tissue-specific Expression of *nuo-1* in *C. elegans*

By

Sarah Ndegwa

A thesis submitted to the Faculty of Graduate Studies and Research in partial fulfillment of the requirements for the degree of Master of Science

Department of Biochemistry

Edmonton, Alberta
Spring 2004

Your file Votre référence
ISBN: 0-612-96527-9
Our file Notre référence
ISBN: 0-612-96527-9

ABSTRACT

Complex I deficiency is one of the most commonly diagnosed mitochondrial respiratory chain disorders. An example of complex I dysfunction arises from mutations within the nuclear gene *NDUFV1* that encodes a 51-kDa subunit containing the NADH, the FMN and one iron-sulfur binding site. The *Caenorhabditis elegans* homologue of *NDUFV1* is *nuo-1*. *C. elegans* strains homozygous for a *nuo-1* deletion arrest early in development at the third larval stage. The main objective of this project was to identify the tissues involved in the larval arrest phenotype of the *nuo-1* mutant.

Transgenic worm strains expressing wild-type *nuo-1* in the nervous system proceed with development to the fourth larval stage or early adulthood, exit the dauer pathway, and have enhanced muscular and neurological function, but have an underdeveloped gonad and are infertile. Results observed with ubiquitous expression of *nuo-1* were similar to the transgenic strain with nervous system expression of *nuo-1*. Worms expressing wild-type *nuo-1* in pharyngeal muscle also bypass the third larval stage arrest and progress to fourth larval stage but do not exit the dauer pathway. Neither body-wall muscle nor germ-line expression of *nuo-1* allow for rescue of third larval stage arrest or exit from the dauer pathway. Further work to characterize these transgenic strains in order to gain insight into the connections between energy metabolism, development, and mitochondrial disease is discussed.

Table of Contents

List of Tables

List of Figures

ABBREVIATIONS AND NOMENCLATURE:

ADP	adenosine diphosphate
Amp^R	ampicillin resistant
ATP	adenosine triphosphate
bp	base pairs
cAMP	cyclic adenosine monophosphate
Cm^R	chloramphenicol resistant
dATP	deoxyadenosine triphosphate
dCTP	deoxycytidine triphosphate
dGTP	deoxyguanosine triphosphate
DNA	deoxyribonucleic acid
dNTP	deoxynucleoside triphosphate
Dpy	dumpy
dTTP	deoxythymidine triphosphate
EMS	ethyl methanesulfonate
FAD	flavin adenine dinucleotide
Fe-S	iron sulfur group
FMN	flavin mononucleotide
g	standard acceleration of gravity (9.81 m/s^2)
GFP	green fluorescent protein
Kan^R	kanamycin resistant
kb	kilobase
kDa	kilodaltons
LB	Luria-Bertani broth
MDa	megadaltons
ml	milliliter
mM	millimolar
MRC	mitochondrial respiratory chain
mRNA	messenger ribonucleic acid
mtDNA	mitochondrial DNA

NADH	nicotinamide adenine dinucleotide (reduced form)
NDUFV1	NADH dehydrogenase ubiquinone oxidoreductase flavoprotein 1
nm	nanometer
nM	nanomolar
ng	nanogram
NGM	nematode growth medium
NUO-1	NADH-ubiquinone oxidoreductase 1
PCR	polymerase chain reaction
P_i	inorganic phosphate
p.s.i.	pounds per square inch
Q	ubiquinone
RNA	ribonucleic acid
ROS	reactive oxygen species
rpm	revolutions per minute
SDS	sodium dodecyl sulfate
Unc	uncoordinated
UTR	untranslated region
°C	degree(s) Celsius
µl	microliter
µM	micromolar
µg	microgram

I. Introduction

I-1. Mitochondrial Disease

Mitochondria are essential organelles that generate energy by respiration and oxidative phosphorylation. Substantial progress has been achieved over the last century in understanding the biochemical roles of mitochondria. In addition to being the site of oxidative phosphorylation, mitochondria are also involved in several other important biological processes. These include maintaining intracellular homeostasis of calcium and hydrogen ions, heme, lipid, and amino acid biosynthesis, and intermediary metabolism (Schatz, 1995). While long recognized for their role in metabolism, the importance of mitochondria in organismal development and disease has more recently been appreciated. Although the first mitochondrial disease was described in 1962 (Luft and Landau, 1995), it would take another 26 years for the identification of a mutation in a mitochondrial disease (Holt *et al.*, 1988). Over the last decade, studies involving mitochondrial diseases have increased exponentially and the molecular mechanisms underlying disease pathology have become a hot topic of research. Animal models have provided valuable evidence to help elucidate the molecular mechanisms of mitochondrial pathophysiology and disease in humans.

Mitochondrial dysfunction is associated with the development of myopathies and encephalomyopathies, heart disease, diabetes, and neurodegenerative conditions (Beal, 1995; Luft and Landau, 1995; Wallace, 1992). Mitochondrial dysfunction has also been associated with ageing (Wallace, 1999). Three concepts help explain the role of mitochondria in disease pathology (Wallace, 1992). Firstly, mitochondrially-generated ATP acts as the major source of cellular energy in a variety of metabolically active

tissues including the nervous system, skeletal muscle, endocrine organs, and the heart myocardium (Chinnery and Turnbull, 1997). Clinical manifestations of mitochondrial dysfunction can therefore be tissue-specific due to tissue-specific thresholds for ATP requirements (Mazat *et al.*, 2001). By extension, the cellular origin of mitochondria may play a role in pathogenesis. Protein isoforms of respiratory chain components may be variably expressed in different tissues, thus predisposing certain tissues to disease pathology (Grossman and Shoubridge, 1996; Poyton and McEwan, 1996). Secondly, mitochondria are a major source of reactive oxygen species (ROS), which are associated with the damage of cellular components including lipids, proteins, and DNA and with pathways that provoke apoptosis (Raha and Robinson, 2001). The extent to which ROS are involved in pathogenesis varies in different tissues (Raha and Robinson, 2001). Finally, the requirement for two genomes, mitochondrial and nuclear (Wallace, 1992), in the assembly of respiratory chain components adds an extra level of complexity that potentiates pathologic outcome.

The work in the Lemire laboratory is focused on exploring the relationships between mitochondrial mutations, mitochondrial dysfunction, and disease manifestation using *Caenorhabditis elegans* as a model system. The conservation of mitochondrial function and the many technological and anatomical advantages offered by the nematode have helped to contribute to our understanding of mitochondria in more complex eukaryotic organisms. Previous studies analyzing mutations within nuclear encoded genes have provided molecular clues that contribute to our understanding of how energy metabolism and development in *C. elegans* may relate to human mitochondrial disease. Determining which tissues are most susceptible to mitochondrial dysfunction may help

address issues of phenotypic variability in human mitochondrial diseases. The goal of my thesis work was to analyze the tissue-specific role of a nuclear encoded complex I gene in *C. elegans* larval development and maturation. The aim of this introduction is to present an overview of previous results that link nuclear encoded genes with development, life-span determination, and ageing in *C. elegans* and to serve as a platform for this study.

I-2. The Mitochondrial Respiratory Chain

Mitochondria are subcellular organelles whose primary role is to generate ATP via oxidative phosphorylation, the major source of cellular energy for metabolism in most eukaryotic cells. Mitochondria are defined by two highly specialized membranes. The inner membrane forms convoluted and folded structures known as cristae, which are believed to increase the surface area of the inner membrane. The inner membrane encloses the matrix, is impermeable to ions and most metabolites, and contains numerous transporters that mediate metabolic communication with other cellular compartments. The matrix contains enzymes involved in the Krebs cycle, in fatty acid oxidation, in heme synthesis, and in the urea cycle. The outer membrane is permeable to most small molecules less than 10 kDa. A series of transporters are present for the transport of larger molecules.

Respiration and oxidative phosphorylation are coupled processes that provide the cell with the major source of cellular energy. These processes require a series of inner membrane bound complexes that constitute the mitochondrial respiratory chain (MRC) (Figure I-1). Complex I (NADH-ubiquinone oxidoreductase), complex II (succinate-ubiquinone oxidoreductase), complex III (ubiquinol-cytochrome *c* oxidoreductase) and

complex IV (cytochrome *c* oxidase) are involved in electron transport. Electrons are transferred down the chain to oxygen as the terminal acceptor. The transfer of electrons through the respiratory chain occurs via redox groups such as flavins (FMN, FAD), iron-sulfur clusters (Fe-S), heme, and copper ions (Cu). Ubiquinone (Q) is a mobile lipophilic carrier that shuttles electrons between complex I or II and complex III. Cytochrome *c* (C) is a water-soluble heme-containing protein that mediates electron transfer between complexes complexes III and IV. The oxidation of nicotinamide adenine dinucleotide (NADH) and succinate coupled to the reduction of oxygen generates an electrochemical proton gradient across the inner membrane by pumping protons from the matrix into the intermembrane space. Complex V (ATP synthase) uses this proton gradient to power ATP synthesis. A small decrease in ATP concentration due to an increase in metabolic demand results in a relatively large percentage increase in cellular ADP (whose cellular concentration is approximately 10-fold lower than that of ATP). Thus, the rate of ATP synthesis is tightly regulated by ADP concentration.

Biogenesis of these complexes requires the coordination of two genomes. Mitochondria have their own genome and are capable of synthesizing proteins in the matrix. Mitochondrial DNA (mtDNA) resides in the mitochondrial matrix and is maternally inherited (Jacobs *et al.*, 2000). However, the mitochondrial genome only encodes approximately 0.1% of mitochondrial proteins. All mammalian mtDNAs are circular double-stranded molecules encoding 13 different protein subunits of the MRC, ribosomal RNAs, and transfer RNAs necessary for mitochondrial translation. The approximately 1000 remaining mitochondrial proteins are nuclear-encoded and imported into the organelle from the cytosol.

In view of the key role each complex in the MRC plays in energy metabolism, damage to one or more could lead to an impairment of cellular ATP synthesis. However, *in vitro* studies using specific inhibitors of different complexes indicate that a considerable loss of activity of any individual complex may be required before ATP synthesis is compromised (Heales *et al.*, 2002). Interestingly, the degree of control each complex has over respiration varies. By extension, the degree of control a particular complex exerts over respiration may differ between cell types. For example, mitochondria extracted from rat brain appear to be heterogeneous in the degree of control complex I has over respiration. For complex I of nonsynaptic origin, activity had to be inhibited by over 70% before ATP synthesis was compromised (Davey *et al.*, 1997). However, for synaptic mitochondria, complexes I, III, and IV activities were decreased by approximately 25, 80, and 70%, respectively, before dramatic changes in the rate of oxygen consumption and ATP synthesis were observed (Davey *et al.*, 1998). These results suggest that in mitochondria of synaptic origin, complex I activity has the tightest control over oxidative phosphorylation such that when the threshold level of inhibition of 25% is reached, energy metabolism is impaired and ATP synthesis is reduced (Davey *et al*, 1998). We believed that it would be fascinating to see if the control complex I exerts on energy metabolism and development varies in different tissues in *C. elegans.*

I-3. Complex I: NADH-ubiquinone oxidoreductase

Complex I is the largest and most complicated component of the MRC. The most intricate membrane-bound enzyme known to date, complex I is composed of at least 46 different subunits (Caroll *et al.*, 2002) with a molecular mass of approximately 1 MDa

(Yagi and Matsuno-Yagi, 2003). The subunits are encoded by two distinct genomes. 7 are encoded by mitochondrial DNA (mtDNA) and the remaining 39 are encoded by nuclear DNA. Over a hundred genes are considered to be involved in the biosynthesis of complex I including genes needed for transcription, translation, transport, processing, cofactor insertion, and complex assembly (Yano, 2002).

Complex I contains a noncovalently-bound flavin mononucleotide (FMN) molecule, two ubiquinone binding sites, and at least eight iron-sulfur clusters as prosthetic groups (Ohnishi *et al.*, 1998). Catalyzed by key glycolytic and Krebs cycle enzymes, electrons are transferred to the coenzyme NAD^+ to generate NADH (Voet and Voet, 1995). At complex I, NADH is reoxidized back to NAD^+ by FMN initiating the process of electron transfer through the Fe-S clusters to ubiquinone. The reoxidation of NADH to NAD^+ initiates the sequential redox process of electron transfer through the MRC. Concomitant with the oxidation of NADH, complex I is a proton pump that uses the redox energy to translocate protons across the inner membrane from the mitochondrial matrix to the intermembrane space. The generation of a proton gradient by complex I subsequently results in a significant contribution to ATP production via complex V (Yagi and Matsuno-Yagi, 2003).

Unlike other components of the MRC with published X-ray structures, the only available information on the 3-D structures of complex I is based on electron microscopic analyses. The three-dimensional structures of complex I from *Escherichia coli* (Guénebaut *et al.*, 1998), *Neurospora crassa* (Guénebaut *et al.*, 1997), *Yarrowia lipolytica* (Djafarzadeh *et al.*, 2000), and bovine heart (Grigorieff, 1998) have been determined at low resolution by electron microscopy. All structures indicate that

complex I consists of 2 major segments arranged in a characteristic L-shape (Figure I-2). A peripheral segment protrudes into the mitochondrial matrix while the other segment is embedded in the membrane. The peripheral segment, also known as the catalytic domain, is globular in structure and is composed of 7 (bacteria) to 12 (mitochondria) subunits (Yagi and Matsuno-Yagi, 2003). The membrane segment is connected to the peripheral segment by a narrow stalk and consists mainly of hydrophobic subunits including, in the case of mitochondrial enzyme, all mitochondrial DNA-encoded subunits (Yagi and Matsuno-Yagi, 2003).

Although four decades have passed since the first isolation of complex I from bovine heart mitochondria, information on its structure and enzymatic regulation is still limited. Complex I research has recently taken on greater significance since the finding that many human neurodegenerative diseases including Leigh syndrome and Parkinson's disease involve structural and functional defects of this enzyme complex. It has become increasingly important to understand at the molecular level how impairment of complex I is linked to the onset of disease.

I-4. Complex I and Mitochondrial Disease

Complex I deficiency is one of the most commonly identified respiratory chain phenotypes. Over the past 15 years, the search for mutations underlying complex I disorders has recovered numerous mutations in mtDNA associated with a wide spectrum of clinical phenotypes. However, attention has now been shifted to finding nuclear genes associated with complex I disease. Recently, nuclear-encoded mutations in human MRC subunits have been described in six essential subunits and one accessory subunit (Bénit *et*

al., 2001; Rubio-Gozalbo *et al.*, 2000; Smeitink and Heuvel, 1999). For the purpose of this thesis, I will focus on results associated with the nuclear encoded NADH-dehydrogenase (ubiquinone) oxidoreductase flavoprotein 1 (*NDUFV1*) gene. *NDUFV1* encodes a 51-kDa subunit that contains the NADH and FMN binding sites and one iron-sulfur motif (Shoubridge, 2001)(Figure I-2). Ten different mutations within the *NDUFV1* gene are currently known and have been associated with abnormal neurological conditions including myoclonic epilepsy, hypotonia, ataxia, psychomotor retardation, Leigh syndrome, and leukodystrophy (Bénit *et al.*, 2001; Schuelke *et al.*, 1999; Schuelke *et al.*, 2002). Of the reported mutations, 5 are non-conservative point mutations (Y204C, C206G, A211V, E214K, and T423M)(Bénit *et al.*, 2001; Schuelke *et al.*, 1999; Schuelke *et al.*, 2002). All these mutations lie in highly conserved domains of the protein. The Y204C, C206G, A211V and E214K mutations are located within the FMN binding domain of the protein (Bénit *et al.*, 2001; Schuelke *et al.*, 2002). The T423M mutation resides in a specific motif that is only found in NADH dehydrogenases of the aerobic metabolic pathway and likely constitutes an essential functional domain of the protein (Schuelke *et al.*, 1999).

How complex I dysfunction produces pathophysiological effects is not clear. Several molecular mechanisms have been put forth as to the etiology of complex I disease. Respiratory activity is usually accompanied by compromised ATP synthesis, but the magnitude of the loss does not always correlate with disease severity (DiMauro *et al.*, 1998; Robinson, 1998). An increase in the NADH/NAD^+ ratio has been implicated in acidosis and cancer (Yano, 2002). Complex I deficiency may result in the elevated production of reactive oxygen species and in an upregulation of mitochondrial superoxide

dismutase (Yano, 2002). An increase in the production of free radicals has been associated with DNA mutations, lipid peroxidation, and protein damage (Wallace, 1999; Yano, 2002). Increased levels of ROS may also trigger inappropriate cellular apoptosis and mitosis (Yano, 2002). Mitochondrial dysfunction may also interfere with normal gene expression (Heddi *et al.*, 1999) and can lead to ragged red muscle fibers that signify mitochondrial hyperproliferation (DiMauro *et al.*, 1998). One study reported a 48-bp long 100% antisense sequence identity between the 3′ UTR of the *NDUFV1* mRNA and the 5′ UTR of the mRNA for a γ-interferon inducible protein (IP-30) (Schuelke *et al.*, 1998). This finding suggests that *NDUFV1* mRNA may act as an antisense suppressor for the translation of IP-30, a protein involved in inflammation, in tissues with high-energy requirements (Schuelke *et al.*, 1998). Mutations in *NDUFV1* may lead to significantly higher levels of IP-30, suggesting a molecular explanation for the occurrence of inflammatory myopathy and encephalomyelitis with complex I deficiency (Campos *et al.*, 1995; Zielasek *et al.*, 1995). Genetic analyses developed for the study of mitochondrial disease have been performed on various model systems including mice, *Drosophila melanogaster*, *Saccharomyces cerevisiae*, and *C. elegans* (Liolitsa and Hanna, 2002). In this lab, the *C. elegans* model system is used to study the molecular mechanisms that underlie complex I dysfunction in humans.

I-5. *C. elegans* as a Model System for Human Biology

C. elegans provides a powerful yet simple genetic and developmental model system to study mitochondria. Figure I-3 highlights key anatomical features in the *C. elegans* model system. In the 1960's, Brenner pioneered work with *C. elegans* by using it

as a simple model to study the genetics and development of the nervous system (Brenner, 1974). Today, our knowledge of *C. elegans* is extensive. *C. elegans* shares many of the essential biological characteristics that pose fundamental questions in human biology. Studies on nematode embryogenesis, morphogenesis, development, nerve function, behavior and ageing, and how they are dictated by genes, provide us with a simple yet effective model for most of the fundamental mysteries of human pathology. The growth and development of *C. elegans* are energy dependent processes that rely on the MRC as a major source for ATP. Various features including the structure, metabolism and bioenergetics of the nematode MRC are very similar to the mammalian counterpart (Murfitt *et al.*, 1976). Several pathways of intermediary metabolism, including the Krebs cycle, are known to be conserved in *C. elegans* (Wadsworth and Riddle, 1989).

The complete *C. elegans* life cycle takes about 3 days at 25 °C (Figure I-4) (Lewis and Fleming, 1995). A single wild-type adult hermaphrodite is capable of producing approximately 300 eggs (Hodgkin, 1999). Following fertilization, the embryo undergoes cell proliferation, organogenesis, and morphogenesis, and hatches as a L1 larva after about 14 h (Sulston, 1988). Over the next 2 days, development proceeds through three additional larval stages, L2, L3, and L4 until an adult emerges from the final molt. The average life-span for normal populations is 2 to 3 weeks (Wood, 1988). Under environmental stress, including low food supply, temperature extremes, and overcrowded conditions, wild type worms can enter the dauer state, a developmentally arrested and morphologically distinct alternative third larval stage (Cassada and Russell, 1975). Response to these environmental stress conditions is mediated by several amphid sensory neurons (Thomas and Lockery, 1999). Being resistant to dessication and having

very low metabolic activity (Wadsworth and Riddle, 1989), dauer larvae can survive for several months. When returned to more favorable growth conditions, dauer larvae resume normal development to adulthood (Riddle and Albert, 1997).

The progression of development through the larval stages toward adulthood is controlled by heterochronic genes that regulate the timing of cell fate determination (Ambros, 1997). Mutations in these heterochronic genes such as *lin-4*, *lin-14*, *lin-28*, and *lin-29* lead to abnormal developmental patterns such that larvae will exhibit tissues at the adult stage, or conversely tissues in adult worms will arrest at the larval stage. The developmentally arrested phenotype of dauer larvae is also regulated by heterochronic genes (Ambros, 1997). Mutations in *lin-4* or *lin-14* alter the stage that worms enter the dauer pathway (Ambros, 1997). Although the actions of these genes are pleiotropic, the heterochronic genes that have so far been identified do not have major effects on gonadal development, suggesting independent regulation of developmental timing in the gonad (Ambros, 1997).

Anatomically, *C. elegans* provides an elegant model to study tissue specificity. Multiple highly-differentiated tissue types such as neurons, muscles, intestine, and hypodermis are contained in the 959 somatic cells of the hermaphrodite (Wood, 1988). Cell lineage is invariant (Sulston and Horvitz, 1977). All 959 somatic cell nuclei are visible with a light microscope facilitating morphological analysis. Of the 959 somatic cells, 302 are neurons. In *C. elegans*, the nervous system functions in movement, providing sensory cues including those of the dauer pathway, egg laying, and feeding (Wood, 1988). The majority of the neurons are situated in the tail, surrounding the pharynx, and along the ventral midline (Figure I-5) (Wood, 1988). Processes from these

neurons either form bundles along the length of the worm as the dorsal and ventral nerve cords or form the circumpharyngeal nerve ring that has often been referred to as the central processing unit or 'brain' of the worm (Wood, 1988). The nerve ring receives input from sensory organs (sensilla) in the head and sends out this sensory information via motor neuron axons to body-wall muscles (Wood, 1988). Sensory information also gets transmitted to body-wall muscle via the dorsal and ventral nerve cords (Wood, 1988).

Muscle cells in the nematode send processes to motor neurons in the dorsal and ventral nerve cords, which is interestingly the reverse of what happens in other organisms (Wood, 1988). Muscle plays a role in movement, egg laying, feeding, and defecation in *C. elegans* (Wood, 1988). The body-wall and pharyngeal muscle cells exhibit organized sarcomeres (Ardizzi and Epstein, 1987). Several additional groups of muscle cells include the vulval muscles of hermaphrodites, the male sex muscles, the anal-intestinal muscles, and the gonadal sheath of the hermaphrodite do not exhibit sarcomeres and therefore may be characterized as smooth muscle (Ardizzi and Epstein, 1987). Locomotion in *C. elegans* is achieved by movement of the body in sinusoidal waves (Thomas and Lockery, 1999). Movement is produced by 95 body-wall muscle cells under the control of motor neurons, interneurons, and sensory neurons (Thomas and Lockery, 1999). Normal feeding occurs by pharyngeal pumping, a process of contraction and relaxation of the muscles of the corpus and terminal bulb (Thomas and Lockery, 1999). Contraction of the terminal bulb muscles breaks up ingested bacteria by the movement of a specialized grinder structure and passes it to the intestine (Thomas and Lockery, 1999). Pharyngeal pumping is regulated by a distinct part of the nervous-

system that consists of 14 classes of neurons that are directly interconnected with the rest of the nervous system by a single neuron class (Thomas and Lockery, 1999).

The *C. elegans* reproductive system consists of the somatic gonad and the germ-line (Jin, 1999). At hatching, a mere four cells make up the gonad (Schedl, 1997). In the late L2 stage, the somatic gonad primordium is formed to enclose the proliferating germ cells into anterior and posterior arms centered around the future vulva (Jin, 1999). As the hermaphrodite gonad develops, it extends anteriorly and posteriorly. This morphogenesis is led by two somatic cells located at the distal ends of each gonad arm called the distal tip cells (Jin, 1999). The two arms eventually turn and migrate toward the centre forming a U-shaped gonad with a central opening that will eventually connect to the vulva (Jin, 1999). During the L4 stage, the vulval cells form a triangular shaped invagination (Greenwald, 1997). At the L4 to adult transition, the vulval invagination pushes outward to form the mature protruding vulva (Greenwald, 1997). Spermatogenesis, beginning early at the L4 stage, occurs in the spermathecae connected to the uterus (Wood, 1988). At the L4 molt, sperm production ceases (Wood, 1988). As the worm reaches adulthood, the hermaphrodite produces oocytes, which pass through the spermathecae, become fertilized, and progress through the early stages of embryogenesis (Wood, 1988).

In 2002, the *C. elegans* genome sequence was completed by the Sanger Institute in Cambridge, UK and by the Washington University School of Medicine in St. Louis, USA. The *C. elegans* genome size is approximately 100 Mb, which is about one-thirtieth the size of its human counterpart, and has over 19,000 distinct protein coding genes. The mitochondrial genome is 13,794 bp. As a diploid organism, *C. elegans* has five pairs of autosomal chromosomes and a pair of sex (X) chromosomes (Wood, 1988).

Hermaphrodites are diploid for all six chromosomes (XX), while males arise at an approximately 0.05% frequency and have only one X chromosome (X0) (Wood, 1988). As a self-fertilizing hermaphrodite, homozygous mutant animals can be easily isolated from a heterozygous parent carrying mutant alleles. Outcrossing of hermaphrodites with males allows for genetic analysis and strain construction (Wood, 1988). Over 95% of the genome is currently available in *E. coli* cosmid and yeast artificial chromosome (YAC) clone libraries, facilitating the process of cloning by complementation of recessive mutant phenotypes (Coulson *et al.*, 1995). Comparing human and *C. elegans* protein sequences reveals that the majority of mammalian MRC polypeptides have highly conserved homologs in the worm (Tsang and Lemire, 2003b).

I-6. Nuclear Mutations in *C. elegans* and Mitochondrial Disease

Currently, approximately 42% of genes known to be associated with human diseases have an orthologue in *C. elegans* (Culetto and Sattelle, 2000). The nematode model has already yielded important insights into the pathophysiology of some of these diseases (Aboobaker and Blaxter, 2000; Culetto and Sattelle, 2000). Since the completion of the genome sequencing project, the availability of the complete mtDNA and nuclear DNA sequences has facilitated the rapid investigation of gene function using either forward or reverse genetic approaches (Okimoto *et al.*, 1992; *C. elegans* Sequencing Consortium, 1998). Surprisingly, while over 300 mutations have been identified in the human mitochondrial genome (MITOMAP: A Human Mitochondrial Genome Database. http://www.mitomap.org, 2002), genetic screens for mutations that affect motility, reproduction, or development in *C. elegans* have yet to recover any

mtDNA mutations (Jorgensen and Mango, 2002). In the following paragraphs, a mutation is considered "lethal" if it blocks survival or reproduction (Edgley *et al.*, 1995).

I-6. a) Mutations Affecting Life-Span

Several genetic studies have linked MRC function with life-span and ageing in *C. elegans*. The "free radical theory of ageing" proposed by Harman (1956) states that increased respiration will lead to the increased production of reactive oxygen species (ROS) such as superoxide anions, hydrogen peroxide, and hydroxyl radicals. For example, superoxide anions are produced during the reduction and subsequent oxidation of ubiquinone during the transport of electrons from complexes I and II to complex III. Increased ROS production leads to the damage of cellular components and is believed to be a major contributor to the premature ageing process that leads to a shorter life-span. The *mev-1(kn1)* mutation in *C. elegans* is a missense allele in the *cyt-1* gene of the cytochrome *b* subunit in complex II (Ishii *et al.*, 1990). Isolated by screening for hypersensitivity to methyl viologen (paraquat), a compound that drastically increases ROS generation, the life-span of *mev-1(kn1)* mutants decreases significantly with rising oxygen concentration (Ishii *et al.*, 1998). Interestingly, *mev-1(kn1)* mutants show increased levels of protein carbonyl derivatives, markers associated with an accelerated rate of ageing (Ishii *et al.*, 2002; Hosokawa *et al.*, 1994) and are hypermutable, especially with high oxygen concentration (Hartman *et al.*, 2001). Therefore, the *mev-1* phenotype has been correlated with an increased production of ROS at the level of complex II, either through the release of electrons directly to oxygen or through the premature release of ubisemiquinone radicals (Senoo-Matsuda *et al.*, 2001). This notion is supported by the

fact that ROS scavengers such as EUK-8 and EUK-134, can restore normal life-span to *mev-1(kn1)* mutants, indicating that endogenous ROS production is a significant cause of accelerated ageing in this strain (Melov *et al.*, 2000). In addition to ROS production, a recent study has reported that abnormal levels of *ced-3*- and *ced-4*-dependent apoptosis is likely to contribute to the short life-span phenotype of *mev-1* mutants (Senoo-Matsuda *et al.*, 2003).

The *gas-1(fc21)* (general anesthetic sensitive) mutation, affects the 49-kDa subunit of complex I and impairs complex I activity (Kayser *et al.*, 1999). Similar to *mev-1(kn1)* mutants, *gas-1(fc21)* mutants are hypersensitive to free radical damage and hyperoxia and have a shorter life span (Hartman *et al.*, 2001; Kayser *et al.*, 1999). However, the molecular basis of the effect on life span is not well understood. Unlike *mev-1* mutants, *gas-1* mutants are not hypermutable and do not generate an excess of superoxide anions (Hartman *et al.*, 2001). It is postulated that the *gas-1* mutation impairs the proper assembly of complex I but the mechanism of its influence on life span remains to be elucidated.

MRC mutations can also prolong life span via decreased ROS production, caloric restriction, and increased stress resistance. Worms carrying the *isp-1(qm150)* missense mutation in the iron-sulfur protein of complex III display slower embryonic development and twice the maximum life span (Feng *et al.*, 2001). *isp-1(qm150)* mutants exhibit a large decrease in oxygen consumption, indicating that electron transport along the MRC is compromised (Feng *et al.*, 2001). Because electron transport is slowed down, the *isp-1* mutation should increase superoxide formation by increasing the half-life of the semiquinone intermediate (Raha and Robinson, 2000). However, in contrast to what

might be expected, the *isp-1* mutation reduces ROS production through a mechanism that is not yet understood (Hekimi and Guarente, 2003).

Mutations in the *daf-2* (abnormal dauer formation) gene, which encodes an insulin receptor-like transmembrane tyrosine kinase (Kimura *et al.*, 1997) involved in the dauer pathway, also result in an increased life span (Kenyon, *et al.*, 1993). This result is explained by an elevated expression of superoxide dismutase, an enzyme that decreases levels of superoxide anions. Interestingly, *daf-2 isp-1* double mutant worms do not live longer than either single mutant, indicating a common mechanism for life-span extension that likely operates through lower levels of ROS by either preventing their formation in *isp-1* mutants or by increasing their detoxification in *daf-2* mutants (Hekimi and Guarente, 2003). This result also indicates that the maximum life-span extension attributed to low levels of ROS is reached in both *isp-1* and *daf-2* mutants (Hekimi and Guarente, 2003).

RNAi-mediated inactivation of the *nuo-2* (NADH-ubiquinone oxidoreductase), *cyc-1* (cytochrome c reductase), *cco-1* (cytochrome c oxidase), and *atp-3* (ATP synthase) genes encoding subunits of complexes I, III, IV, and V, respectively extended life span, reduced the size of the adult without affecting cell number, and reduced ATP levels (Dillin *et al.*, 2002). Interestingly, when *cco-1* RNAi treatment imposed throughout development is removed during adulthood, *cco-1* mRNA levels increased to almost normal levels, but did not restore ATP levels (Dillin *et al.*, 2002). These results suggest that the low level of ATP experienced during development results in a morphological and physiological state that leads to increased life-span. It is possible that the irreversible developmental alterations are a result of ROS acting as intracellular second messengers

(Kamata and Hirata, 1999). Therefore, energy metabolism in *C. elegans* may be monitored early in life and in response, a fixed rate of respiration is established throughout development to influence growth rate, body size, life-span, and ageing during adulthood (Dillin *et al.*, 2002).

Mutations in the *clk-1* (biological clock abnormal) gene, which encodes a mitochondrial protein necessary for ubiquinone biosynthesis, results in significant life span extension (Wong *et al.*, 1995). Deregulation of larval stage development also occurs, as *clk-1* mutants display a lengthening of embryonic and post-embryonic development, an extended cell cycle period, a longer defecation cycle, in conjunction with reduced mobility, pharyngeal pumping rates, and brood sizes (Wong *et al.*, 1995). *clk-1* mutants maintain normal rates of respiration by relying on bacterial Q_8 and perhaps demethoxyubiquinone-9 (DMQ_9) (Jonassen *et al.*, 2002). However, since the main form of ubiquinone, Q_9, is required for normal mitochondrial function, development and physiological function, the precise role of DMQ_9 is unclear. Accelerated ageing occurs with an overexpression of CLK-1 in a wild-type background, indicating that in addition to quinone synthesis, the mitochondrial protein may regulate developmental and behavioral processes (Felkai *et al.*, 1999). Biochemical analysis of *clk-1* mutants reveals that decreased energy production may not be completely responsible for increased life span since *clk-1* animals have ATP levels that resemble wild-type (Felkai *et al.*, 1999; Braeckman *et al.*, 2002). In addition to its role as a redox cofactor, ubiquinone acts as an antioxidant in all cellular membranes (Dallner and Sindelar, 2000). However, recent evidence suggests that DMQ_9 may be a better antioxidant than ubiquinone and its redox cycle less prone to the production of ROS (Miyadera *et al.*, 2002). *clk-1* mutants have

low levels of detoxifying enzymes and accumulate by-products of oxidative damage, such as lipofuscin at slower rates than wild-type worms (Braeckman *et al.*, 2002). Therefore, these results suggest that longevity in *clk-1* mutants may result from a decrease in ROS attributed to the presence of DMQ. Interestingly, the longevity of *clk-1* mutants is dependent on the presence of a reproductive system (Dillin *et al.*, 2002). The life-span extending properties of the *clk-1* mutation are inhibited with the ablation of somatic gonad precursor cells (Dillin *et al.*, 2002). Curiously, laser ablation of the germ-line in *daf-2* mutants further extends life span (Hsin and Kenyon, 1999). This finding suggests that in addition to energy status, signals arising from somatic and germ-line cells act reciprocally to regulate life-span.

An *eat-2* (eating abnormal) mutation, which disrupts normal pharyngeal pumping and results in a low caloric intake, also increases life-span (Lakowski and Hekimi, 1998). A *clk-1, eat-2* double mutant does not result in a further extension in life span suggesting that both mutations may utilize the same pathway(s) (Lakowski and Hekimi, 1998). It is likely that *clk-1* mutations may promote longevity by lowering metabolic rates and concomitantly ROS production in mitochondria (Hekimi and Guarente, 2003). *clk-1* and *daf-2* mutations are additive as *daf-2 clk-1* double mutants can live up to five times longer than wild-type animals (Lakowski and Hekimi, 1996). Although the major source of ROS is mitochondria, ROS are also produced in the cytoplasm and by redox reactions in other membrane-bound organelles, including peroxisomes and the endoplasmic reticulum, and at the plasma membrane (Borges *et al.*, 2002). It has been suggested that *daf-2* protects cells from mitochondrially produced ROS while *clk-1* reduces extramitochondrially produced ROS (Hekimi and Guarente, 2003). This hypothesis is

consistent with the observation that *clk-1* mutations increase life-span only moderately in seclusion, but the increase becomes much more significant in combination with a *daf-2* background (Hekimi and Guarente, 2003).

I-6. b) Mutations Resulting in Developmental Arrest

In addition to mutations that affect life-span, mutations that cause more severe losses of mitochondrial function and result in lethality (L2, L3, or L4 arrest) have been observed in *C. elegans*. The *C. elegans nuo-1* gene encodes a 51-kDa active site subunit of NADH-ubiquinone oxidoreductase (complex I) (Tsang *et al.*, 2001). The NADH and FMN binding sites, as well as one iron-sulfur cluster motif are encoded by six exons (Figure I-7). The first MRC gene to be studied using target-selected mutagenesis, the recovered *nuo-1(ua1)* mutation is a 1.2-kb deletion of the first three of the six exons including the mitochondrial localization sequence, the NADH, and the FMN binding sites (Tsang *et al.*, 2001). The *nuo-1(ua1)* allele is likely a null mutation and is homozygous lethal. Heterozygous hermaphrodites (*nuo-1(ua1)*/+) produce 1/4 homozygous *nuo-1(ua1)* progeny that progress past the first two larval stages but never reach sexual maturity and arrest at the L3-larval stage (Tsang *et al.*, 2001). More severely affected is gonadogenesis, which is arrested earlier at the L2 stage (Tsang *et al.*, 2001). Impaired feeding and mobility and a slower defecation cycle in mutant animals are suggestive of neurological and/or muscular defects (Tsang *et al.*, 2001). *nuo-1* is the *C. elegans* homologue for the human *NDUFV1* gene. Figure I-8 illustrates that the two proteins are highly conserved. Currently, mutations within the *NDUFV1* gene affect amino acids conserved within the worm NUO-1.

The *atp-2* gene encodes the β-subunit of the peripheral catalytic domain of ATP synthase (complex V) (Tsang *et al.*, 2001). Also targeted by reverse genetics, the *atp-2(ua2)* mutation deletes the first exon and partially the second resulting in the removal of the mitochondrial targeting sequence. Similar to the *nuo-1(ua1)* mutation, the *atp-2(ua2)* mutation is homozygous lethal with homozygous mutant progeny arresting at the L3 larval stage with L2-sized gonads (Tsang *et al.*, 2001). Interestingly, the *nuo-1* and *atp-2* mutants also live significantly longer and have reduced mobilities, reduced pharyngeal pumping rates, and longer defecation cycles (Tsang *et al.*, 2001).

The *coq-3(qm188)* mutation is a deletion in a methyltransferase-encoding gene of coenzyme Q biosynthesis that results in homozygous mutant animals that reach adulthood but with a large proportion that are sterile (Hihi *et al.*, 2002). The few worms that are viable have significantly lower brood sizes and most of the progeny die at the L1 stage. Surprisingly, homozygous *coq-3* mutants complemented with a *coq-3(+)* extrachromosomal transgenic array follow a normal pattern of development, but worms that lose the array arrest as L2 larvae (Hihi *et al.*, 2002). Recent RNA interference studies using *nuo-1* dsRNA or *atp-2* dsRNA revealed that 10% and 65% respectively of progeny arrest as embryos before tissue differentiation takes place (Tsang *et al.*, 2001). Embryonic lethality in the *nuo-1*(RNAi) or *atp-2*(RNAi) phenotypes is more severe than the corresponding *nuo-1(ua1)* or *atp-2(ua2)* null alleles. This finding suggests that the *nuo-1(+)* or *atp-2(+)* genes in the heterozygous hermaphrodite contribute to the survival of homozygous mutant progeny to the L3 stage due to maternal rescue of the embryonic arrest phenotype.

For the *nuo-1(ua1)*, *atp-2(ua2)*, and *coq-3(qm188)* mutations, development is normal in the early stages of development. This is due to a maternal effect that provides wild-type gene product, potentially mRNA, to the oocyte and supports development until zygotic expression can no longer supply the higher energy demands of later larval stages. All three mutations suggest that a functional MRC is essential for development past the L3 stage and for viability. This hypothesis is further supported by the fact that *clk-1* mutants also have a conditional lethal phenotype (Jonassen *et al.*, 2001). When cultured on a ubiquinone-deficient strain of *E. coli*, *clk-1* mutants do not proceed past the L2 larval stage (Jonassen *et al.*, 2001). By extension, the *clk-1* mutation also indicates a maternal effect in that the slow development and long-life phenotypes are only seen in second generation progeny and beyond (Ewbank *et al.*, 1997).

The reasons that worms with impaired mitochondrial function arrest at the L2 or L3 stage are currently under investigation. We propose that development to the L4-larval stage, which involves a large increase in body size and the process of reproductive maturation, are associated with substantially higher energy demands than earlier stages of development. Three observations support this concept. Firstly, aerobic respiration measured by oxygen consumption peaks at the L3 or L4 stage (Vanfleteren and De Vreese, 1996). This finding is consistent with a shift from the glyoxylate cycle in L1 larvae toward respiration via the Krebs cycle to support further development in the L2 to L4 stages (Wadsworth and Riddle, 1989). Second, there is a 5-fold increase in mtDNA copy number in the L3 to L4 transition (Tsang and Lemire, 2002). Finally, ATP-2 protein levels also significantly increase as worms progress to the L4-larval stage (Tsang and Lemire, 2003b). In summary, all these changes reflect an upregulation of MRC

components and increased energy requirement to sustain further development. Therefore, a dysfunctional MRC culminates in developmental arrest.

I-7. Thesis Objective

The work in the Lemire laboratory is focused on exploring the molecular mechanisms by which MRC mutations are pathogenic as a potential avenue for developing more effective therapies. Figure I-9 summarizes what has been proposed for the connection between energy metabolism, development, and life-span in *C. elegans* and how mitochondrial dysfunction may lead to disease. Our studies may identify new molecular mechanisms relating energy metabolism and development by which to better understand mitochondrial diseases.

The aim of my research was to investigate the tissue-specific role of *nuo-1* in development using a series of transgenic worm strains. The design and rationale of my experiments were based on the observation that mutations in various MRC nuclear encoded genes, and specifically the *nuo-1(ua1)* allele, result in developmental arrest at the L3-larval stage. Because mitochondrial diseases in humans are characterized by a plethora of organ specific phenotypes, it seemed important to ask whether L3-arrest in worm MRC mutants is due to a tissue-specific energy deficit. This raises the questions of what roles different tissues could have in energy metabolism and of how mitochondrial dysfunction in these tissues could lead to disease. We wished to see whether the L3-arrest phenotype of *nuo-1* mutants could be complemented by expressing a *nuo-1(+)* transgene in a subset of tissues. Identifying which tissues have the lowest threshold for MRC

dysfunction could help compartmentalize the global L3-arrest phenotype into tissue-specific components.

We hypothesized that the L3-arrest phenotype is due to the failure of a common energy-requiring checkpoint in development. We propose an energy-requiring checkpoint rather than an energy deficit to explain the L3-arrest phenotype that occurs almost invariably when worms are homozygous for the *nuo-1(ua1)* allele. An energy deficit would typically result in larval arrest at various stages as energy became limiting, which is not what is observed. Several possible explanations as to how this checkpoint functions should be considered. Firstly, all tissues may be involved equally in the developmental decision to proceed to L4. Secondly, tissues may make differential contributions to the developmental decision. Tissue hierarchy may exist where some tissues are more important than others, perhaps because they have lower thresholds for MRC dysfunction. Thirdly, one tissue may act as a " master tissue" acting exclusively in checkpoint regulation. Finally, some tissues may be capable of developing past the L3 stage when an MRC dysfunction is present, but MRC dysfunction in neighboring tissues prevents further development. Previous evidence indicates that this latter case is the least likely in *C. elegans* because an all-or-none developmental response is usually observed in complementation studies (Tsang and Lemire, 2003a).

We analyzed whether *nuo-1* functions in a cell non-autonomous manner such that a signal arising from a specific tissue allows a genotypically mutant cell in other tissue to develop as a wild-type cell would. Essentially, a one-to-one correspondence between a cell's genotype and phenotype is absent. We placed the *nuo-1(+)* gene under the control of a variety of tissue-specific promoters for muscle, nervous system, germ-line, and

general expression. Several expression plasmids were created and transformed into *nuo-1(ua1)*/+ heterozygotes. Introducing DNA by ballistic transformation, we created a series of transgenic worm strains that should only have wild-type MRC function in tissues in which the specific promoter is active. Our results revealed that *nuo-1* expression controls development in a cell non-autonomous manner. This suggests that development beyond the L3 stage is regulated by a global mechanism that allows all cells to reach a consensus decision based on energy status on whether or not to continue with development. My results indicate that transgenic strains containing nervous system and pharyngeal specific expression of *nuo-1* are partially complemented and able to develop beyond the L3 stage. Several approaches to further characterize these strains are outlined in the future studies section in the discussion chapter.

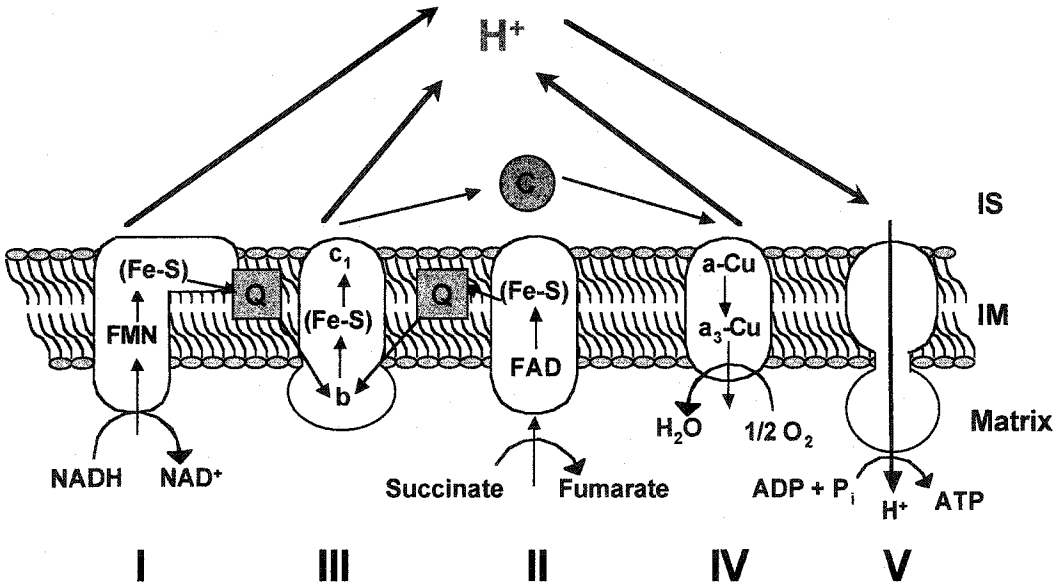

Figure I-1. Schematic Representation of the Mitochondrial Respiratory Chain

The mitochondrial respiratory chain consists of a series of inner membrane bound complexes. Complex I (NADH-ubiquinone oxidoreductase), complex II (succinate-ubiquinone oxidoreductase), complex III (ubiquinol-cytochrome *c* oxidoreductase) and complex IV (cytochrome *c* oxidase) are involved in electron transport. Electrons are transferred down the chain to oxygen as the terminal acceptor. The transfer of electrons through the respiratory chain occurs via redox groups such as flavins (FMN, FAD), iron-sulfur clusters (Fe-S), heme, and copper ions (Cu). Ubiquinone (Q) shuttles electrons between complex I or II and complex III. Cytochrome *c* (C) mediates electron transfer between complexes complexes III and IV. The oxidation of nicotinamide adenine dinucleotide (NADH) and succinate coupled to the reduction of oxygen generates an electrochemical proton gradient across the inner membrane (IM) by pumping protons (H^+) from the matrix into the intermembrane space (IS). Complex V (ATP synthase) uses this proton gradient to power ATP synthesis.

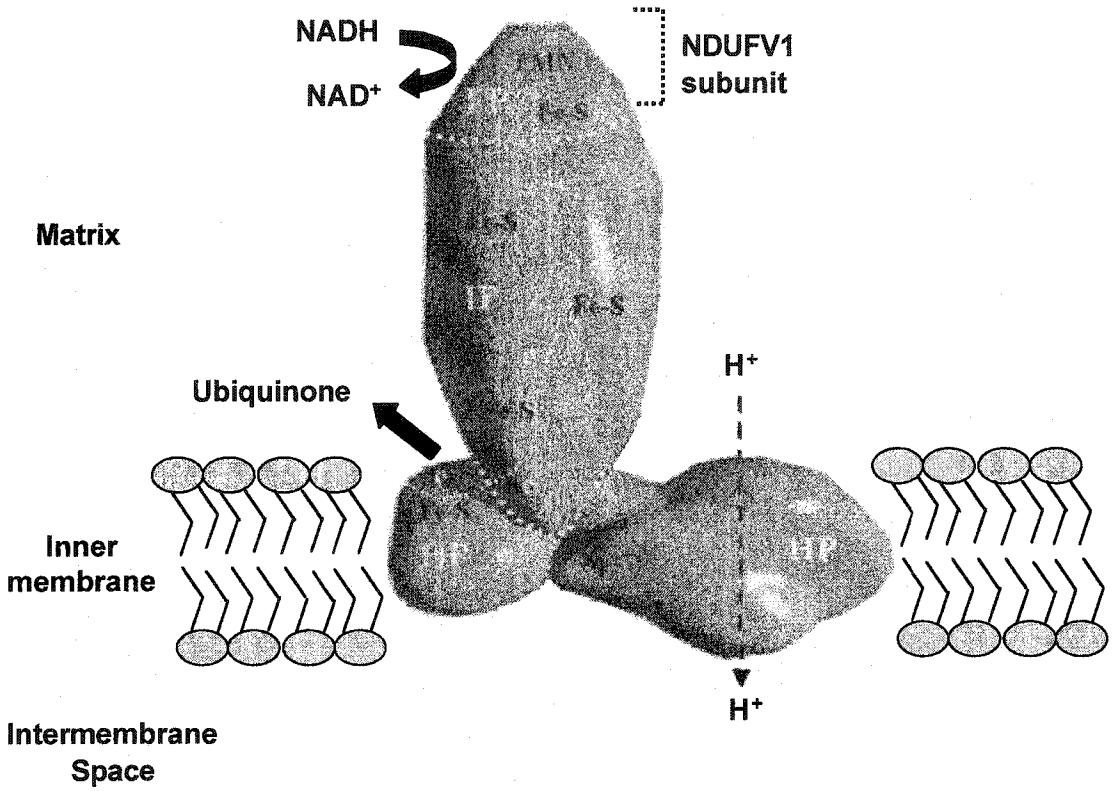

Figure I-2. Two-dimensional drawing of Complex I

Complex I consists of two major segments arranged in a L-shape. Complex I can be fragmented into a hydrophobic membrane fraction (HP) that attaches the complex to the inner membrane, the flavoprotein (FP), and the iron-sulfur protein (IP) fractions. The proposed location of the NDUFV1 subunit, the FMN binding site, the transport of electrons (e^-) from NADH to ubiquinone via the iron-sulfur (Fe-S) clusters, and the generation of a proton gradient across the inner membrane are shown (adapted from Triepels *et al.*, 2001).

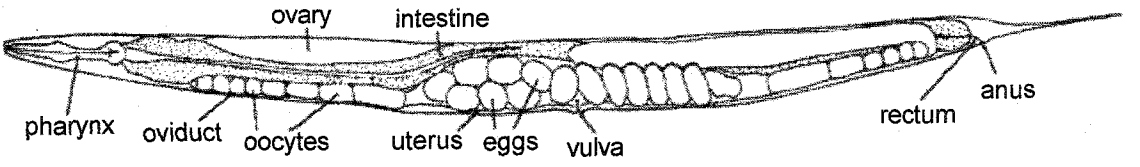

Figure I-3. The *C. elegans* Model System

The major anatomical features of the *C. elegans* adult hermaphrodite. Anterior left, posterior right (adapted from Riddle *et al.*, 1997).

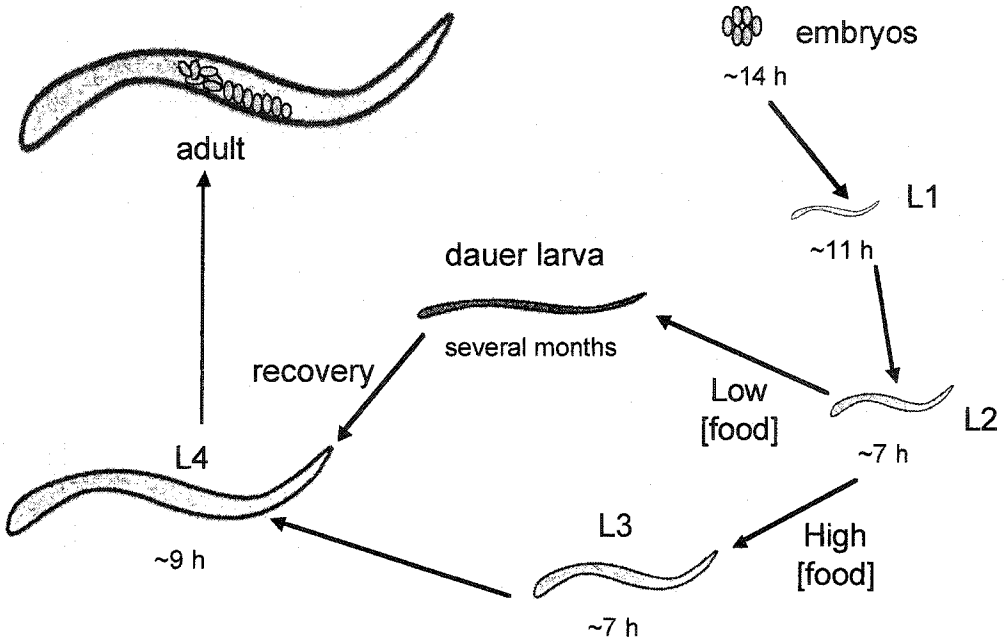

Figure I-4. The *C. elegans* Life-Cycle

The duration of each developmental stage is shown for growth on plates at 25 °C. Under favorable conditions and a high food supply, development proceeds through four larval stages to adulthood. The entire life-cycle is completed in 3 days. In adverse conditions and a low food supply L2 larvae moult to produce dauer larvae, and survive for several months. Upon improvement of environmental conditions, dauers moult to the L4 larvae stage and proceed with normal development to adulthood (adapted from Wood, 1988).

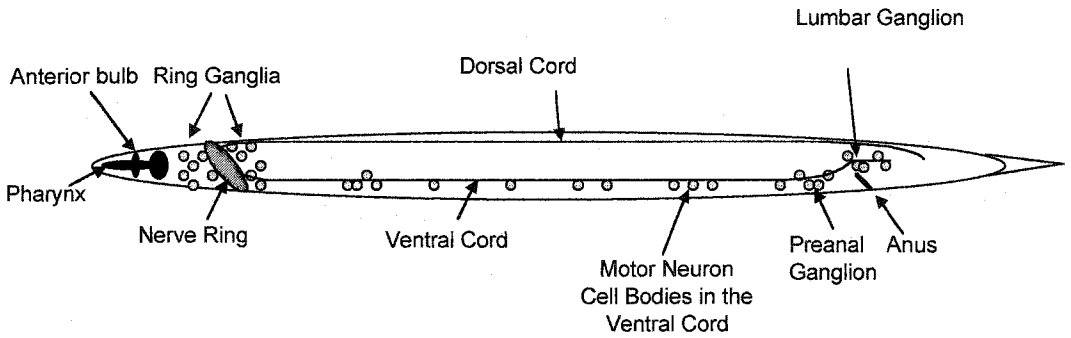

Figure I-5. The *C. elegans* Nervous system

The major cell body ganglia, nerve ring, and nerve cords that run the length of the body forming sensory tracts are shown. Anterior left, posterior right (adapted from Thomas and Lockery, 1999).

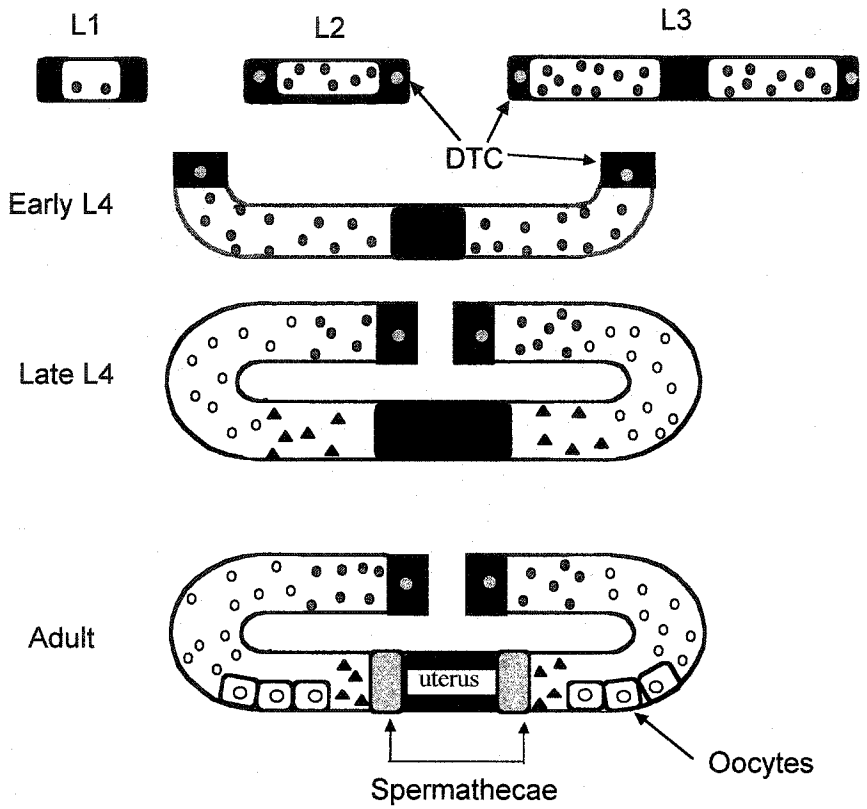

Figure I-6. The Reproductive System in the Hermaphrodite Worm

Somatic gonad cells with mitotic nuclei (open circles), germ-line meiotic nuclei (closed circles), sperm (triangles), distal tip cells (DTC), are shown. The somatic primordium encloses proliferating germ cells forming anterior and posterior arms. The gonad extends anterior and posteriorly led by DTC, and eventually loops at the L4 stage to from a U-shaped gonad. Sperm produced in the spermathecae at the L4 stage fertilize oocytes in the adult hermaphrodite initiating embryogenesis. Anterior is left (adapted from Schedl, 1997).

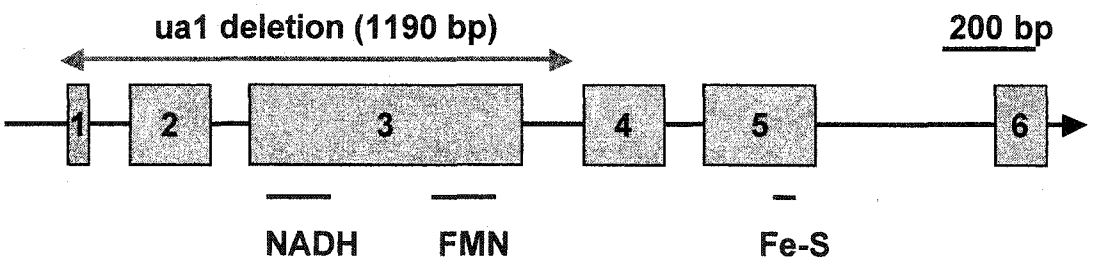

Figure I-7. Structure of the *nuo-1* gene

The six exons of the *nuo-1* gene are depicted as rectangles. The position of predicted substrate-binding (NADH) or cofactor-binding (FMN) regions, and the iron sulfur cluster (Fe-S) are shown below the exons. The ethyl methanesulfonate induced 1.2-kb *ua1* deletion was confirmed by sequencing (Tsang *et al.*, 2001).

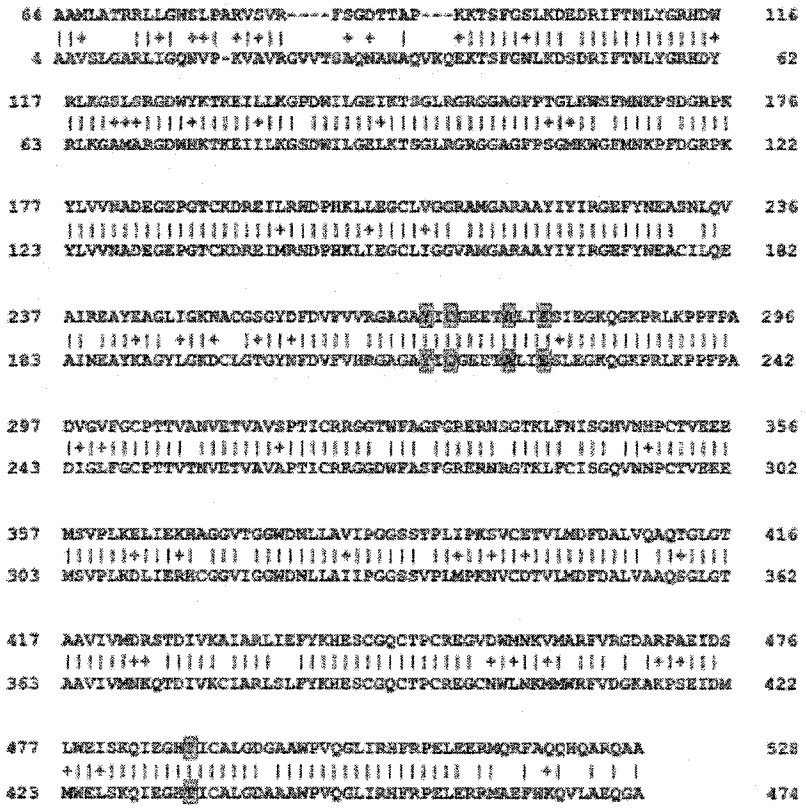

Figure I-8. Sequence Alignment of *C. elegans* NUO-1 and Human NDUFV1 Proteins

The human NDUFV1 protein sequence was compared with the *C. elegans* Wormpep database using the Blast 2.0 algorithm with default parameters (http://www.wormbase.org/db/searches/blat). Results indicated that the predicted gene C09H10.3 corresponding to the *nuo-1* locus has a P value of 6.7 X 10^{-203}. A sequence identity of 77% and sequence similarity of 88% are reported. |, amino acid identical to *C. elegans*; -, gap introduced to optimize alignment; +, conserved residue. The boxes indicate the amino acid residues affected by the non-conservative point mutations (Y204C, C206G, A211V, and E214K) located within the FMN binding domain and the T423M mutation likely in an essential functional domain of the protein (Bénit *et al.*, 2001; Schuelke *et al.*, 2002).

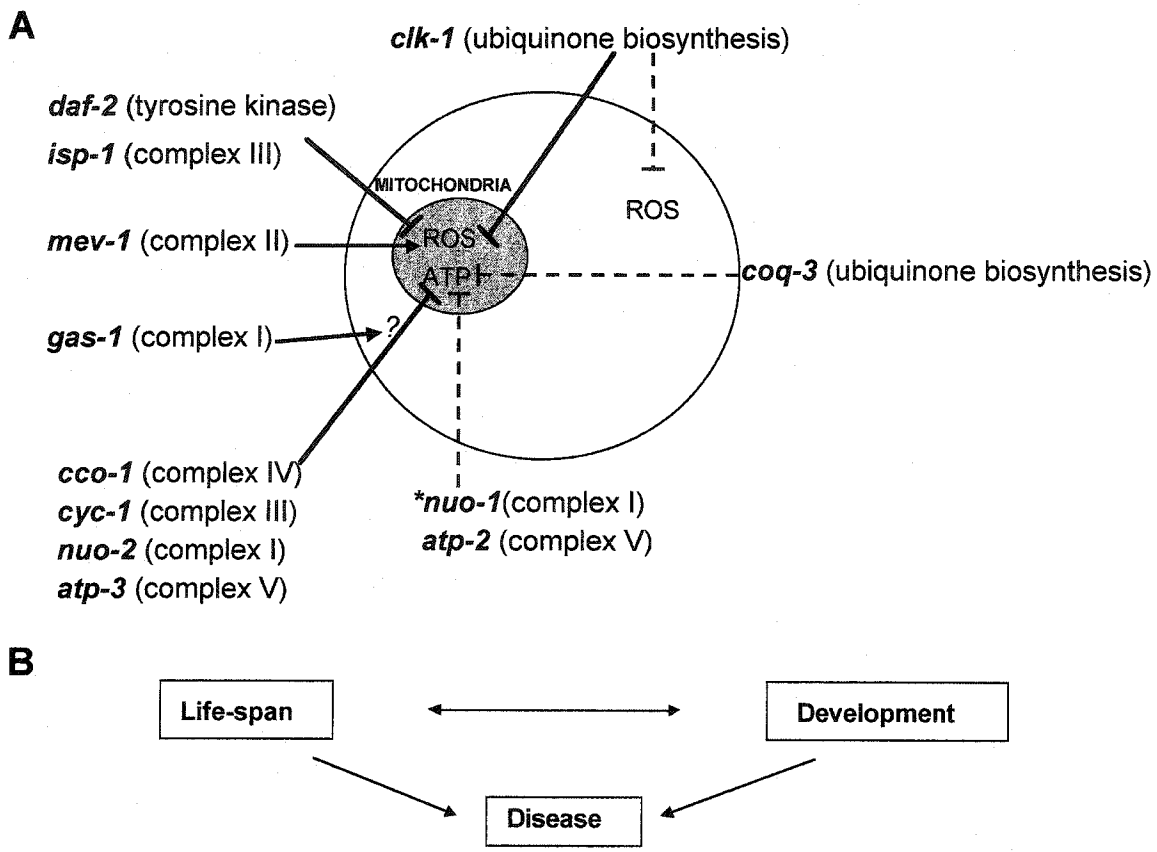

Figure I-9. Proposed actions of nuclear encoded genes in life-span and development and potential links to mitochondrial disease

A, Nuclear mutations that influence levels of mitochondrial or cytoplasmic reactive oxygen species (ROS) or ATP levels are included in the diagram. The dotted lines represent actions that are likely but have not yet been formally demonstrated. Mutations that affect life-span are illustrated on the left. Mutations that influence development are shown on the right. Mutations that play a role in both development and life-span are illustrated in the centre. The asterisk indicates the gene of interest. **B**, Potential interdependence between life-span, development, and disease.

BIBLIOGRAPHY:

Aboobaker, A.A., and M.L. Blaxter. 2000. Medical significance of *Caenorhabditis elegans*. *Ann. Med.* **32:**23-30.

Ambros, V. 1997. Heterochronic Genes, pp. 501-518 in *C. elegans* Volume II, edited by D.L. Riddle, T. Blumenthal, B.J. Meyer, and J. Preiss. Cold Spring Harbor Laboratory, Cold Spring Harbor, NY.

Ardizzi, J.P., and H.F. Epstein. 1987. Immunochemical localization of myosin heavy chain isoforms and paramyosin in developmentally and structurally diverse muscle cell types of *C. elegans*. *J. Cell Biol.* **105:**2763-2770.

Beal, M.F. 1995. Aging, energy, and oxidative stress in neurodegenerative diseases. *Ann. Neurol.* **38:**357-366.

Bénit, P., D. Chretien, N. Kadhom, P. de Lonlay-Debeney, V. Cormier-Daire, A. Cabral, S. Peudenier, P. Rustin, A. Munnich, and A. Rötig. 2001. Large-scale deletion and point mutations of the nuclear *NDUFV1* and *NDUFS1* genes in mitochondrial complex I deficiency. *Am. J. Hum. Genet.* **68:**1344-1352.

Borges, F., E. Fernandes, and F. Roleira. 2002. Progress towards the discovery of xanthine oxidase inhibitors. *Curr. Med. Chem.* **9:**195-217.

Braeckman, B.P., K. Houthoofd, K. Byrs, I. Lenaerts, A. De Vreese, S. Van Eygen, H. Raes, and J.R.Vanfleteren 2002. No reduction of energy metabolism in *Clk* mutants. *Mech. Ageing Dev.* **123:**1447-1456.

Brenner, S. 1974. The genetics of *Caenorhabditis elegans*. *Genetics* **77:**71-94.

***C. elegans* Sequencing Consortium.** 1998. Genome Sequence of the Nematode *C. elegans*: A Platform for Investigating Biology. *Science* **282:**2012-2018.

Campos, Y., J. Arenas, A. Cabello, and J.J. Gomez-Reino. 1995. Respiratory chain enzyme defects in patients with idiopathic inflammatory myopathy. *Ann. Rheum. Dis.* **54:**491-493.

Caroll, J., R.J. Shannon, I.M. Fearnley, J.E. Walker, and J. Hirst. 2002. Definition of the Nuclear Encoded Protein Composition of Bovine Heart Mitochondrial Complex I. *J. Biol. Chem.* **277:**50311-50317.

Cassada, R.C., and R.L. Russell. 1975. The dauer larva, a post-embryonic developmental variant of the nematode *C. elegans*. *Dev. Biol.* **46:**326-342.

Chinnery, P.F., and D.M. Turnbull. 1997. Mitochondrial Medicine. *Q. J. Med.* **90:**657-667.

Coulson, A., C. Huynh, Y. Kozono, and R. Shownkeen. 1995. The physical map of the *Caenorhabditis elegans* genome. *Methods Cell Biol.* **48:**533-550.

Culetto, E. and D.B. Sattelle. 2000. A role for *Caenorhabditis elegans* in understanding the function and interactions of human disease genes. *Hum. Mol. Genet.* **9:**869-877.

Dallner, G., and P.J. Sindelar. 2000. Regulation of ubiquinone metabolism. *Free Radic. Biol. Med.* **29:**285-294.

Davey, G.P., L. Canevari, and J.B. Clark. 1997. Threshold effects in Synaptosomal and Nonsynaptic Mitochondria from Hippocampal CA1 and Paramedian Neocortex Brain Regions. *J. Neurochem.* **69:**2564-2570.

Davey, G.P., S. Peuchen, and J.B. Clark. 1998. Energy Thresholds in Brain Mitochondria. *J. Biol. Chem.* **273:**12753-12757.

Dillin, A., A.-L. Hsu, N. Arantes-Oliveira, J. Lehrer-Graiwer, H. Hsin, A.G. Fraser, R.S. Kamath, J. Ahringer, C. Kenyon. 2002. Rates of Behavior and Aging Specified by Mitochondrial Function During Development. *Science* **298:**2398-2401.

DiMauro, S., E. Bonilla, M. Davidson, M. Hirano, and E.A. Schon. 1998. Mitochondria in neuromuscular disorders. *Biochim. Biophys. Acta* **1366:**199-210.

Djafarzadeh, R., S. Kerscher, K. Zwicker, M. Radermacher, M. Lindahl, H. Shagger, and U. Brandt. 2000. Biophysical and structural characterization of proton-translocating NADH-dehydrogenase (complex I) from the strictly aerobic yeast *Yarrowia lipolytica. Biochim. Biophys. Acta* **1459:**230-238.

Edgley, M.L., D.L. Baillie, D.L. Riddle, and A.M. Rose. 1995. Genetic Balancers. *Methods Cell Biol.* **48:**147-184.

Ewbank, J.J., T.M. Barnes, B. Lakowski, M. Lussier, H. Bussey, and S. Hekimi. 1997. Structural and functional conservation of the *Caenorhabditis elegans* timing gene *clk-1. Science* **275:**980-983.

Felkai, S., J.J. Ewbank, J. Lemieux, J.C. Labbe, G.G. Brown, and S. Hekimi. 1999. CLK-1 controls respiration, behavior and aging in the nematode *Caenorhabditis elegans. EMBO J.* **18:**1783-1792.

Feng, J., F. Bussiere, and S. Hekimi. 2001. Mitochondrial electron transport is a key determinant of life span in *Caenorhabditis elegans. Dev. Cell.* **1:**633-644.

Greenwald, I. 1997. Development of the Vulva, pp. 519-541 in *C. elegans* Volume II, edited by D.L. Riddle, T. Blumenthal, B.J. Meyer, and J. Preiss. Cold Spring Harbor Laboratory, Cold Spring Harbor, NY.

Grigorieff, N. 1998. Three-dimensional structure of bovine NADH:ubiquinone oxidoreductase (complex I) at 22 Å in ice. *J. Mol. Biol.* **277:**1033-1046.

Grossman, L.I. and E.A. Shoubridge. 1996. Mitochondrial Genetics and Human Disease. *Bioessays* **18:**983-991.

Guénebaut, V., R. Vincentelli, D. Mills, H. Weiss, and K. Leonard. 1997. Three-dimensional structure of NADH-dehydrogenase from *Neurospora crassa* by electron microscopy and conical tilt reconstruction. *J. Mol. Biol.* **265:**409-418.

Guénebaut, V., A. Schlitt, H. Weiss, K. Leonard, and T. Friedrich. 1998. Consistent structure between bacterial and mitochondrial NADH:ubiquinone oxidoreductase (complex I). *J. Mol. Biol.* **276:**105-112.

Harman, D. 1956. Aging: A Theory Based on Free Radical and Radiation Chemistry. *J. Gerontol.* **11:**298-300.

Hartman, P.S., N. Ishii, E.B. Kayser, P.G. Morgan, and M.M. Sedensky. 2001. Mitochondrial mutations differentially affect aging, mutability and anesthetic sensitivity in *Caenorhabditis elegans. Mech. Ageing Dev.* **122:**1187-1201.

Heales, S.J.R., M.E. Gegg, and J.B. Clark. 2002. Oxidative Phosphorylation: Structure, function, and intermediary metabolism. *Int. Rev. Neurobiol.* **53:**25-56.

Heddi, A., G. Stepien, P.J. Benke, and D.C. Wallace. 1999. Coordinate induction of energy gene expression in tissues of mitochondrial disease patients. *J. Biol. Chem.* **274:**22968-22976.

Hekimi, S., and L. Guarente. 2003. Genetics and the Specificity of the Aging Process. *Science* **299:**1351-1354.

Hihi, A.K., Y. Gao, and S. Hekimi. 2002. Ubiquinone is necessary for *Caenorhabditis elegans* development at mitochondrial and non-mitochondrial sites. *J. Biol. Chem.* **277:**2202-2206.

Hodgkin, J. 1999. Conventional genetics, pp.245-270 in *C. elegans* A Practical Approach, edited by I.A. Hope. Oxford University Press Inc., NY.

Holt, I.J., A.E. Harding, and J.A. Morgan-Hughes. 1988. Deletions of muscle mitochondrial DNA in patients with mitochondrial myopathies. *Nature* **331:**717-719.

Hosokawa, H., N. Ishii, H. Ishida, K. Ichimore, H. Nakazawa, and K. Suzuki. 1994. Rapid accumulation of fluorescent material with aging in an oxygen-sensitive mutant *mev-1* of *Caenorhabditis elegans. Mech. Ageing Dev.* **74:**161-170.

Hsin, H., and C. Kenyon. 1999. Signals from the reproductive system regulate the lifespan of *C. elegans*. *Nature* **399**:362-366.

Ishii, N., K. Takahashi, S. Tomita, T. Keino, S. Honda, K. Yoshino, and K. Suzuki. 1990. A methyl viologen-sensitive mutant of the nematode *Caenorhabditis elegans*. *Mutat. Res.* **237**:165-171.

Ishii, N., M. Fujii, P.S. Hartman, M. Tsuda, K. Yasuda, N. Senoo-Matsuda, S. Yanase, D. Ayusawa, and K. Suzuki. 1998. A mutation in succinate dehydrogenase cytochrome *b* causes oxidative stress and ageing in nematodes. *Nature* **394**:694-697.

Ishii, N., S. Goto, and P.S. Hartman. 2002. Protein oxidation during aging of the nematode *Caenorhabditis elegans*. *Free Radic. Biol. Med.* **33**:1021-1025.

Jacobs, H.T., S.K. Lehtinen, and J.N. Spelbrink. 2000. No sex please, we're mitochondria: a hypothesis on the somatic unit of inheritance of mammalian mtDNA. *Bioessays* **22**:564-572.

Jin, Y. 1999. Transformation, pp. 69-96 in *C. elegans* A Practical Approach, edited by I.A. Hope. Oxford University Press Inc., NY.

Jonassen, T., P.L. Larsen, and C.F. Clarke. 2001. A dietary source of coenzyme Q is essential for growth of long-lived *Caenorhabditis elegans clk-1* mutants. *Proc. Natl. Acad. Sci. USA* **98**:421-426.

Jonassen, T., B.N. Marbois, K.F. Faull, C.F. Clarke, and P.L. Larsen. 2002. Development and fertility in *Caenorhabditis elegans clk-1* mutants depend upon transport of dietary coenzyme Q_8 to mitochondria. *J. Biol. Chem.* **277**:45020-45027.

Jorgensen, E.M., and S.E. Mango. 2002. The art and design of genetic screens: *Caenorhabditis elegans*. *Nat. Rev. Genet.* **3**:356-369.

Kamata, H., and H. Hirata. 1999. Redox regulation of cellular signalling. *Cell Signal.* **11**:1-14.

Kayser, E.B., P.G. Morgan, and M.M. Sedensky. 1999. GAS-1: a mitochondrial protein controls sensitivity to volatile anesthetics in the nematode *Caenorhabditis elegans*. *Anesthesiology* **90**:545-554.

Kenyon, C., J. Chang, E. Gensch, A. Rudner, R. Tabtiang. 1993. A *C. elegans* mutant that lives twice as long as wild type. *Nature* **366**:461-464.

Kimura, K.D., H.A. Tissenbaum, Y. Liu, G. Ruvkun. 1997. *daf-2*, an insulin receptor-like gene that regulates longevity and diapause in *Caenorhabditis elegans*. *Science* **277**:942-946.

Lakowski, B., and S. Hekimi. 1996. Determination of life-span in *Caenorhabditis elegans* by four clock genes. *Science* **272:**1010-1013.

Lakowski, B., and S. Hekimi. 1998. The genetics of caloric restriction in *Caenorhabditis elegans*. *Proc. Natl. Acad. Sci. USA* **95:**13091-13096.

Lewis, J.A., and J.T. Fleming. 1995. Basic culture methods, pp.3-29 in *Caenorhabditis elegans*: Modern Biological Analysis of an Organism, edited by H.F. Epstein and D.C. Shakes. Academic Press, San Diego.

Liolitsa, D., and M.G. Hanna. 2002. Models of Mitochondrial Disease. *Int. Rev. Neurobiol.* **53:**429-466.

Luft, R., and B.R. Landau. 1995. Mitochondrial Medicine. *J. Intern. Med.* **238:**405-421.

Mazat, J.-P., R. Rossignol, M. Malgat, C. Rocher, B. Faustin, and T. Lettelier. 2001. What do mitochondrial diseases teach us about normal mitochondrial functions...that we already knew: threshold expression of mitochondrial defects. *Biochim. Biopyhs. Acta* **1504**:20-30.

Melov, S. J. Ravenscroft, S. Malik, M.S. Gill, D.W. Walker, P.E. Clayton, D.C. Wallace, B. Malfroy, S.R. Doctrow, and G.J. Lithgow. 2000. Extension of life-span with superoxide dismutase/catalase mimetics. *Science* **289:**1567-1569.

Miyadera, H., K. Kano, H. Miyoshi, N. Ishii, S. Hekimi, K. Kita. 2002. Quinones in long-lived *clk-1* mutants of *Caenorhabditis elegans*. *FEBS Lett.* **512:**33-37.

Murfitt, R.R., K. Vogel, and D.R. Sanadi. 1976. Characterization of the mitochondria of the free-living nematode, *Caenorhabditis elegans*. *Comp. Biochem. Physiol.* **53B:**423-430.

Ohnishi, T., V.D. Sled, T. Yano, T. Yagi, D.S. Burbaev, and A.D. Vinogradov. 1998. Structure-function studies of iron-sulfur clusters and semiquinones in the NADH-Q oxidoreductase segment of the respiratory chain. *Biochim. Biophys. Acta* **1365:**301-308.

Okimoto, R., J.L. Macfarlane, D.O. Clary, and D.R. Wolstenholme. 1992. The mitochondrial genomes of two nematodes, *Caenorhabditis elegans* and *Ascaris suum*. *Genetics* **130:**471-498.

Poyton, R.O., and J.E. McEwen. 1996. Crosstalk Between Nuclear and Mitochondrial Genomes. *Annu. Rev. Biochem.* **65:**563-607.

Raha, S., and B.H. Robinson. 2000. Mitochondria, oxygen free radicals, disease and ageing. *Trends Biochem. Sci.* **25:**502-508.

Raha, S. and B.H. Robinson. 2001. Mitochondria, oxygen free radicals, and apoptosis. *Am. J. Med. Genet.* **106:**62-70.

Riddle, D.L., T. Blumenthal, B.J. Meyer, and J.R. Priess. 1997. Introduction to *C. elegans*, pp. 1-22 in *C. elegans* Volume II, edited by D.L. Riddle, T. Blumenthal, B.J. Meyer, and J. Preiss. Cold Spring Harbor Laboratory, Cold Spring Harbor, NY.

Riddle, D.L., and P.S. Albert. 1997. Genetic and Environmental Regulation of Dauer Larva Development, pp.739-768 in *C. elegans* II, edited by D.L. Riddle, T. Blumenthal, B.J. Meyer, and J. Priess. Cold Spring Harbor Laboratory Press, NY.

Robinson, B.H. 1998. Human Complex I deficiency: Clinical spectrum and involvement of oxygen free radicals in the pathogenicity of the defect. *Biochim. Biophys. Acta* **1364:**271-286.

Rubio-Gozalbo, M.E., K.P. Dijkman, L.P. van den Heuvel, R.C. Sengers, U. Wendel, and J.A. Smeitink. 2000. Clinical differences in patients with mitochondriocytopathies due to nuclear versus mitochondrial DNA mutations. *Hum. Mutat.* **15:**522-532.

Schatz, G. 1995. Mitochondria: beyond oxidative phosphorylation. *Biochim. Biophys. Acta* **1271:**123-126.

Schedl, T. 1997. Developmental Genetics of the Germ Line, pp. 241-269 in *C. elegans* Volume II, edited by D.L. Riddle, T. Blumenthal, B.J. Meyer, and J. Preiss. Cold Spring Harbor Laboratory, Cold Spring Harbor, NY.

Schuelke, M., J. Loeffen, E. Mariman, J. Smeitink, and L. van den Heuvel. 1998. Cloning of the Human Mitochondrial 51 kDa Subunit (NDUFV1) Reveals a 100% Antisense Homology of Its 3′ UTR with the 5′ UTR of the γ-Interferon Inducible Protein (IP-30) Precursor: Is This a Link between Mitochondrial Myopathy and Inflammation? *Bioch. Biophys. Res. Commun.* **245:**599-606.

Schuelke, M., J. Smeitink, E. Mariman, J. Loeffen, B. Plecko, F. Trijbels, S. Stockler-Ipsiroglu, and L. van den Heuvel. 1999. Mutant *NDUFV1* subunit of mitochondrial complex I causes leukodystrophy and myoclonic epilepsy. *Nature Genet.* **21:**260-261.

Schuelke, M., A. Detjen, L. van den Heuvel, C. Korenke, A. Janssen, A. Smits, F. Trijbels, and J. Smeitink. 2002. New Nuclear Encoded Mitochondrial Mutation Illustrates Pitfalls in Prenatal Diagnosis by Biochemical Methods. *Clin. Chem.* **48:**772-775.

Senoo-Matsuda, N., K. Yasuda, M. Tsuda, T. Ohkubo, S. Yoshimura, H. Nakazawa, P.S. Hartman, and N. Ishii. 2001. A defect in the cytochrome *b* large subunit in

complex II causes both superoxide anion overproduction and abnormal energy metabolism in *Caenorhabditis elegans*. *J. Biol. Chem.* **276:**41553-41558.

Senoo-Matsuda, N., P.S. Hartman, A. Akatsuka, S. Yoshimura, and N. Ishii. 2003. A complex II defect affects mitochondrial structure, leading to *ced-3*- and *ced-4*-dependent apoptosis and aging. *J. Biol. Chem.* **278:**22031-22036.

Shoubridge, E.A. 2001. Nuclear Gene Defects in Respiratory Chain Disorders. *Sem. Neurol.* **21:**261-267.

Smeitink, J., and L. van den Heuvel. 1999. Human mitochondrial complex I in health and disease. *Am. J. Hum. Genet.* **64:**1505-1510.

Sulston, J.E., and H.R. Horvitz. 1977. Post-embryonic cell lineages of the nematode, *Caenorhabditis elegans*. *Dev. Biol.* **56:**110-156.

Sulston, J. 1988. Cell Lineage, pp. 123-155 in The Nematode *Caenorhabditis elegans*, edited by W.B. Wood. Cold Spring Harbor Laboratory, Cold Spring Harbor, NY.

Thomas, J.H., and S. Lockery. 1999. Neurobiology, pp. 143-179 in *C. elegans* A Practical Approach, edited by I.A. Hope. Oxford University Press Inc., NY.

Triepels, R.H., L.P. Van Den Heuvel, J.M. Trijbels, and J.A. Smeitink. 2001. Respiratory Chain Complex I Deficiency. *Am. J. Med. Genet.* **106:**37-45.

Tsang, W.Y., L.C. Sayles, L.I. Grad, D.B. Pilgrim, and B.D. Lemire. 2001. Mitochondrial Respiratory Chain Deficiency in *Caenorhabditis elegans* Results in Developmental Arrest and Increased Life Span. *J. Biol. Chem.* **276:**32240-32246.

Tsang, W.Y., and B.D. Lemire. 2002. Mitochondrial genome content is regulated during nematode development. *Biochem. Biophys. Res. Commun.* **291:**8-16.

Tsang, W.Y., and B.D. Lemire. 2003a. Mitochondrial ATP synthase controls larval development cell nonautomously in *Caenorhabditis elegans*. *Dev. Dyn.* **226:**719-726.

Tsang, W.Y., and B.D. Lemire. 2003b. The role of mitochondria in the life of the nematode, *Caenorhabditis elegans*. *Biochim. Biophys. Acta,* **1638:**91-105.

Vanfleteren, J.R., and A. De Vreese. 1996. Rate of aerobic metabolism and superoxide production rate potential in the nematode *Caenorhabditis elegans*. *J. Exp. Zool.* **274:**93-100.

Voet, D., and J.G. Voet. 1995. Electron transport and oxidative phosphorylation, pp. 563-598 in Biochemistry 2nd Edition. Wiley, NY.

Wadsworth, W.G. and D.L. Riddle. 1989. Developmental Regulation of Energy Metabolism in *Caenorhabditis elegans*. *Dev. Biol.* **132:**167-173.

Wallace, D.C. 1992. Mitochondrial genetics: A new paradigm for aging and degenerative diseases? *Science* **256:**628-632.

Wallace, D.C. 1999. Mitochondrial Diseases in Man and Mouse. *Science* **283:**1482-1488.

Wong, A., P. Boutis, and S. Hekimi. 1995. Mutations in the *clk-1* gene of *Caenorhabditis elegans* affect developmental and behavioral timing. *Genetics* **139:**1247-1259.

Wood, W.B. 1988. Introduction to *C. elegans* Biology, pp.1-16 in The Nematode *Caenorhabditis elegans*, edited by W.B. Wood. Cold Spring Harbor Laboratory, Cold Spring Harbor, NY.

Yagi, T., and A. Matsuno-Yagi. 2003. The Proton-Translocating NADH-Quinone Oxidoreductase in the Respiratory Chain: The Secret Unlocked. *Biochemistry* **42:**2266-2274.

Yano, T. 2002. The energy-transducing NADH:quinone oxidoreductase, complex I. *Mol. Aspect. Med.* **23:**345-368.

Zielasek, J., H. Reichmann, H. Kunzig, S. Jung, H.P. Hartung, and K.V. Toyka. 1995. Inhibition of brain macrophage/microglial respiratory chain enzyme activity in experimental autoimmune encephalomyelitis of the Lewis rat. *Neurosci Lett.* **184:**129-132.

II. Materials and Methods

II-1. Cloning Rationale and Design

Our cloning strategy was chosen to facilitate the creation of constructs containing a series of tissue-specific promoters driving *nuo-1* expression. We chose to study the expression of *nuo-1* in tissues that we thought could have a higher rate of respiration and energy requirement than other tissues. We obtained plasmids containing a promoter specific for the nervous system, *unc-119* (Maduro and Pilgrim, 1995), for the pharyngeal muscle, *myo-2* (Jantsch-Plunger and Fire, 1994), for the body-wall muscle, *unc-54* (MacLeod *et al.*, 1977), and for the germ-line, *pie-1* (Tenenhaus *et al.*, 2001). For general expression, we obtained a plasmid containing the promoter for the *let-858* gene, which is ubiquitously expressed throughout development (Kelly *et al.*, 1997). A list of plasmids used in this study is presented in Table II-1.

We chose to use Gateway™ Cloning Technology (Invitrogen Canada Inc., Burlington, Ontario) because of its high cloning efficiency and its directionality in cloning DNA segments. The Gateway Cloning System provides an alternative to restriction endonucleases and ligase by employing phage lambda-based site-specific recombination (Gibco BRL: Instruction Manual, 1999). The system is based on the switch between the lytic and lysogenic pathways used by *E. coli* bacteriophage lambda (λ) to integrate into and excise out of the host's genome (Ptashne, 1999). The integrative and excisive recombination reactions are site-specific and mediated by proteins encoded by λ and *E. coli* (Ptashne, 1999). These recombination reactions performed *in vitro* are the basis of the Gateway Cloning Technology (Landy, 1989).

II-2. Tissue Specificity

The following section describes the promoters that were used to study the tissue-specific expression of *nuo-1*.

II-2. a) Nervous system

The promoter from the *unc-119* gene, a member of the uncoordinated gene class (Maduro and Pilgrim, 1995), was used to study the expression of *nuo-1* in the nervous-system. UNC-119 is conserved in a spectrum of organisms (Maduro *et al.*, 2000) and has been shown to inhibit axon branching to maintain appropriate nervous system structure (Knobel *et al.*, 2001). The pattern of expression of the *unc-119* gene has been previously described in *C. elegans* using *unc-119::lacZ* and *unc-119::GFP* transgenic worms (Maduro and Pilgrim, 1995). Staining or fluorescence was seen very early in the embryo and continued through to adulthood in the dorsal and ventral nerve cords, the nerve ring, and the nerve bodies that innervate the preanal and lumbar ganglia (Maduro and Pilgrim, 1995). There is also evidence of expression outside the nervous system antecedent to the anterior pharyngeal bulb where no neuronal cell bodies are found (Maduro and Pilgrim, 1995).

II-2. b) Muscle

The *unc-54* (MacLeod *et al.*, 1977) and the *myo-2* (myosin heavy chain structural genes gene class) promoters (Jantsch-Plunger and Fire, 1994) were used for *nuo-1* expression in muscle. Myosin is a major component of the thick filament in muscle consisting of two heavy and two light chains. The *unc-54* gene encodes myosin heavy

chain B (MHC B), the major myosin heavy chain expressed in *C. elegans* (Ardizzi and Epstein, 1987). Using a monoclonal antibody to UNC-54 immunolocalization revealed expression in several muscle cell types including body wall, intestinal, anal depressor, and sphincter muscles, the contractile sheath of the somatic gonad, and vulval muscle cells (Ardizzi and Epstein, 1987). In addition, UNC-54 is expressed in the adult male sex muscles (Ardizzi and Epstein, 1987). The *myo-2* gene encodes myosin heavy chain C (MHC C), a unique type of myosin heavy chain that is limited to pharyngeal muscle cells (Ardizzi and Epstein, 1987). Using *myo-2::lacZ* (Jantsch-Plunger and Fire, 1994) and *myo-2::gfp* (Gaudet and Mango, 2002) transgenic worms, expression of *myo-2* was reported exclusively in pharyngeal muscle.

II-2. c) The Germ-line

The *pie-1* gene, a member of the pharynx and intestine in excess gene class, encodes a zinc finger protein that is an essential regulator of germ cell fate (Tenenhaus *et al.*, 2001). PIE-1 segregates with the germ lineage during the first embryological cleavages and functions as a global transcriptional repressor (Zhang *et al.*, 2003). PIE-1 promotes primordial germ cell development by blocking the transcription of genes involved in somatic development (Reese *et al.*, 2000). PIE-1 localization is concentrated in the posterior germ cell lineages (Mello *et al.*, 1996). Using *pie-1::gfp* transgenic worms, it was observed that at each division, PIE-1 inheritance is favored in germ-line daughter cells and excluded in somatic daughter cells (Reese *et al.*, 2000).

II-2. d) Ubiquitous Expression

As a positive control, we used the promoter of a globally expressed gene. The *let-858* gene is a member of member of the lethal gene class and encodes nucampholin, a highly conserved protein rich in acidic and basic residues (Kelly *et al.*, 1997). LET-858 is required for early embryogenesis and tissue differentiation and is expressed ubiquitously throughout development (Kelly *et al.*, 1997). LET-858 is speculated to be involved in protein synthesis and/or RNA binding (Kelly *et al.*, 1997). Northern blot analysis suggested that *let-858* is expressed at all stages but is most abundant at the embryo and larval stages (Kelly *et al.*, 1997).

II-3. General DNA Isolation, Purification, and Cloning Techniques

Unless otherwise stated, molecular biology methods were performed as described in Sambrook *et al.*, 1989. Plasmid DNA was isolated for cloning and restriction analysis by a modified alkaline-lysis method (Morelle, 1989). Further purification of plasmid DNA and of polymerase chain reaction-generated DNA for sequencing was accomplished using the Qiagen Plasmid Mini Preparation Kit (Qiagen, Mississauga, Ontario).

Restriction endonuclease enzymes for final construct analysis were purchased from New England BioLabs (New England Biolabs Inc., Pickering, Ontario) and Gibco BRL Life Technologies (Invitrogen Canada Inc., Burlington, Ontario). Enzyme digestions and inactivations were carried out as specified by the manufacturers. Routinely, ethanol precipitation of DNA for restriction endonuclease inactivation was carried out using the selective alcohol precipitation protocol (Innis, 1990) by adding 1/2

volume 7.5 M ammonium acetate, mixing, adding 9 volumes of ice-cold 95% ethanol, and precipitating at –70 °C for at least 15 minutes.

DNA was analyzed by gel electrophoresis in 1% agarose gels in TBE buffer (45 mM Tris-borate, 1 mM EDTA, pH 8.0) (Sambrook *et al.*, 1989). Restriction fragment sizes were determined relative to size standards run in adjacent lanes and visualized by ethidium bromide staining. Ligations were carried out in a final volume of 15 μl using 1 Unit T4 DNA Ligase (New England BioLabs). Different vector to insert ratios were used to optimize cloning efficiency. For transformation into electrocompetent *E. coli* DH5α, 1-2 μl of the ligation reaction was used. Unless otherwise specified, transformation of *E. coli* was carried out by electroporation (Hanahan *et al.*, 1991) using the Gibco BRL Cell-Porator *E. coli* Electroporation System (Invitrogen, Canada Inc., Burlington, Ontario) at 2.44 kV. For selection on kanamycin or chloramphenicol plates, transformants were allowed to recover in 1 ml Luria Broth (LB) without antibiotics for 1 hr at 37°C before plating on LB plates (5g/L NaCl, 10g/L tryptone, 5g/L yeast extract, 2% agar, pH 7.4) (Sambrook *et al*, 1989). Correct transformants were confirmed by restriction enzyme digestion of plasmid DNA isolated from single colonies. The antibiotics ampicillin, kanamycin, and chloramphenicol were used at final concentrations of 50 μg/ml.

II-4. Recombination Reactions of the Gateway Cloning System

Gateway Cloning Technology is based on reactions mediated by recombinant proteins. The cocktail of recombinant proteins used are Integrase (Int) and excisionase (Xis), which are encoded by the λ genome, and integration host factor (IHF), which is an *E. coli* protein (Gibco BRL: Instruction Manual, 1999). Four recombination sites (labeled

as 'att' sites) are specifically recognized by these proteins and allow for directional cloning.

Two reactions constitute Gateway cloning. The BP reaction is the *in vitro* version of the λ integration reaction mediated by the Int and IHF recombinant proteins (Gibco BRL: Instruction Manual, 1999). A recombination reaction between the attB sites on a PCR product of your gene of interest and the attP sites on a Donor Vector yields a Gateway compatible Entry Clone containing the PCR fragment. Entry Clones contain the rrnB sequence making them transcriptionally silent (Gibco BRL: Instruction Manual, 1999). The cloned gene is flanked by attL sites in the Entry Clone and can be transferred into new Expression Clones by recombination with Destination Vectors.

The LR reaction is the *in vitro* version of the λ excision reaction mediated by the Int, IHF, and Xis recombination proteins. A recombination reaction between the attL sites on the Entry Clone (flanking the gene of interest) and the attR sites on a Destination Vector (containing the tissue-specific promoter) yields an Expression Clone. The orientation and reading frame of the gene are maintained throughout the subcloning because the attL1 site recombines specifically with the attR1 site and the attL2 site recombines specifically with the attR2 site. The Expression Clone consists of the tissue-specific promoter driving the expression of the gene of interest and is selected for the antibiotic resistance marker it carries. Due to the presence of a ccdB gene that is toxic to most *E. coli* strains, the unreacted Destination Vector does not give rise to ampicillin-resistant colonies even though it carries an ampicillin resistance gene.

II-5. Construction of a *nuo-1* Entry Vector

A schematic diagram outlining the construction of the *nuo-1* Entry Vector, pENTRnuo-1 is shown in Figure II-1. A detailed account of the cloning process is outlined in the steps below.

II-5. a) Mun1 Deletion of nuo-1 Sequence

The 2.4-kb region of *nuo-1* genomic sequence to be cloned extended from the ATG start codon (downstream of the TATA box) to approximately 200 bp downstream of the coding sequence, including a putative polyadenylation signal. To avoid the need to sequence the entire region, a 1.4-kb deletion was made between two *Mun 1* restriction sites within the *nuo-1* gene. A 10 μl restriction digest of pceNuo-1C, which contains a 5.4-kb fragment of genomic DNA encoding the *nuo-1* gene, with 5 units *Mun 1* was incubated at 37 °C for 2 h. The products were run on a 1% agarose gel to confirm that the digest had gone to completion. Ethanol precipitation was used to inactivate the *Mun 1* enzyme and the DNA was resuspended in 20 μl sterile water. A 10-μl self-ligation reaction was set up and incubated at 16 °C overnight. A 1-μl aliquot of the ligation was transformed into DH5α and transformants were selected for chloramphenicol resistance. Plasmid DNA of selected colonies was analyzed by restriction digest to identify clones with the *Mun 1* deletion. A *Mun 1* deleted clone, pceNuo-1m, was used as a template for PCR reactions with Gateway compatible oligonucleotide primers.

II-5. b) Design of attB Oligonucleotide Primers

Forward and reverse primers for the attB PCR consisted of 29 nucleotides of attB sequence (including 4 guanosine residues) and 24 or 21 nucleotides of *nuo-1* gene-specific sequence. The sequences of the attB primers are shown in Table II-2. The four guanosine residues at the 5′-ends of the primers are recommended for the synthesis of an efficiently recombining Gateway compatible PCR product for use as a substrate in the BP reaction. The oligonucleotide primers (40 nmol) were synthesized on an Applied Biosystems 392 DNA Synthesizer by the DNA Core Facility in the Department of Biochemistry, University of Alberta. The oligonucleotides were dissolved in 100 μl TE (10mM Tris-HCl, 1mM EDTA, pH 8.0) and their concentrations determined by absorbance spectroscopy at 260 nm.

II-5. c) Polymerase Chain Reaction

PCR was performed using the Expand™ High Fidelity PCR System kit from Roche Diagnostics (Basel, Switzerland). The kit contains a mix of the thermostable *Taq* and *Pwo* DNA polymerases designed for both high yield and high fidelity amplifications.

All reactions were carried out in a final volume of 50 μl using thin walled PCR reaction tubes. For each reaction, two separate master mixes were prepared on ice. Master mix 1 consisted of 200 μM of each dNTP (dATP, dTTP, dCTP, dGTP), 300 nM of the upstream primer (attB1), 300 nM of the downstream primer (attB2), and 0.1- 0.75 μg of template DNA. Master mix 2 consisted of 10X High Fidelity buffer (with 15 mM $MgCl_2$), sterile H_2O, and 2.6 U of *Taq* DNA polymerase mix. The two Master Mixes were pipetted together on ice and cycling was immediately initiated. Cycles of

denaturation at 94 °C for 45 sec, annealing at 55 °C for 30 sec, and elongation at 72 °C for 1.5 min were repeated 35 times. The reaction was incubated for an additional 10 min at 72 °C.

To remove unincorporated primer and primer-dimers, the amplified product was purified by polyethylene glycol (PEG) precipitation. To the 50-µl PCR reaction, 150 µl of TE and 100 µl of a solution of 30% PEG-8000 containing 30 mM $MgCl_2$ were added. The reaction was immediately centrifuged at 10,000 x *g* for 10 min at room temperature. The supernatant was removed and the pellet was resuspended in 50 µl TE. An aliquot of the purified PCR product was run on a 1% agarose gel to confirm its recovery and size.

II-5. d) Sequencing of the nuo-1 PCR Fragment

DNA sequence analysis, based on the dideoxy chain termination method (Sanger *et al.*, 1977), was performed by the Department of Biochemistry DNA Core Laboratory (University of Alberta) using 200 ng/µl of PCR product. Table II-2 lists the primers used for sequencing. The sequencing results are presented in Figure II-2 and confirm that the sequence of the PCR product is as expected.

II-5. e) BP Reaction to create a nuo-1 Entry Clone

The *nuo-1* PCR fragment was recombined into the Donor Vector pDONR201 via the BP reaction to create an Entry Clone. A reaction mixture of 6 µl TE, 4 µl BP Clonase Reaction Buffer, 2 µl pDONR201 (150 ng/µl) and 4 µl PCR (10 ng/µl) product was prepared and mixed well on ice. To this, 4 µl of BP Clonase Enzyme Mix was added and the reaction was incubated at 25 °C for 60 minutes. Following the incubation, 2 µl

Proteinase K solution (200 μg/ml) was added and the reaction was incubated at 37 °C for 10 minutes. A 2-μl aliquot of BP reaction was transformed into DH5α and transformants were selected for kanamycin resistance. Plasmid DNA of selected colonies was analyzed by restriction enzyme digests to confirm the structure of the *nuo-1* Entry Clone, pENTRnuo-1m.

To restore the complete *nuo-1* coding sequence, the 1.4-kb *Mun 1* fragment was ligated into the *Mun 1* digested Entry Clone. In a 15-μl reaction, the Entry Clone was digested with *Mun 1* for 3 h at 37 °C. Shrimp alkaline phosphatase (0.5 U) was added in the last hour of the digest to dephosphorylate the DNA ends and thus decrease the probability of self-ligation. Simultaneously, in a 15-μl reaction, pceNuo-1C was digested with *Mun 1* for 3 h at 37 °C to generate the 1.4-kb fragment. In 10-μl ligation reactions, different vector to insert ratios were incubated with 1 unit of T4 DNA ligase at 16 °C overnight. A 1-μl aliquot of the ligation reaction was transformed into electrocompetent DH5α and correct transformants were selected for kanamycin resistance. Restriction digests of isolated pENTRnuo-1 plasmid DNA confirmed the insertion of the *Mun 1* fragment in the correct orientation.

II-6. Construction of Destination Vectors

Standard vectors can be converted into Gateway compatible Destination Vectors by inserting the Gateway Reading Frame Cassette into the multiple cloning site (MCS) of that vector. Destination Vectors created in this way will have two recombination sites (attR1 and attR2) flanking a chloramphenicol resistance gene and a ccdB gene arranged contiguously. Because the reading frame cassettes are blunt-ended, they can insert in both

orientations. Destination Vectors must be constructed and propagated in the *gyrA462* strain of *E. coli,* DB3.1, as the presence of the ccdB gene is otherwise lethal (Gibco BRL. Instruction Manual, 1999).

The Gateway Reading Frame Cassette was inserted into the MCS at the 3′ end of the various tissue-specific promoters of pBY103, pPD118.25, pPD118.33, and pPD30.38 (Table II-1) to create Destination Vectors. To clone in Gateway Cloning System Reading Frame Cassette B, each plasmid was cut with a blunt end generating enzyme in a 10-µl restriction digest for 2.5 h at 37 °C. Shrimp alkaline phosphatase (0.5 U) was added for 1 h to remove 5′ phosphates and decrease the probability of self-ligation of the vector. After incubation, the enzymes were heat inactivated by incubation at 65 °C for 15 min. In a 10-µl ligation reaction, 10-50 ng of digested plasmid, 10-20 ng of Gateway Cloning System Reading Frame Cassette B, and 1 unit of T4 DNA ligase were combined and incubated overnight at 16 °C. 1 µl of ligation reaction was transformed into 100 µl DB3.1 competent cells using a heat shock transformation protocol. A 20-µl aliquot of DB3.1 cells was put into chilled sterile microcentrifuge tubes. To this, 1 µl of the ligation reaction was added and incubated on ice for 30 min. The cells were heat shocked for 15 sec in a 42 °C water bath and then placed on ice. The cells were allowed to recover in 100 µl S.O.C. (20 mg/ml Bactotryptone, 5.5 mg/ml yeast extract, 10 mM $MgSO_4$, 10 mM $MgCl_2$, 10 mM KCl, 10 mM NaCl, 20 mM Glucose, pH 7.0) medium for 1 h. Transformants were selected on LB plates containing chloramphenicol. Plasmid DNA was isolated from single ampicillin resistant colonies grown in liquid culture and cut with restriction enzymes to determine the orientation of the cassette. Clones with the correct orientation had the attL1 site next to the 3′ end of each promoter.

II-7. Construction of Expression Clones via the LR Reaction

Recombination between the Entry Clone, pENTRnuo-1, and the various Destination Vectors by the LR reaction resulted in a series of Expression Clones listed in Table II-1. A schematic diagram outlining the construction of Expression Clones via the LR reaction is presented in Figure II-3.

A reaction mixture of 8 μl pENTRnuo-1 (15 ng/μl), 4 μl Destination Vector (15 ng/μl), 4 μl LR Clonase Reaction Buffer was prepared on ice. The reaction was incubated with 4 μl LR Clonase Enzyme mix at 25 °C for 60 minutes. Following the incubation, 2 μl Proteinase K solution (200 μg/ml) were added and the reaction was incubated at 37 °C for 10 minutes. A 1-μl aliquot of the recombination reaction was transformed into 20 μl DH5α electrocompetent cells and transformants selected for on LB plates containing ampicillin. Restriction enzyme digest analysis of plasmid DNA was used to confirm the structure of the Entry Clone pENTRnuo-1, and each Expression Clone pEXPunc-54, pEXPunc-119, and pEXPlet-858 as illustrated in Figure II-4. Restriction enzyme digest analysis was also used to confirm the pEXPmyo-2 and pEXPpie-1 constructs (results not shown.)

II-8. Creation of Transgenic Worm Strains

To investigate the tissue-specific role of the *nuo-1* gene in the development of *C. elegans*, we wished to generate a series of transgenic worm strains expressing *nuo-1* under the control of the tissue-specific promoters. For example, the *unc-119* promoter, which is specific for the nervous system, should drive *nuo-1* expression in the nervous-

system and produce worms with a functional mitochondrial respiratory chain exclusively in neurons (Maduro and Pilgrim, 1995). Previous experiments carried out by Wilm *et al.* (1999) and Praitis *et al.* (2001) showed that microparticle bombardment could be used as an effective alternative to microinjection to create transgenic lines in *C. elegans.* Microparticle bombardment is a method of transformation that uses helium pressure to introduce DNA-coated gold beads into the cells of the target organism (Bio-Rad Instruction Manual, 2001). We reasoned that since a large number of worms are bombarded simultaneously (approximately 10^4 worms per bombardment), transformation would occur at a more detectable frequency.

To identify transformants, we used a conditional lethal method of selection based on the rescue of the *unc119(ed3)* mutant phenotype (Praitis *et al.,* 2001). The ethyl methanesulfonate (EMS) induced mutant allele, *ed3*, consists of a C to T point mutation in exon IV of the *unc-119* gene, creating an in-frame stop codon (Maduro and Pilgrim, 1995). Mutant worms display a strongly uncoordinated (Unc) phenotype, are almost paralyzed, and tend to curl (Maduro and Pilgrim, 1995). The effects of the mutation are nervous system specific and worms display normal muscle ultrastructure (Maduro and Pilgrim, 1995). *unc-119(ed3)* mutants cannot form dauers, an alternative larval stage that normally allows *C. elegans* to survive for months without food (Cassada and Russell, 1975). As a result, *unc-119(ed3)* mutants transformed with a plasmid containing *unc-119(+)* are motile and survive starvation. Untransformed worms display the Unc phenotype and eventually starve and die. Therefore, although positive transformants from microparticle bombardment occur at a relatively low frequency (~0.5 X 10^{-4}), this *unc-*

119 based selection permits the surviving non-Unc transformant worms to be easily identified (Praitis *et al.*, 2001).

II-9. Worm Strains

A list of the worm strains that were used in this study is presented in Table II-3. The following outlines special features of each strain and how they were constructed.

II-9. a) The LB21B balanced nuo-1 worm strain

The *nuo-1(ua1)* mutation is lethal in worms resulting in developmental arrest at the L3 larval stage (Tsang *et al.*, 2001). The mutation is maintained in the balanced heterozygote strain, LB21B. Figure II-5 illustrates the genetic balancer for chromosome II, *mIn1*, found in LB21B. The balancer contains a chromosomal inversion of a central portion of the chromosome, which includes the wild-type *nuo-1(+)* allele, the recessive *dpy-10(e128)* mutation, and a GFP marker, *mIs14[myo2::gfp; pes-10::gfp]* that contains the pharyngeal *myo-2* and the gut *pes-10* promoters and a gut enhancer fused individually to the gene encoding GFP (Edgley and Riddle, 2001). The chromosomal inversion on the *mIn1* balancer virtually eliminates crossover events and recombination in heterozygotes, producing a stable line (Hodgkin, 1999).

Homozygous mutant progeny *nuo-1(ua1)/nuo-1(ua1),* which do not contain the balancer, are non-fluorescent and arrest at the L3 larval stage. Heterozygous worms are wild-type and display pharyngeal fluorescence when visualized using a fluorescence stereomicroscope (Leica MZ FLIII, Leica Microsystems AG, Heerbrugg, Switzerland). Homozygous *nuo-1(+)* worms display brighter pharyngeal fluorescence and are dumpy

(morphologically shorter and fatter than wild-type) (Levy *et al.*, 1993) as they carry two copies of the balancer chromosome with the recessive *dpy-10(e128)* allele. Following the self-fertilization of a heterozygous worm, Mendelian genetics dictates that 25% of the progeny in a mixed population are homozygous for the mutation. Our goal was to identify homozygous *nuo-1(ua1)* worms complemented with the tissue-specific transgene that developed past the L3 larval stage.

II-9. b) Construction of the LB77 strain

In order to utilize microparticle bombardment to mediate transformation, we needed to create an *unc-119(ed3)* strain with a balanced *nuo-1(ua1)* mutation. To construct the desired strain, we started with the LB22 *nuo-1(ua1)* balanced strain that is also homozygous for the *him-8(e1489)* mutation (a member of the High Incidence of Males gene class) (Broverman and Meneely, 1994). The *him-8(e1489)* mutation results in the increased loss of X chromosomes during hermaphrodite gametogenesis, resulting in a significantly higher occurrence of males in self-progeny (Broverman and Meneely, 1994). Four heterozygous LB22 males picked as L4 larvae were crossed with one DP38 *(unc-119 (ed3))* hermaphrodite also picked at the L4 stage to enhance the production of outcross progeny (Hodgkin, 1999). The resulting *unc-119(ed3)*/+ III ; *nuo-1(ua1)*/+ II and *unc-119(ed3)*/+ III ; *mIn1*/+ II outcross progeny were mated to each other. Progeny from the second cross were screened for fluorescent Unc worms. Verification of the genotype of the *unc-119(ed3)* III ; *nuo-1(ua1)/mIn1* II mutant strain, LB77 was made by using PCR and by determining the Mendelian segregation pattern for the balancer.

II-10. Microparticle Bombardment and Screening for Transformants

Unless otherwise specified, the basic protocols followed for worm preparation and bombardment are as described (Praitis *et al.*, 2001).

II-10. a) Preparation of DNA

Purification of plasmid DNA was accomplished using the Qiagen Plasmid Mini Preparation Kit (Qiagen, Mississauaga, Ontario). To create transgenic lines, the transforming plasmids listed in Table II-4 were used. The plasmids pDP#MM016b and pAZ119 contain an *unc-119(+)* rescuing genomic fragment (consisting of the whole *unc-119* gene, including its promoter and 3′-untranslated region) as a selectable co-transformation marker (Maduro and Pilgrim, 1995). Each Expression Clone was co-bombarded with either pDP#MM016b or pAZ119 with the exception of pEXPpie-1, which already contains the *unc-119(+)* rescuing fragment. To optimize co-transformation, the initial concentrations of both plasmids were kept approximately the same at 1-2 μg/μl.

II-10. b) Preparation of gold particles

15 mg of 1 micron gold beads were weighed into an Eppendorf tube. 1 ml of 70% ethanol was added and vortexed for 5 min. The particles were allowed to settle for 15 min. Once the beads settled, the tube was centrifuged briefly for 3-5 sec and the supernatant discarded. The next steps were repeated three times. 1 ml distilled water was added and vortexed for 1 min. After the particles were allowed to settle for 1 min, the tube was centrifuged briefly for 3-5 sec and the supernatant was discarded. To the

pellet, 250 µl of 50% glycerol was added. The suspension of gold beads in 50% glycerol was stored at –20 °C.

II-10. c) Preparation of DNA-coated gold microcarriers

The quantities in the following protocol are for a single bombardment. Gold beads suspended in 50% glycerol were vortexed for 5 min and an aliquot of 10 µl per bombardment was added to an Eppendorf tube. While vortexing, 0.5 µl of each plasmid, pEXPunc-119 and pDP#MM016b (1-2 µg/µl), 10 µl 2.5 M $CaCl_2$, and 4 µl 0.1 M spermidine were added. Following vortexing for 5 min, the beads were allowed to settle for 1 min. The tube was centrifuged briefly for 3-5 sec and the supernatant discarded. The pellet was resuspended in 30 µl 70% ethanol, centrifuged briefly, and the supernatant removed. The pellet was resuspended in 10 µl 100% ice cold ethanol and vortexed thoroughly until ready to bombard.

II-10. d) Preparation of worms

A synchronous population of L4 and young adult hermaphrodite worms were used for bombardment. Nematode Growth Medium (NGM) agar 100-mm plates (3 g NaCl, 17 g agar, 5 g peptone, 1 ml of 5 mg/ml cholesterol in ethanol, 975 ml sterile water, 1 ml 1M $CaCl_2$, 1 ml 1M $MgSO_4$, 25 ml 1M potassium phosphate, pH 6) seeded with a lawn of *E. coli* (OP50) were used to culture LB77 worms (Lewis and Fleming, 1995). Worms and eggs were washed off plates containing a high proportion of gravid adults and eggs with M9 buffer (3g/L KH_2PO_4, 6g/L Na_2HPO_4, 5g/L NaCl, sterile water, 1 ml 1M $MgSO_4$) into 50 ml Falcon tubes (Lewis and Fleming, 1995). The tubes were

centrifuged at 1000 rpm for 5 min and the supernatant discarded. The worms were resuspended in M9 buffer and pelleted another two times to remove most of the *E. coli.* To 5 ml of worms in M9, 35 ml of an alkaline hypochlorite mix (8.75 ml 4M NaOH, 14 ml bleach, and 28.25 ml sterile water) were added and incubated at room temperature for 7 min. Following incubation, the tubes were centrifuged at 1400 rpm for 5 min and the supernatant discarded. The resulting egg pellet was deposited on unseeded plates and incubated overnight to allow the worms to hatch. Starved L1 worms were transferred to seeded plates to resume development. The synchronized worms were allowed to mature to the L4-early adult stage at 20 °C for 3-4 days.

When ready to bombard, the worms were washed off using M9 buffer into 50 ml Falcon tubes and allowed to settle for 5 min. The tubes were centrifuged at 1000 rpm for 5 min. Most of the supernatant was discarded and approximately 75 µl of worms were spread in a monolayer onto a 2-cm spot of *E. coli* in the centre of a 60-mm NGM target plate. The target plates were placed on ice to immobilize the worms for bombardment.

II-10. e) Bombardment parameters and procedure

The Biolistic® PDS-1000/He system (Bio-Rad, Hercules, California) uses a high helium pressure created by a rupture disk and a partial vacuum to accelerate a thin macrocarrier sheet toward target tissue (Bio-Rad Instruction Manual, 2001). The macrocarrier sheet contains gold microcarriers that are coated with the transforming plasmid DNA. The macrocarrier sheet is abruptly stopped by a screen, propelling the DNA-coated microcarriers toward the target to result in transformation (Bio-Rad Instruction Manual, 2001).

Before placing DNA-coated gold on the macrocarrier, the tube was vortexed to break up gold particle aggregates. 10 μl of DNA-coated gold beads were spread over the central region of each macrocarrier and the ethanol allowed to evaporate. The NGM target plate containing the worms to be bombarded was taken from the ice and placed on the target shelf. The launch velocity of DNA-coated gold microcarriers for each bombardment was determined by the following parameters: 1350 p.s.i rupture discs were used, a vacuum in the bombardment chamber of 26.5 inches of Hg was created, the distance from the rupture disk to the macrocarrier was set to 0.25 inches, the macrocarrier travel distance to the stopping screen was set to 9 mm, and the distance between the stopping screen and the target cells was set to 9 cm.

Following bombardment, the target plates were incubated at 20 °C for 7-14 days allowing untransformed worms to starve and die. The target plates were screened for worms rescued for the *unc-119(ed3)* mutation based on their ability to form dauers and a non-Unc phenotype. Of these, 10-15 individual transformants were cloned and their F_1 progeny scored for presence of Unc worms. From a series of bombardments, we obtained several independent transmitting lines.

II-10. f) Polymerase Chain Reaction of Transmitting Lines

To confirm the presence of transforming DNA in transmitting lines, oligonucleotide primers were designed to specifically recognize DNA sequences present only in the transforming plasmids. Forward and reverse primers for all PCR reactions are presented in Table II-5. All oligonucleotide primers were synthesized and prepared as previously described. Worm lysates served as the source of template DNA for all PCR

reactions. Worms were washed off NGM plates with M9 buffer and digested in single worm lysis buffer containing 200 μg/ml proteinase K. The lysis reaction was incubated at 50 °C for 1 h followed by 10 min at 95 °C to inactivate the proteinase K.

All PCR reactions were carried out using a Gene Amp PCR System 9700 (PE Applied Biosystems, Foster City, California). A final reaction volume of 15 μl in thin walled PCR reaction tubes was used. For each reaction, the following mix was prepared on ice: 200 μM of each dNTP (dATP, dTTP, dCTP, dGTP), 0.4 μM of upstream primer, 0.4 μM of downstream primer, 10X PCR buffer (with 15 mM $MgCl_2$), 4.5 U *Taq* DNA polymerase, sterile H_20, and approximately 0.1 – 1.0 μg template DNA. Cycles of denaturation at 92 °C for 35 sec, annealing at 58 °C for 45 sec, and elongation at 72 °C for 1.5 min were repeated 35 times. The reactions were incubated for an additional 10 min at 72 °C. The amplification products were analyzed by agarose gel electrophoresis and visualized by ethidium bromide staining.

II-10. g) Inheritance Patterns of Transgenic DNA

Transgenic DNA becomes heritable within an organism by integration into the genome or extrachromosomally in the form of tandemly repeated copies of the transgene (Mello and Fire, 1995). It is still unclear how integration occurs via microparticle bombardment but it is suggested that double strand breakage occurs and DNA repair mechanisms use the array to repair DNA at random. Stinchcomb *et al.* (1985) first described the formation of extrachromosomal arrays as the ligation of several hundred copies of plasmid. Co-bombarded DNAs could essentially be mixed in an array in random order and in proportion to the relative DNA concentrations in the original

microcarrier suspension. Arrays greater than 700-kb are transmitted through the germ-line as extrachromosomal elements, whereas smaller arrays are lost due to mitotic instability (Mello and Fire, 1995).

Strains homozygous for an integrated *unc-119* rescuing transgene would segregate 100% non-Unc progeny. Obligate heterozygotes could occasionally occur when the transforming DNA is either toxic or its integration is in an essential gene (Mello and Fire, 1995). For these strains, worms homozygous for the insertion would be inviable resulting in a 2:1 ratio of viable wild-type:Unc progeny. Extrachromosomal arrays behave like chromosomal free duplications and display non-Mendelian segregation patterns (Mello and Fire, 1995). The transmission of extrachromosomal arrays from one generation to the next depends on the size of the array and can range from 10 to 90% (Mello and Fire, 1995).

Table II-1. Plasmids Used in This Study

Plasmid	Relevant Features	Source
pceNuo-1C	Contains a 5.4-kb *Xho* 1 fragment from the cosmid CO9H10 encoding the *nuo-1* gene cloned into the pBC (KS-) vector, Cm^R	Lab collection
pceNuo-1m	Derived from pceNuo-1C. Contains a 1.4-kb *Mun 1* deletion within the *nuo-1* gene, Cm^R	this study
pDONR201	Gateway compatible Donor Vector with attP sites; used in the BP reaction to create Entry Clones, Cm^R, Kan^R	Gateway Cloning kit
pBY103	Contains a 1.2-kb fragment encoding the *unc-119* nervous system-specific promoter, Amp^R	David Pilgrim, University of Alberta
pPD118.25	Contains a 3.4-kb fragment encoding the promoter of the ubiquitously expressed *let-858* gene, Amp^R	Andrew Fire, Carnegie Institution of Washington 1997 vector kit
pPD118.33	Contains a 1.3-kb fragment encoding the *myo-2* pharyngeal muscle-specific promoter, Amp^R	Andrew Fire, Carnegie Institution of Washington 1997 vector kit
pID2.02	Gateway compatible vector with attR sites; contains a 5.7-kb *unc-119* rescuing fragment, and the 3.5-kb *pie-1* germline-specific promoter, Amp^R	Geraldine Seydoux, Johns Hopkins University School of Medicine
pPD30.38	Contains a 0.8–kb fragment encoding the *unc-54* body wall muscle-specific promoter and enhancer, Amp^R	Andrew Fire, Carnegie Institution of Washington pre-1995 vector kit
pENTRnuo-1	Gateway compatible Entry Clone with attL sites containing *nuo-1* gene PCR fragment; used in LR reaction to create Expression Clones, Kan^R	this study
pDESTunc-119	Gateway compatible vector with attR sites containing the *unc-119* promoter; used in LR reaction with pENTRnuo-1 to create pEXPunc-119, Amp^R, Cm^R	this study
pDESTlet-858	Gateway compatible vector with attR sites containing the *let-858* promoter; used in LR reaction with pENTRnuo-1 to create pEXPlet-858, Amp^R, Cm^R	this study
pDESTmyo-2	Gateway compatible vector with attR sites containing the *myo-2* promoter; used in LR reaction with pENTRnuo-1 to create pEXPmyo-2, Amp^R, Cm^R	this study
pDESTunc-54	Gateway compatible vector with attR sites containing the *unc-54* promoter; used in LR reaction with pENTRnuo-1 to create pEXPunc-54, Amp^R, Cm^R	this study
***pEXPunc-119**	Gateway compatible vector with attB sites; contains the *unc-119* promoter upstream of the *nuo-1* coding region, Amp^R	this study
***pEXPlet-858**	Gateway compatible vector with attB sites; contains the *let-858* promoter upstream of the *nuo-1* coding region, Amp^R	this study
***pEXPmyo-2**	Gateway compatible vector with attB sites; contains the *myo-2* promoter upstream of the *nuo-1* coding region, Amp^R	this study
***pEXPpie-1**	Gateway compatible vector with attB sites; contains the *unc-119* rescue fragment, and *pie-1* promoter upstream of the *nuo-1* coding region, Amp^R	this study
***pEXPunc-54**	Gateway compatible vector with attB sites; contains the *unc-54* promoter upstream of the *nuo-1* coding region, Amp^R	this study

*Vectors used in expression studies.

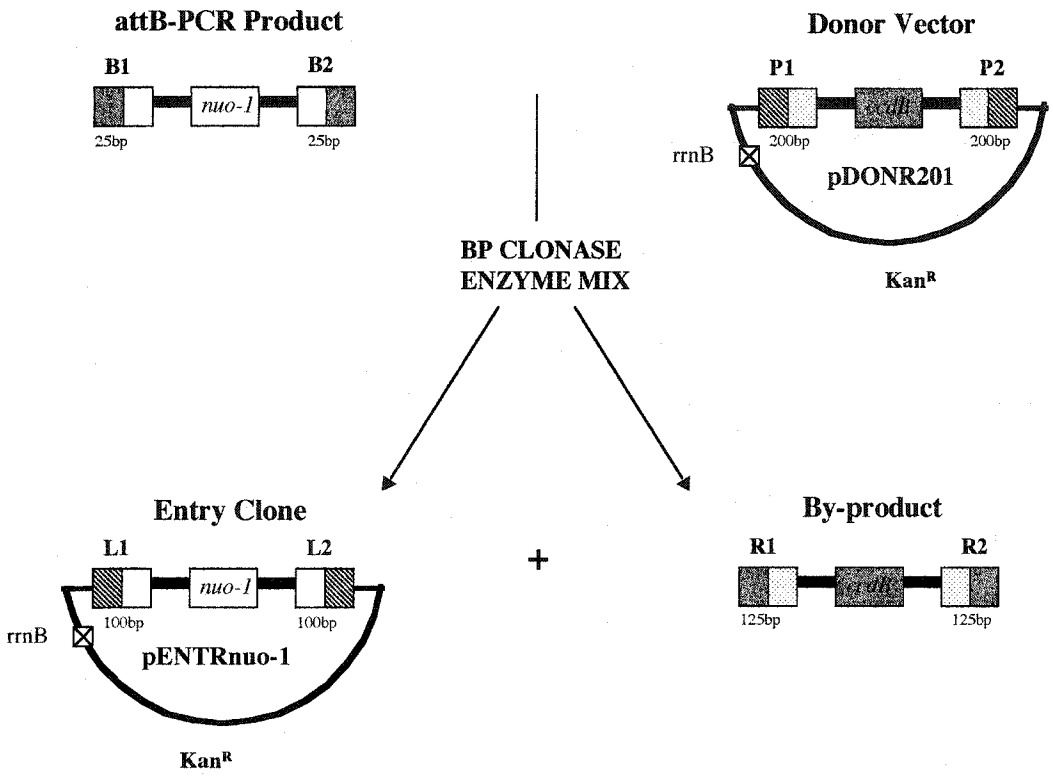

Figure II-1. Cloning the *nuo-1* PCR Product by the BP Reaction

The *nuo-1* gene containing a *Mun 1* deletion was amplified with primers containing terminal 25-bp attB sites. The PCR product was used as a substrate in the BP reaction. Recombination between the attB-PCR product and a Donor Vector results in an Entry Clone.

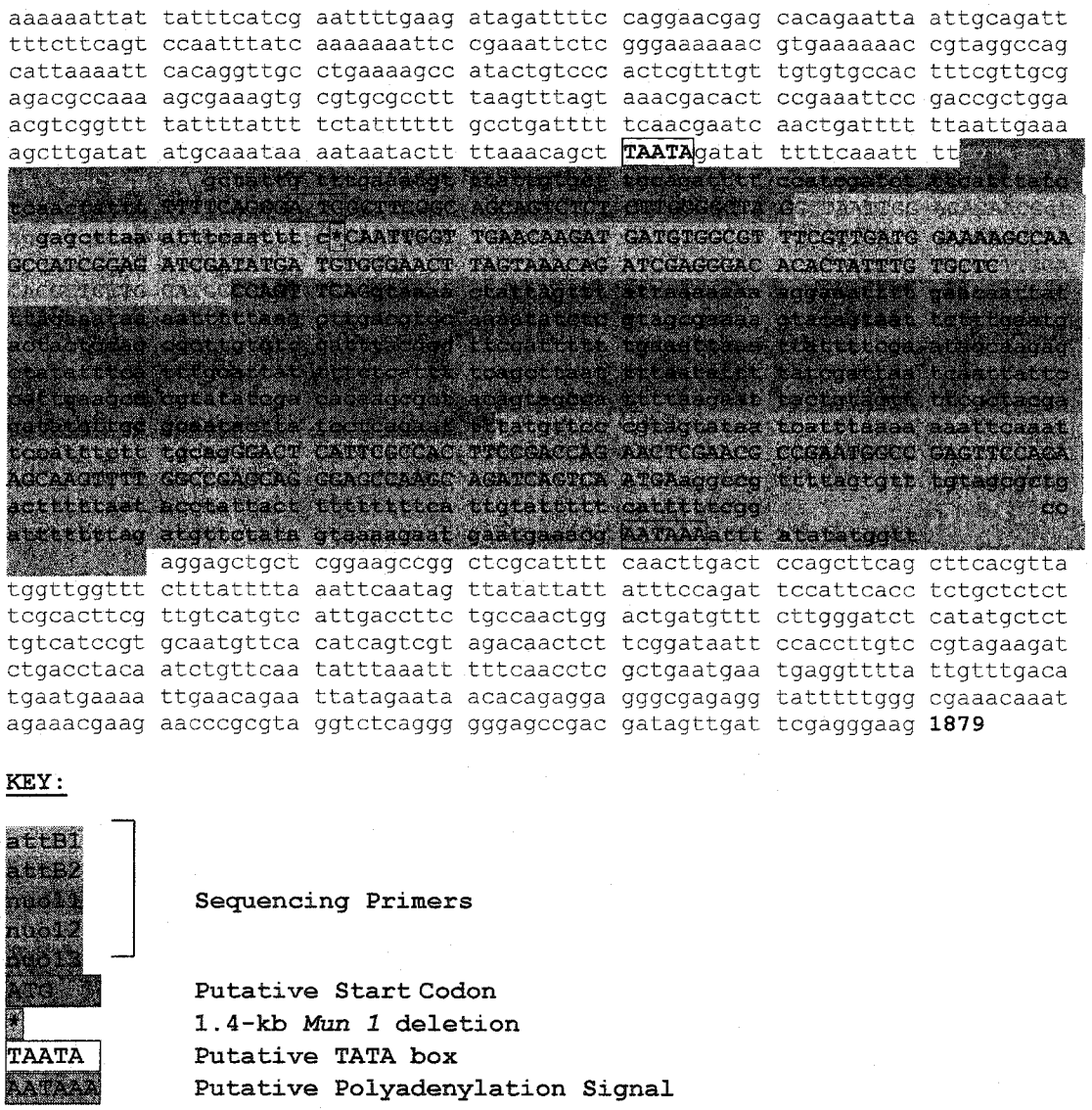

Figure II-2. Sequence of the *nuo-1* PCR Product

The cloned region begins upstream of the ATG start codon and extends to a putative polyadenylation signal. Coding regions are capitalized. The location of the 1.4-kb *Mun 1* deletion is indicated with an asterisk. Sequencing results obtained with various primers are color coded to indicate the region correctly sequenced.

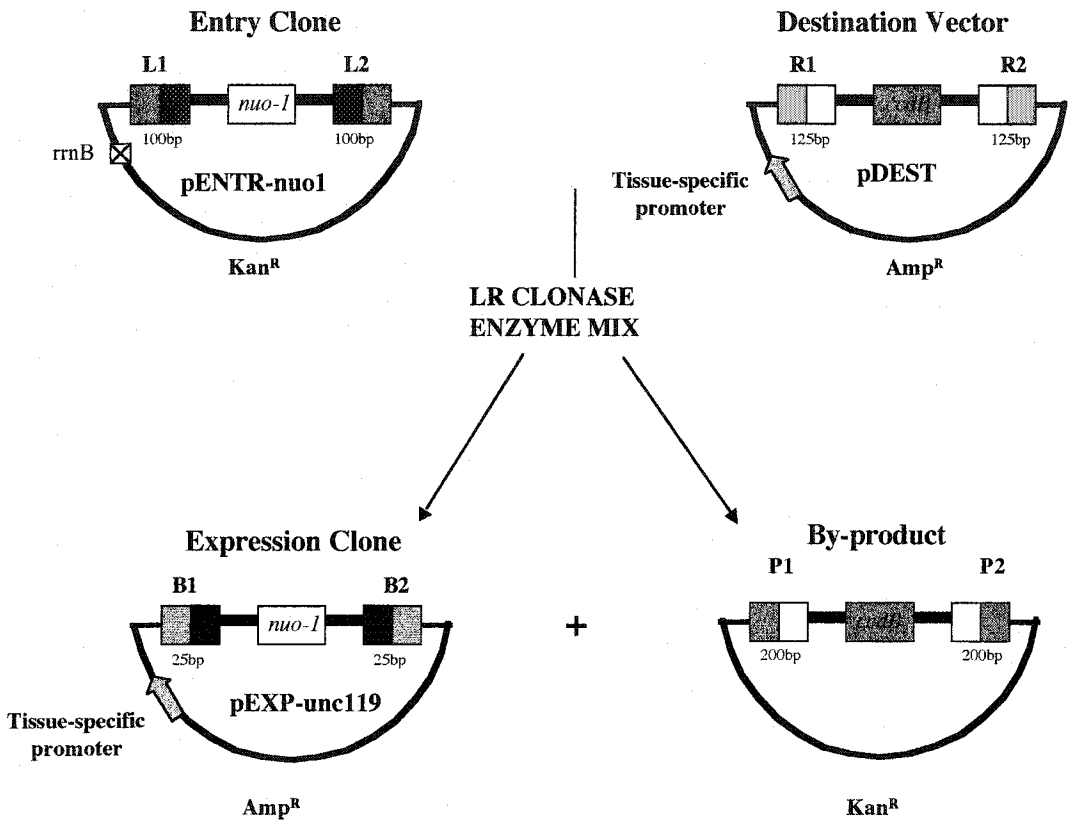

Figure II-3. Creation of an Expression Clone By the LR Reaction

Recombination between an Entry Clone carrying the *nuo-1* sequence, pENTRnuo-1 and a Destination Vector containing a tissue-specific promoter yields an Expression Clone. Each Expression Clone contains a tissue-specific promoter driving *nuo-1* expression.

Primer	Sequence (5'-3')	Purpose
attB1 (53 bp)	ggggacaagtttgtacaaaaaagcaggcttacgtagcattatt gactggaaag	PCR, Recombination, Sequencing
attB2 (50 bp)	ggggaccactttgtacaagaaagctgggtcagcaacacaact aggcaacc	PCR, Recombination, Sequencing
nuo11 (21 bp)	ctacCGTTCTGTCCAATTAGC	Sequencing
nuo12 (18 bp)	ctcgatttcgtctcctcc	Sequencing
nuo13 (20 bp)	TTGGAGACGCTGCTGCATGG	Sequencing

Table II-2. Sequences of Oligonucleotide Primers

The underlined nucleotides are necessary for BP reaction recombination. All other nucleotides are *nuo-1* specific. Coding regions are capitalized.

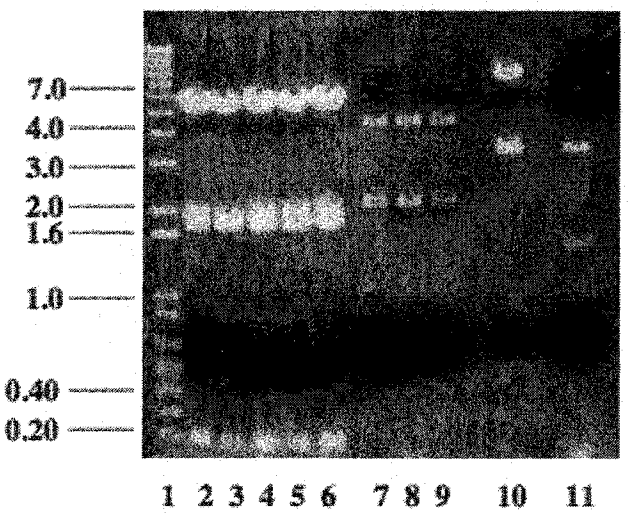

Figure II-4. Restriction Digest Analysis of the Expression and Entry Clones

Plasmid DNA of Expression Clones and pENTRnuo-1 were digested overnight at 37 °C with restriction enzymes. Aliquots of the digests were run on a 1% agarose gel along with a 1-kb DNA ladder (lane 1). pEXPunc-54 clones produced bands of the expected sizes of 0.2, 1.8, and 5.2 kb when digested with *Bgl II* (lanes 2-6). pEXPunc-119 clones produced bands of the expected sizes of 1.0, 2.0, and 4.0 kb when digested with *Hind III* (lanes 7-9). The pEXPlet-858 clone produced bands of the expected sizes of 0.4, 3.0, and 6.4 kb when digested with *Nsi I* (lane 10). The pENTRnuo-1 clone used in the LR reaction produced bands of the expected sizes of 1.3, 2.0, and 3.0 kb when digested with *Nsi I* (lane 11).

Strain	Genotype	Source
LB21B	*nuo-1(ua1)/mIn1* [*dpy-10(e128) mIs14*] II	Lab collection
LB22	*nuo-1(ua1)/mIn1* [*dpy-10(e128) mIs14*] II; *him-8(e1489)* IV	Lab collection
DP38	*unc-119(ed3)* III	CGC, University of Minnesota
LB77	*nuo-1(ua1)/mIn1* [*dpy-10(e128) mIs14*] II, *unc-119(ed3)* III	this study

Table II-3. Worm Strains Used In This Study

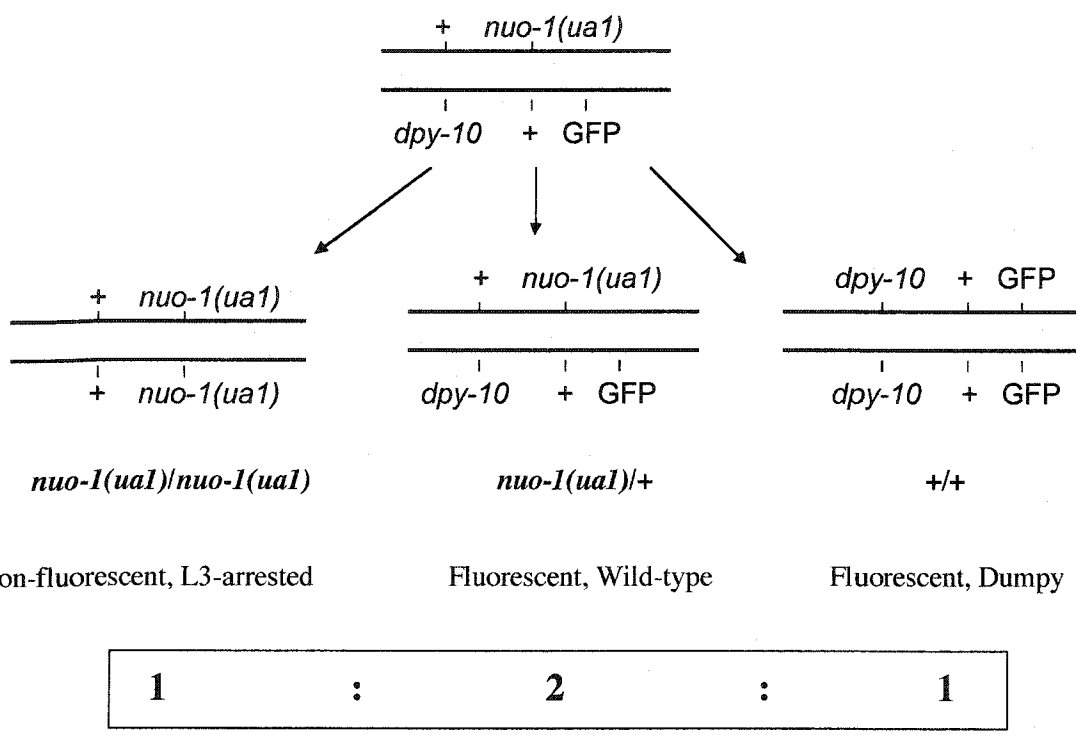

Figure II-5. The *mIn1* Balancer Chromosome

Schematic of the *mIn1* balancer on chromosome II. The balancer chromosome consists of the wild-type *nuo-1* allele (+), a recessive mutation of the *dpy-10* gene, and a pharyngeal green fluorescent protein marker (GFP). The exact location of the GFP locus has not been determined. The opposing chromosome contains the *nuo-1(ua1)* mutation and the wild-type *dpy-10* (+) gene. The arrows point to the progeny of a self-fertilized hermaphrodite. The box indicates the Mendelian ratios of the progeny genotypes.

Plasmid	Relevant Features	Source
pDP#MM016b	Contains a 5.7-kb *Hind III-Xba I* rescue fragment encoding the *unc-119* gene cloned into BS(SK-), Amp^R	Judith Austin, University of Chicago
pAZ119	Contains the 5.7-kb *unc-119* rescue fragment and a *myo-2* enhancer oligo fused to a *myo-2* minimal promoter driving GFP expression, Amp^R	Judith Austin, University of Chicago
pEXPunc-119	Contains the 1.2-kb nervous system-specific *unc-119* promoter upstream of the *nuo-1* coding region, Amp^R	this study
pEXPlet-858	Contains the 3.5-kb ubiquitous *let-858* promoter upstream of the *nuo-1* coding region, Amp^R	this study
pEXPmyo-2	Contains the 1.3-kb pharyngeal muscle-specific *myo-2* promoter upstream of the *nuo-1* coding region, Amp^R	this study
pEXPunc-54	Contains the 0.8-kb body wall muscle-specific *unc-54* promoter upstream of the *nuo-1* coding region, Amp^R	this study
pEXPpie-1	Contains the 5.7-kb *unc-119* rescue fragment and the 3.5-kb germline-specific *pie-1* promoter upstream of the *nuo-1* coding region, Amp^R	this study

Table II-4. Transforming Plasmids

Table I1-5. Sequences of Oligonucleotide Primers Used in Transmitting Lines

Primer Name	Sequence (5′ - 3′)	Purpose
NFP2	GTAAACGACACTCCGAAATTCC	Forward primer for genomic *nuo-1*; located upstream of the *nuo-1* gene.
NFP3	CTCATTCATTCAGCGAGGTTG	Reverse primer for genomic *nuo-1*; located downstream of the *nuo-1* gene.
NFP7	TCGATGAGCTTATGTGGGTCG	Reverse primer for genomic *nuo-1* and for all transgenic expression clones; located within the *ua1* deletion of the *nuo-1* coding region.
U1191	TAGACCGAGATAGGGTTGAGTG	Forward primer for transgenic pAZ119; located upstream of *unc-119* in vector specific sequence.
U1192	TGGGTAACTATAGGACTATAGG	Reverse primer for transgenic pAZ119; located within the promoter region of *unc-119*.
U1193	CTCGCTTCTCTTTTCCTAGACG	Forward primer for transgenic pEXPunc-119; located within the *unc-119* promoter region.
U1194	TTCCATTCGCCATTCAGGCTG	Forward primer for transgenic pDP#MM016b; located downstream of *unc-119* in vector specific sequence.
U1195	GTTATCAGTAGGAGAAGCCTCC	Reverse primer for transgenic pDP#MM016b; located within the non-coding region of *unc-119*.
U541	ACTCCCGATCTATCTCTATCCC	Forward primer for transgenic pEXPunc-54; located within the *unc-54* promoter region.
L8582	GAGGCGACAACGGTATTTTCG	Forward primer for transgenic pEXPlet-858; located within the *let-858* promoter region.
MYO21	GACCACATGGTCCTTCTTGAG	Forward primer for transgenic pEXPmyo-2; located within the *myo-2* promoter region.
PIE11	ATTCAGCACGGAGCACTTCTC	Forward primer for transgenic pEXPpie-1; located within the *pie-1* promoter region.

BIBLIOGRAPHY

Ardizzi, J.P., and H.F. Epstein. 1987. Immunochemical localization of myosin heavy chain isoforms and paramyosin in developmentally and structurally diverse muscle cell types of *C. elegans*. *J. Cell Biol.* **105:**2763-2770.

Bio-Rad Laboratories Instruction Manual. 2001. Biolistic® PDS-1000/He Particle Delivery System. Molecular Bioscience Group, Hercules, California.

Broverman, S.A., and P.M. Meneely. 1994. Meiotic mutants that cause a polar decrease in recombination on the X chromosome in *Caenorhabditis elegans*. *Genetics* **136:**119-127.

Cassada, R.C., and R.L. Russell. 1975. The dauer larva, a post-embryonic developmental variant of the nematode *C. elegans*. *Dev. Biol.* **46:**326-342.

Edgley, M.L., and D.L. Riddle. 2001. LG II balancer chromosome in *Caenorhabditis elegans*: mT1 (II;III) and the mIn1 set of dominantly and recessively marked inversions. *Mol. Genet. Genom.* **266:**385-395.

Gaudet, J., and S.E. Mango. 2002. Regulation of organogenesis by the *Caenorhabditis elegans* FoxA protein PHA-4. *Science* **295:**821-825.

Gibco BRL: Instruction Manual. 1999. Gateway Cloning Technology (for Early Access Program). Life Technologies. www.lifetech.com/gateway

Hanahan, D., J. Jesse, and F.R. Bloom. 1991. Plasmid transformation of *Escherichia coli* and other bacteria. *Methods Enzymol.* **204:**63-113.

Hodgkin, J. 1999. Conventional genetics, pp.245-270 in *C. elegans* A Practical Approach, edited by I.A. Hope. Oxford University Press Inc., NY.

Innis, M.A. 1990. Selective Alcohol Precipitation PCR Protocols, p.482 in PCR Protocols: A guide to Methods and Applications, edited by M.A. Innis, D.H. Gelfand, J.J. Sninsky, and T.J. White. Academic Press, San Diego.

Jantsch-Plunger, V., and A. Fire. 1994. Combinatorial structure of a body muscle-specific transcriptional enhancer in *Caenorhabditis elegans*. *J. Biol. Chem.* **269:**27021-27028.

Kelly, W.G., S.Q. Xu, M.K. Montgomery, and A. Fire. 1997. Distinct requirements for somatic and germline expression of a generally expressed *Caenorhabditis elegans* gene. *Genetics* **146:**227-238.

Knobel, K.M., W.S. Davis, E.M. Jorgensen, and M.J. Bastiani. 2001. UNC-119 suppresses axon branching in *C. elegans*. *Development* **128:**4079-4092.

Landy, A. 1989. Dynamic, structural, and regulatory aspects of lambda site specific recombination. *Annu. Rev. Biochem.* **58**:913-949.

Lewis, J.A., and J.T. Fleming. 1995. Basic culture methods. *Methods Cell Biol.* **48:**3-29.

Levy, A.D., J.Yang, and J.M. Kramer. 1993. Molecular and genetic analyses of the *Caenorhabditis elegans dpy-2* and *dpy-10* collagen genes: A variety of molecular alterations affect organismal morphology. *Mol. Biol. Cell* **4:**803-817.

MacLeod, A.R., R.H. Waterston, and S. Brenner. 1977. An internal deletion mutant of a myosin heavy chain in *C. elegans*. *Proc. Natl. Acad. Sci. USA* **74:**5336-5340.

Maduro, M., and D. Pilgrim. 1995. Identification and Cloning of *unc-119*, a Gene Expressed in the *Caenorhabditis elegans* Nervous System. *Genetics* **141:**977-988.

Maduro, M.F., M. Gordon, R. Jacobs, and D.B. Pilgrim. 2000. The UNC-119 family of neural proteins is functionally conserved between Humans, *Drosophila* and *C. elegans*. *J. Neurogenet.* **13:**191-212.

Mello, C., and A. Fire. 1995. DNA transformation. *Methods Cell Biol.* **48:**451-482.

Mello, C.C., C.M. Schubert, B.W. Draper, W. Zhang, R. Lobel, and J.R. Priess. 1996. The PIE-1 protein and germline specification in *C. elegans* embryos. *Nature* **382:**710-712.

Morelle, G. 1989. Never-Fail Miniprep. *Focus: BRL Newsletter* **11**:7-8.

Praitis, V., E. Casey, D. Collar, and J. Austin. 2001. Creation of Low-Copy Integrated Transgenic Lines in *Caenorhabditis elegans*. *Genetics* **157:**1217-1226.

Ptashne, M. 1992. A Genetic Switch: phage (lambda) and higher organisms, 2nd ed. Cell Press: Blackwell Scientific Publications, Cambridge, Massachusetts.

Reese, K.J., M.A. Dunn, J.A. Waddle, and G.C. Seydoux. 2000. Asymmetric segregation of PIE-1 in *C. elegans* is mediated by two complementary mechanisms that act through separate PIE-1 protein domains. *Mol. Cell* **6:**445-455.

Sambrook, J., E.F. Fritsch, and T. Maniatis (ed.). 1989. Molecular Cloning: a laboratory manual, 2nd ed. CSH Laboratory Press, Cold Spring Harbor, New York.

Sanger, F., S. Nicklen, and A.R. Coulson. 1977. DNA sequencing with chain terminating inhibitors. *Proc. Natl. Acad. Sci. USA* **74:**5463-5467.

Stinchcomb, D.T., J.E. Shaw, S.H. Carr, and D. Hirsch. 1985. Extrachromosomal DNA transformation of *Caenorhabditis elegans*. *Mol. Cell. Biol.* **5**:3484-3496.

Tenenhaus, C., K. Subramaniam, M.A. Dunn, G. Seydoux. 2001. PIE-1 is a bifunctional protein that regulates maternal and zygotic gene expression in the embryonic germ line of *Caenorhabditis elegans*. *Genes Dev.* **15:**1031-1040.

Tsang, W.Y., L.C. Sayles, L.I. Grad, D.B. Pilgrim, and B.D. Lemire. 2001. Mitochondrial Respiratory Chain Deficiency in *Caenorhabditis elegans* Results in Developmental Arrest and Increased Life Span. *J. Biol. Chem.* **276:**32240-32246.

Wilm, T., P. Demel, H.-U. Koop, H. Schnabel, and R. Schnabel. 1999. Ballistic transformation of *Caenorhabditis elegans*. *Gene* **229:**31-35.

Zhang, F., M. Barboric, T.K. Blackwell, and B.M. Peterlin. 2003. A model of repression: CTD analogs and PIE-1 inhibit transcriptional elongation by P-TEFb. *Genes Dev.* **17:**748-758.

III. Results

III-1. Introduction

We sought to characterize the transmitting lines expressing *nuo-1* under the control of tissue-specific promoters with a series of genotypic, phenotypic, and functional assays. We wished to evaluate whether L3 larval arrest in *nuo-1(ua1)* mutants could be complemented by expressing wild-type *nuo-1* only in a subset of tissues. Previous work has suggested that the L3-to-L4 transition may involve an energy-sensing developmental checkpoint (Tsang *et al.*, 2001). Homozygous *nuo-1(ua1)* mutants arrest at the third larval stage with a second larval stage sized gonad (Tsang *et al.*, 2001). We hypothesized that germ-line proliferation and organogenesis, which are associated with sexual maturation during L4, are energy intensive processes and that the transition from L3 to L4 is associated with increased energy requirements. In addition, the severe effect of the *nuo-1(ua1)* mutation on gonad development supports the notion that a substantial energy requirement is necessary for gonadogenesis, even at early stages of development. In this chapter, I describe various features of the transmitting lines that link nervous system and muscle tissue with energy metabolism and development in *C. elegans*.

III-2. Characterization of Transmitting Lines

Table III-1 lists the transmitting lines that were obtained from several bombardments. The following sections describe the genotypic characterization of each strain to determine the presence of transgenic DNA and its inheritance pattern.

III-2. a) Polymerase Chain Reaction

Figure III-1 illustrates the multiplex PCR system that was used to confirm the genotype of LB77, the strain used in all bombardments. The NFP2 and NFP3 primers anneal outside the cloned *nuo-1* sequence in each expression clone. This makes it possible to detect genomic *nuo-1* exclusively. The NFP7 primer anneals within the *ua1* deletion, permitting discrimination between mutant and wild-type *nuo-1* alleles. Along with the observed phenotype of self-progeny (100% Unc self-progeny with pharyngeal fluorescence), the PCR results indicate that the strain was heterozygous for the *nuo-1(ua1)* deletion and properly balanced.

Following bombardment, PCR was used to confirm the presence of transforming plasmids in each transmitting line. Figures III-2 and III-3 illustrate PCR analysis to show the presence of the pDP#MM016b and pAZ119 plasmids, respectively in the *uaEx22* and *uaEx16* control strains. Figures III-4 to III-6 illustrate PCR analysis to confirm the presence of expression plasmids in the *uaEx17*, *uaEx13*, *uaEx14*, *uaIs2*, *uaEx15*, *uaEx19*, and *uaEx20* transmitting lines. PCR analysis was also used to confirm the presence of transforming plasmids in the LB77 *uaEx18*, LB77 *uaEx21*, and LB80 *uaIs3* lines (Table III-1) (results not shown). Unless otherwise stated, negative controls for each primer set were performed by PCR on strains that did not contain the transforming plasmid (results not shown).

III-2. b) Inheritance Patterns of Transmitting Lines

Following verification of transformation by PCR analysis, each transmitting line was cultured as previously described on NGM plates (Lewis and Fleming, 1995). To

elucidate the inheritance pattern, single hermaphrodite L4 worms from the transmitting line were placed on 12 separate NGM plates, allowed to self-fertilize, and the entire broods analyzed. Figure III-7 presents the phenotypic predictions used in brood analysis.

Of our independently derived transmitting lines, two produced 100% non-Unc progeny on each of the 12 plates. The absence of Unc animals over several generations indicated that both the *uaIs2* and *uaIs3* strains contained homozygous integrations of transgenic DNA. Several of our transmitting lines produced three types of progeny: wild-type, Unc, and sterile worms. Two possibilities can explain this segregation pattern. First, the transformed lines may contain extrachromosomal arrays, which are occasionally lost. Second, the lines may contain chromosomal insertions of the transforming DNA and worms homozygous for the insertion are unable to reproduce. On each of the 12 plates, we always recovered Unc progeny in non-Mendelian ratios. Non-fluorescent, Unc, L3-arrested worms indicated the loss of the complementing array. These results confirmed an extrachromosomal inheritance pattern for LB77 *uaEx13* to *uaEx22* (Table III-1). It is speculated that co-bombarding multiple plasmids increases the probability of extrachromosomal inheritance of transgenic DNA over integration into the genome. This may explain the inheritance pattern of our transmitting lines 2 of which contained homozygous integrations of transgenic DNA, and 10 carried extrachromosomal arrays of transgenic DNA.

III-2. c) Genetic Characterization of LB77 uaEx17

To ensure that the LB77 *uaEx17* was properly balanced, we needed to confirm that the *nuo-1(ua1)* allele exhibited Mendelian patterns of inheritance. The progeny from

a single self-fertilized worm were scored according to phenotype as presented in Table III-2. Worms fluorescing in the pharyngeal region carry the balancer chromosome and were separated from non-fluorescent worms and the two groups scored according to sinusoidal movement. The results indicated a ratio of Dpy:WT:non-fluorescent worms of approximately 1:2:1 confirming Mendelian genetics for the balancer. Wild-type worms produce approximately 330 ± 30 progeny at 20 °C (Hodgkin, 1999). The complete brood size of this transmitting line (excluding dead embryos) of 282 was considered to be normal. By calculating the proportion of non-Unc worms in the complete brood, the transmission was determined to be approximately 84%. Some non-Unc, non-fluorescent worms, homozygous for the *nuo-1(ua1)* allele were observed to bypass L3 arrest, indicating partial complementation by the extrachromosomal array. Further developmental and functional assays were performed to analyze the degree of complementation.

III-2. d) Genetic Characterization of LB77 uaEx15

To characterize the LB77 *uaEx15* line, the progeny from five worms were picked at the L4 stage onto separate plates and scored according to phenotype as presented in Table III-3. The complete brood size of the transmitting line was considered to be variable and below normal in some cases. By calculating the proportion of non-Unc worms in the complete brood, the transmission was determined to vary from ~ 20%-50%. Some non-Unc, weakly-fluorescent worms, homozygous for the *nuo-1(ua1)* allele were observed to bypass L3 arrest and become L4 larvae, indicating partial complementation by the extrachromosomal array. Similar results were obtained for the *uaEx18* and

uaEx21 lines (results not shown). Further developmental and functional assays were performed to analyze the degree of complementation.

III-3. Developmental Analysis

To observe the developmental characteristics of the homozygous *nuo-1(ua1)* worms in each transmitting line, non-Unc, non- or weakly-fluorescent animals were grown on NGM plates for 7 days at 20 °C. To examine morphology and developmental stage, worms were mounted on 2% agarose pads on glass slides, immobilized with sodium azide, and observed under a Zeiss Axioskop-2 research microscope with a SPOT-2 digital camera (Carl Zeiss Canada Ltd., Calgary, Canada).

III-3. a) Negative Control Transmitting Lines

As expected, homozygous *nuo-1(ua1)* worms from the negative control strains LB77 *uaEx16*, LB77 *uaEx22*, and LB80 *uaIs3* never progressed past the L3 stage, even after a 7-day incubation. Figure III-8 illustrates that the gonad morphology of control animals with the *uaEx22* array resembled *nuo-1(ua1)* homozygous progeny of LB21B worms. None of these animals displayed signs of vulval development. These results indicate that neither the pDP#MM016b or the pAZ119 plasmids contribute to the complementation of the L3-arrest phenotype.

III-3. b) Muscle and Germ-line specific Transmitting Lines

Some homozgyous *nuo-1(ua1)* worms carrying the pharyngeal muscle-specific *uaEx15*, *uaEx18*, and *uaEx21* arrays progressed to the L4 larval stage. A triangular-

shaped developing vulva and reflexed gonadal arms characteristic of the early L4 larval stage were observed in some animals. The percentage of homozygous *nuo-1(ua1)* animals that bypassed the L3 stage varied with the strain and ranged from approximately 10%-30%. None of the homozygous *nuo-1(ua1)* worms carrying the body-wall muscle-specific array, *uaEx19* or the germ-line specific array *uaEx20* array progressed past the L3 stage. Neither of these lines displayed any signs of vulval development. Because strains carrying the *uaEx19* and *uaEx20* arrays did not display any signs of complementation, we chose not to conduct any further genetic characterization. Figure III-9 illustrates the gonad and vulval development of animals carrying the *uaEx21* array that progressed to the L4 stage and L3-arrested animals carrying the *uaEx21* or *uaEx19* arrays. All worms appeared to have normal muscle structure and displayed no distinct morphological abnormalities. These results suggest that the *myo-2::nuo-1* construct is able to partially complement the complete loss of *nuo-1*. However, the *unc-54::nuo-1* or *pie-1::nuo-1* constructs do not complement this loss.

III-3. c) Nervous system specific Transmitting Lines

Homozygous *nuo-1(ua1)* worms carrying the *uaEx17* array progressed much slower than wild-type worms but by 4-7 days, over 90% of the worms had progressed to the L4 or adult stages. The gonad arms had extended considerably along the ventral surface and reflexed in some worms. Figure III-10 illustrates the gonad and vulval development of L4 and adult worms carrying the *uaEx17* array. All worms appeared to have normal muscle structure and displayed no distinct morphological abnormalities. The triangular-shaped developing vulva characteristic of the L4 larval stage was observed in

some worms while other worms displayed a fully mature protruding vulva characteristic of the adult stage. However, none of the worms that reached adulthood contained any developing oocytes or fertilized eggs in their gonads. Therefore, our results show that most homozygous *nuo-1(ua1)* mutant worms carrying the *uaEx17* array develop an L4-sized gonad and an L4- or adult-stage vulva, but are sterile. These results indicate that the *unc-119::nuo-1* construct is able to partially complement the complete loss of *nuo-1*.

III-3. d) Ubiquitously expressing Transmitting Lines

All homozygous *nuo-1(ua1)* worms from the ubiquitously expressing strains LB77 *uaEx13*, and LB77 *uaEx14* progressed to adulthood but never developed any oocytes or fertilized eggs in their gonads. The LB79 *uaIs2* strain appeared to have a problem that interfered with GFP expression. This made it difficult to isolate homozygous *nuo-1(ua1)* worms, and we chose to exclude this strain from further analysis. Figure III-10 illustrates the vulval morphology of adult worms carrying the *uaEx13* array. All worms appeared to have normal muscle structure and displayed no distinct morphological abnormalities. The heterozygous *nuo-1*/+ progeny of an LB21B worm is shown as an example of a gravid adult. Therefore, our results show that homozygous *nuo-1(ua1)* mutant worms carrying the *uaEx13* and *uaEx14* arrays progress to adulthood, but are sterile. These results indicate that the *let-858::nuo-1* construct is able to partially complement the complete loss of *nuo-1*.

III-3. e) PCR analysis

Once the developmental stage had been elucidated using Nomarski optics, we needed to confirm the genotype of partially complemented worms by PCR using the NFP2, NFP3, and NFP7 primers. The results presented in Figure III-11 of individual L4 and adult worms from the *uaEx13* and *uaEx17* transmitting lines confirmed that these animals were homozygous for the *nuo-1(ua1)* allele. Partially complemented L4 or early adult worms carrying the *uaEx14*, *uaEx15*, *uaEx18*, and *uaEx21* arrays produced similar results (data not shown).

III-4. Functional Assays

We reasoned that due to the normally high rates of respiration in muscle and nerve cells, an impaired mitochondrial respiratory chain might lead to mobility or sensory defects. To test neurological and muscle function, we performed swimming and pumping assays on worms of the same chronological age. Two congenic strains, LB77 *uaEx17*, and the control LB77 *uaEx22* strain were compared in each assay. Plates containing synchronized eggs were incubated at 20 °C and analyzed at various stages of development using stereomicroscopy (Leica MZ FLIII, Leica Microsystems AG, Heerbrugg, Switzerland). To test sensory function, we observed the ability of dauers in each transmitting line to exit the dauer stage and progress to adulthood.

III-4. a) Swimming Assays

Swimming assays are used to assess locomotory function. To perform swimming assays, worms were placed in a drop of M9 buffer and the numbers of sinusoidal waves per minute were counted. As presented in Figure III-12, worms carrying the *uaEx17* array swam faster than control worms carrying the *uaEx22* array. However, the effect of the *uaEx17* array tapered off at 5 days. The swimming rate decreased as chronological age increased. The difference in swimming rates between *uaEx17* and *uaEx22* array carrying *nuo-1(ua1)*/+ L3 worms, and *nuo-1(ua1)/nuo-1(ua1)* L3 worms at 1 day are statistically significant.

III-4. b) Pharyngeal Pumping Assays

Pharyngeal pumping was scored by observing the number of contractions of the terminal bulb of the pharynx on seeded plates. Each worm was scored for 1 min. In worms carrying the *uaEx17* array, pharyngeal pumping rates were similar to that of LB21B worms (Tsang *et al.*, 2001) suggesting that they were able to support development with proper feeding ability. The pharyngeal pumping rates of *uaEx22* carrying animals were decreased and irregular. In concordance with the swimming assay, pharyngeal pumping rates were higher in *uaEx17* array carrying worms than in worms carrying the *uaEx22* array (Figure III-13). Again, the effect of the *uaEx17* array tapered off at 5 days. However, only the difference between *uaEx17* and *uaEx22* array carrying *nuo-1(ua1)*/+ L3 worms is statistically significant.

III-4. c) Exit from the Dauer Stage

Worms homozygous for the *nuo-1(ua1)* mutation are competent to enter dauer, but cannot exit from it (Tsang *et al.*, 2001). The ability of *nuo-1(ua1)* mutants to enter dauer establishes that these worms are physically and developmentally at the L3 larval stage (Tsang *et al.*, 2001). To assess whether worms from each transmitting line would exit the dauer stage, the progeny from single heterozygous *nuo-1(ua1)*/+ worms were grown on NGM plates and left for 7 d to starve. When the *E. coli* supply had been depleted, sodium dodecyl sulfate (SDS) was added to a final concentration of 1% in M9 and gently stirred for 30 min at room temperature. Dauer larvae are resistant to treatment with 1% SDS (Tissenbaum *et al.*, 2000). SDS-resistant dauers were picked onto fresh seeded plates. Non- or weakly-fluorescent homozygous *nuo-1(ua1)* dauers were placed on separate plates and incubated at 15 °C to allow for recovery from dauer.

All homozygous *nuo-1(ua1)* mutant dauers from each transmitting line were morphologically similar to heterozygote *nuo-1(ua1)*/+ dauers. Similar to homozygous *nuo-1(ua1)* mutants, the control strains LB77 *uaEx16*, *uaEx22*, and LB80 *uaIs3* did not exit the dauer stage even after 5d at 15 °C on seeded plates. Transmitting lines carrying the *uaEx15*, *uaEx18*, *uaEx19*, *uaEx20* and *uaEx21* arrays also did not exit the dauer stage. However, over two-thirds of worms carrying the *uaEx17* array recovered from dauer and progressed to the late L4-early adult stage within 4-7d after SDS treatment. As expected, all worms carrying the *uaEx13*, and *uaEx14* arrays also exited dauer and progressed to adulthood within 3-5 days after SDS-treatment.

Table III-1. Transmitting Lines Obtained by Bombardment

Expected Expression	Strain Name	Inheritance Pattern	Complementation of L3 Arrest
Ubiquitous	LB77 uaEx13 [unc-119(+); pExplet-858(let-858::nuo-1)]	Extrachromosomal	**Partial** Sterile Adult Exits Dauer
Ubiquitous	LB77 uaEx14 [unc-119(+); pExplet-858(let-858::nuo-1)]	Extrachromosomal	**Partial** Sterile Adult Exits Dauer
Pharyngeal Muscle	LB77 uaEx15 [unc-119(+); pExpmyo-2(myo-2::nuo-1)]	Extrachromosomal	**Partial** L4-arrested Does not exit Dauer
None	LB77 uaEx16 [unc-119(+)]	Extrachromosomal	**N.O.** L3-arrested Does not exit Dauer
Nervous System	LB77 uaEx17 [unc-119(+); pExpunc-119(unc-119::nuo-1)]	Extrachromosomal	**Partial** L4 or Sterile Adult Exits Dauer
Pharyngeal Muscle	LB77 uaEx18 [unc-119(+); pExpmyo-2(myo-2::nuo-1)]	Extrachromosomal	**Partial** L4-arrested Does not exit Dauer
Body-wall Muscle	LB77 uaEx19 [unc-119(+); pExpunc-54(unc-54::nuo-1)]	Extrachromosomal	**N.O.** L3-arrested Does not exit Dauer
Germ-line	LB77 uaEx20 [pExppie-1(unc-119 (+); pie-1::nuo-1)]	Extrachromosomal	**N.O.** L3-arrested Does not exit Dauer
Pharyngeal Muscle	LB77 uaEx21 [unc-119(+); pExpmyo-2(myo-2::nuo-1)]	Extrachromosomal	**Partial** L4-arrested Does not exit Dauer
None	LB77 uaEx22 [unc-119(+)]	Extrachromosomal	**N.O.** L3-arrested Does not exit Dauer
Ubiquitous	LB79 uaIs2 [unc-119(+);pEXPlet-858(let-858::nuo-1)]	Homozygous Integrated	**N.O.** GFP interference Strain not used
None	LB80 uaIs3 [unc-119(+)]	Homozygous Integrated	**N.O.** L3-arrested Does not exit Dauer

N.O. = not observed

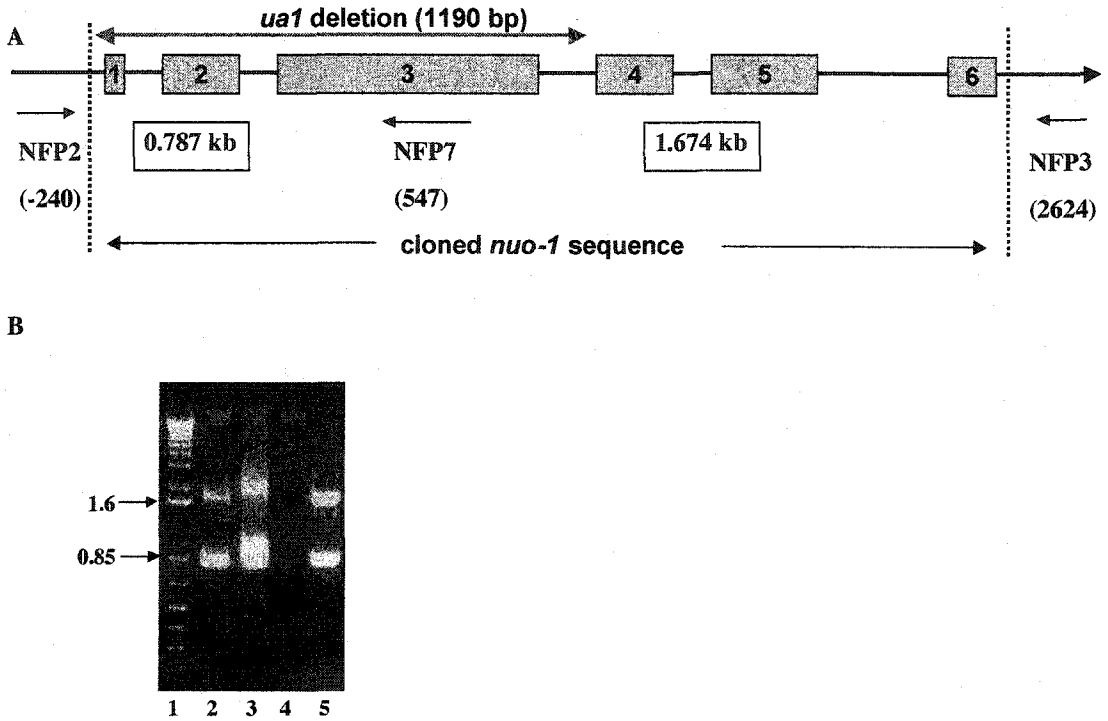

Figure III-1. Confirmation of the LB77 Genotype

A, Schematic of a region of chromosome II showing the six exons of the *nuo-1* gene and the *ua1* deletion. Primer positions are indicated in parentheses and directions are indicated with arrows. The ATG codon for the *nuo-1* gene is regarded as +1. When PCR is performed with the NFP2, NFP3, and NFP7 primers, worms homozygous for the *ua1* mutation will produce a 1.7-kb band. Homozygous wild-type worms will produce a 0.8-kb band. The longer 2.8-kb product produced by the NFP2 and NFP3 primers is not seen under the conditions used. Heterozygous strains will produce both 0.8 and 1.7-kb bands. **B**, PCR using multi-worm lysates of the LB77 strain was performed using the NFP2, NFP3, and NFP7 primers. An aliquot of the PCR reaction was run on a 1% agarose gel along with a 1-kb DNA ladder (lane 1). The expected sizes of 0.8 and 1.7 kb were produced indicating that LB77 is heterozygous (*nuo-1(ua1)*/+) (lanes 2 and 3). Reaction buffer alone is shown as a negative control (lane 4). The PCR products from LB22 are shown as a positive control (lane 5).

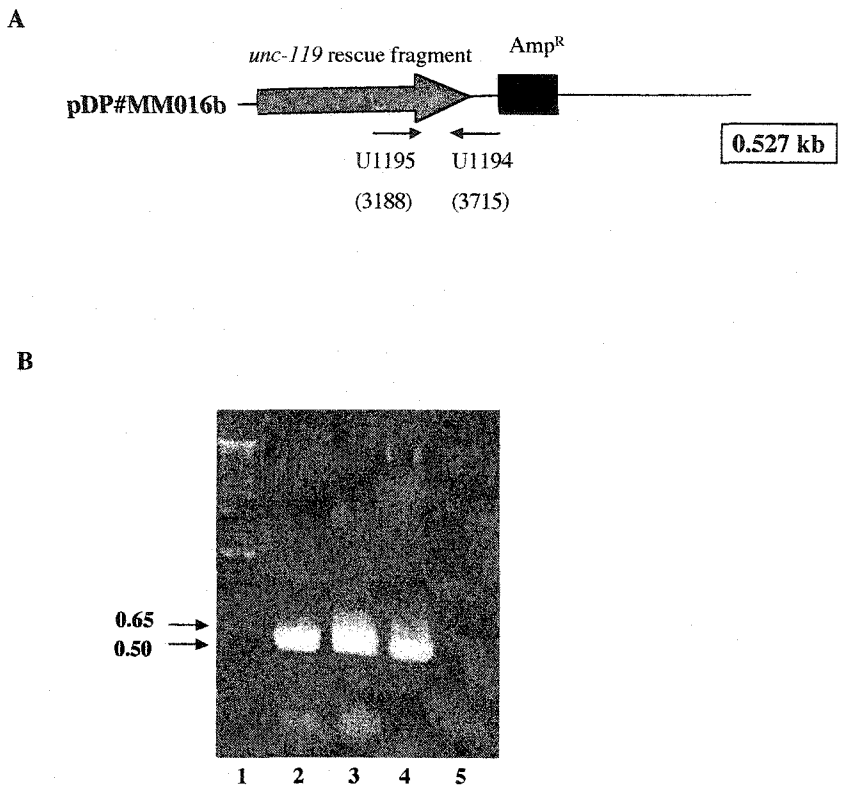

Figure III-2. Confirmation of the presence of pDP#MMO16b

A,Schematic of pDP#MMO16b plasmid sequence. Primer positions are indicated in parentheses and directions are indicated with arrows. The expected PCR product size is indicated in the box. The ATG start codon for the *unc-119* gene on pDP#MM016b is regarded as +1.

B, PCR using a multi-worm lysate of the transmitting line LB77 *uaEx22* was performed using the U1194 and U1195 primers. An aliquot of the PCR reaction was run on a 1% agarose gel along with a 1-kb DNA ladder (lane 1). The PCR product using template DNA from the transmitting line LB77 *uaEx17* was the expected size of 0.5 kb (lanes 2 and 3). The PCR product of the pDP#MM016b plasmid is shown as a positive control (lane 4). Reaction buffer alone is shown as a negative control (lane 5).

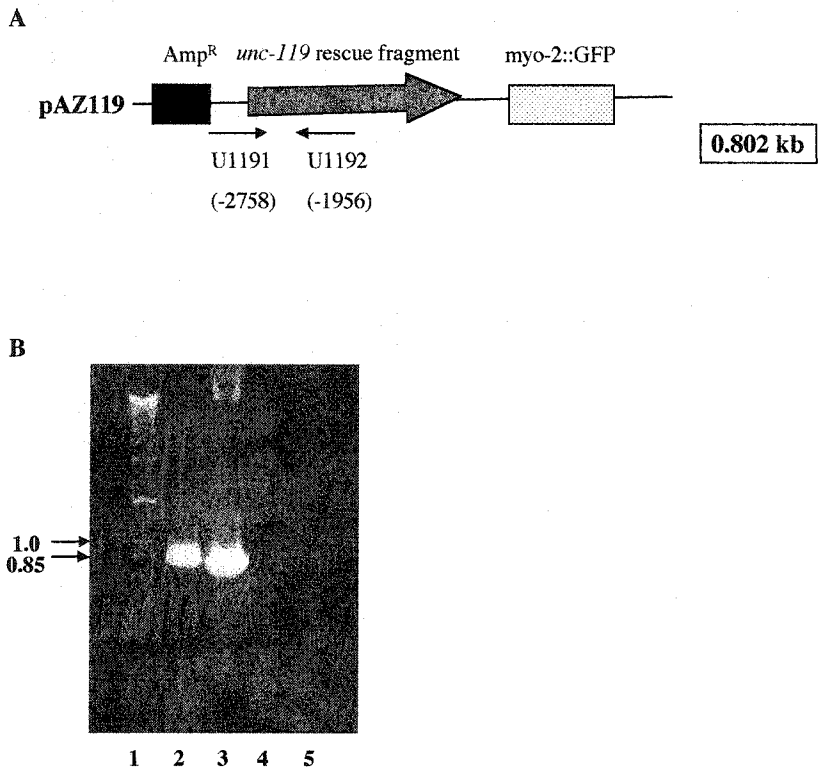

Figure III-3. Confirmation of the presence of pAZ119

A, Schematic of pAZ119 plasmid sequence. Primer positions are indicated in parentheses and directions are indicated with arrows. The expected PCR product size is indicated in the box. The ATG start codon for the *unc-119* gene on pAZ119 is regarded as +1. **B**, PCR using a multi-worm lysate of the transmitting line LB77 *uaEx16* was performed using the U1191 and U1192 primers. An aliquot of the PCR reaction was run on a 1% agarose gel along with a 1-kb DNA ladder (lane 1). The PCR product using template DNA from the transmitting line LB77 *uaEx16* was the expected size of 0.8 kb (lane 2). The PCR product of the pAZ119 plasmid is shown as a positive control (lane 3). PCR reactions using reaction buffer alone (lane 4) and template DNA from the LB77 *uaEx13* transmitting line (lane 5) are shown as a negative controls.

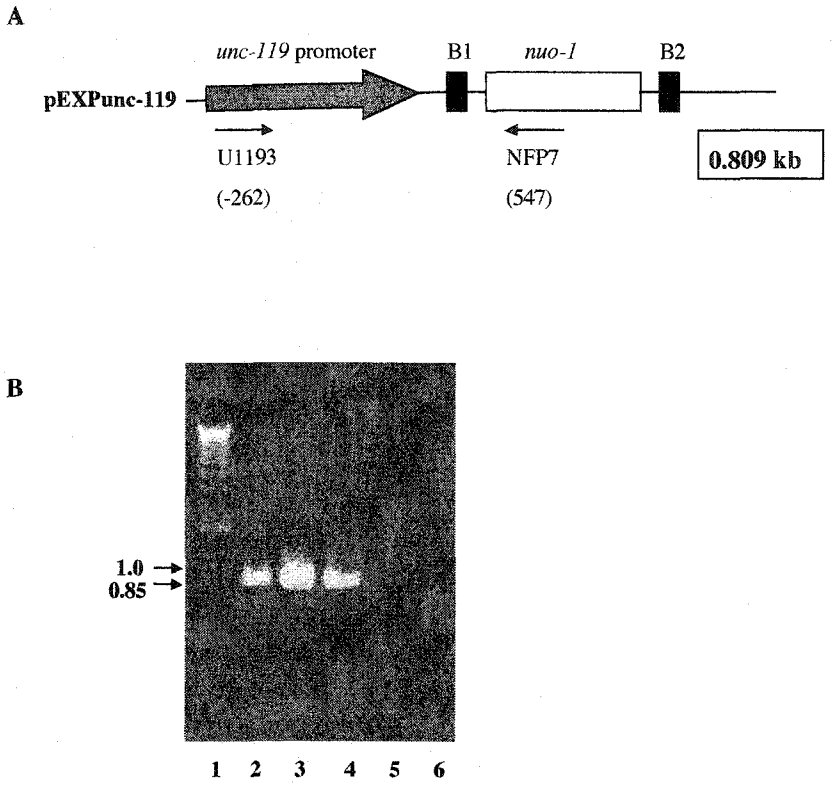

Figure III-4. Confirmation of the presence of pEXPunc-119

A, Schematic of pEXPunc-119 plasmid sequence. Primer positions are indicated in parentheses and directions are indicated with arrows. The expected PCR product size is indicated in the box. The ATG start codon for the *nuo-1* gene on pEXPunc-119 is regarded as +1.

B, PCR using a multi-worm lysate of the transmitting line LB77 *uaEx17* was performed using the U1193 and NFP7 primers. An aliquot of the PCR reaction was run on a 1% agarose gel along with a 1-kb DNA ladder (lane 1). The PCR product using template DNA from the transmitting line LB77 *uaEx17* was the expected size of 0.8 kb (lanes 2 and 3). The PCR product of the pEXPunc-119 plasmid is shown as a positive control (lane 4). PCR reactions using reaction buffer alone (lane 5) and template DNA from the LB77 *uaEx13* transmitting line (lane 6) are shown as a negative controls.

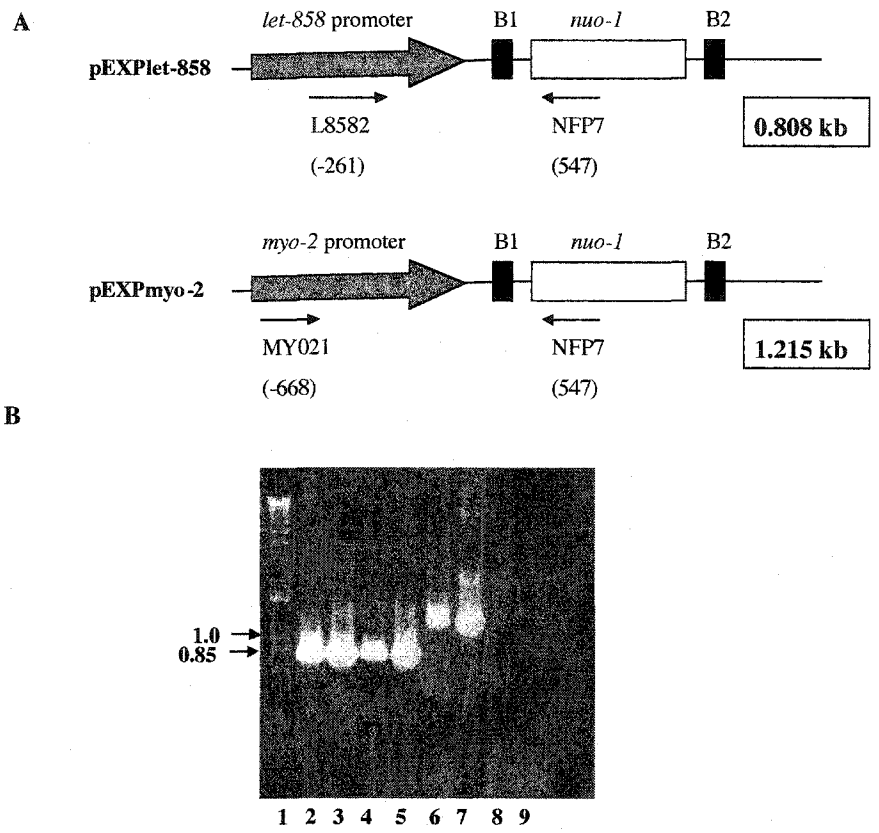

Figure III-5. Confirmation of the presence of pEXPlet-858 and pEXPmyo-2 in Transmitting Lines

A, Schematics of pEXPlet-858 and pEXPmyo-2 plasmid sequences. Primer positions are indicated in parentheses and directions are indicated with arrows. The expected PCR product sizes are indicated in the boxes. The ATG start codon for the *nuo-1* gene on each plasmid is regarded as +1. **B**, PCR using multi-worm lysates from the transmitting lines LB77 *uaEx13*, *uaEx14*, and LB79 *uaIs2* were performed using the L8582 and NFP7 primers. PCR using a multi-worm lysate from the transmitting line LB77 *uaEx15* was performed using the MY021 and NFP7 primers. An aliquot of the PCR reaction was run on a 1% agarose gel along with a 1-kb DNA ladder (lane 1). The PCR products using template DNA from the transmitting lines LB79 *uaIs2*, LB77 *uaEx13*, LB77 *uaEx14* respectively were the expected size of 0.8 kb (lanes 2 to 4). The product of the pEXPlet-858 plasmid is shown as a positive control (lane 5). The PCR product using template DNA from the transmitting line LB77 *uaEx15* was the expected size of 1.2 kb (lane 6). The product of the pEXPmyo-2 plasmid is shown as a positive control (lane 7). PCR reactions using reaction buffer alone with the L8582 and NFP7 primers (lane 8), or the MYO21 and NFP7 primers (lane 9) are shown as a negative controls.

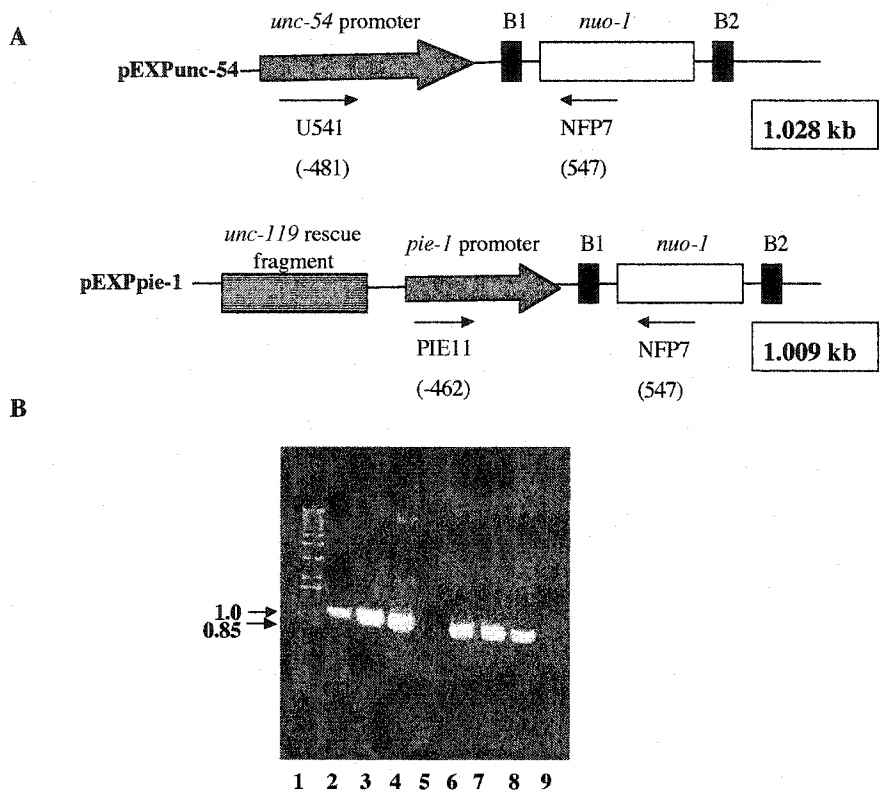

Figure III-6. Confirmation of the presence of pEXPunc-54 and pEXPpie-1 in Transmitting Lines

A, Schematics of pEXPunc-54 and pEXPpie-1 plasmid sequences. Primer positions are indicated in parentheses and directions are indicated with arrows. The expected PCR product sizes are indicated in the boxes. The ATG start codon for the *nuo-1* gene on each plasmid is regarded as +1. **B**, PCR using multi-worm lysates from the transmitting line LB77 *uaEx19* was performed in duplicate using the U541 and NFP7 primers. PCR using multi-worm lysates from the transmitting line LB77 *uaEx20* was performed in duplicate using the PIE11 and NFP7 primers. An aliquot of the PCR reaction was run on a 1% agarose gel along with a 1 kb DNA ladder (lane 1). The PCR product using template DNA from the transmitting line LB77 *uaEx19* was the expected size of 1.0 kb (lanes 2 to 3). The product of the pEXPunc-54 plasmid is shown as a positive control (lane 4). PCR using reaction buffer alone with the U541 and NFP7 primers is shown as a negative control (lane 5). The PCR product using template DNA from the transmitting line LB77 *uaEx20* was the expected size of 1.0-kb (lanes 6 to 7). The product of the pEXPpie-1 plasmid is shown as a positive control (lane 8). PCR using reaction buffer alone with the PIE11 and NFP7 primers is shown as a negative control (lane 9).

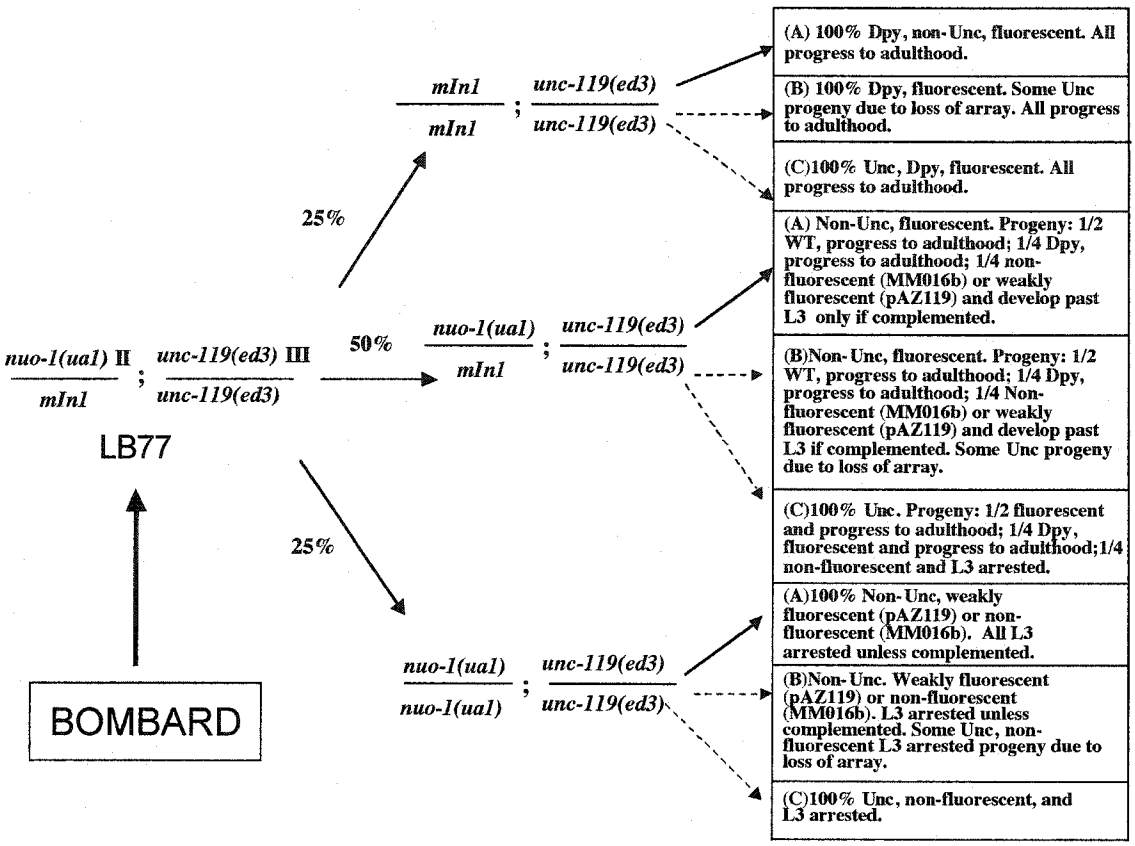

Figure III-7. Phenotypic Analysis of Transmitting Lines

Following bombardment, NGM plates containing LB77 worms were left to starve for 7-14 days at 20 °C and screened for transformants. When transformed worms are picked onto separate plates, progeny were scored for motility, fluorescence, and viability. Homozygous *nuo-1(ua1)* animals that bypassed the L3-larval arrest were considered to be complemented to varying extents by the transgenic DNA. Predicted inheritance patterns in terms of motility and fluorescence in (A), homozygous integrated strains; (B), extrachromosomal strains with the array; (C), extrachromosomal strains once the array has been lost are described for each genotype. The predictions for all extrachromosomal strains assume that both transforming plasmids are present in a single array so that if the array is lost, both the *nuo-1* and the reporter genes are lost.

Genotype	*nuo-1(+)/nuo-1(+)*		*nuo-1(ua1) / +*		*nuo-1(ua1) / nuo-1(ua1)*	
	WT (adult)	Unc (adult)	WT (adult)	Unc (adult)	WT (L4/ Adult)	Unc (L3-arrested)
	45	19	132	16	60*	10
Totals	**64**		**148**		**70**	

Table III-2. Brood Analysis of the LB77 *uaEx17* Line

The self-progeny of a single hermaphrodite worm placed on a plate and incubated at 20 °C were examined. Worms were separated into non-fluorescent and fluorescent based on pharyngeal fluorescence originating from the *mIn1* balancer chromosome. Fluorescent worms were further divided into Dpy [*nuo-1(+)/nuo-1(+)*] and wild-type [*nuo-1(ua1)/+* or *nuo-1(ua1)/nuo-1(ua1)*] categories. All worms were examined for motility and classified as either WT (array present) or Unc (loss of array). Non-fluorescent worms with WT movement (marked with an asterisk) progressed past the L3 larval stage and were further analyzed in swimming, pumping, and dauer-exit assays.

Total Unc	Total Non-Unc	*nuo-1(ua1) / nuo-1(ua1)* Non-Unc (L4)*	Brood Size	Transmittance (%)
90	80	9	170	47
173	52	10	225	23
116	62	11	178	35
38	9	2	47	19
85	29	3	114	25

Table III-3. Brood Analysis of the LB77 *uaEx15* Line

The total self-progeny of single hermaphrodite worms from the LB77 *uaEx15* transmitting line were placed on 5 separate plates and incubated at 20 °C and examined. Worms were separated into weakly fluorescent and strongly fluorescent based on pharyngeal fluorescence originating from transgenic pAZ119 plasmid DNA or the *mIn1* balancer chromosome, respectively. All worms were examined for motility and classified as either non-Unc (array present) or Unc (loss of array). All Unc and/or brightly fluorescent worms were picked off plates before or at the L4 stage. All weakly fluorescent animals were picked onto separate plates and allowed to mature at 20°C for 4-7 days. The transmittance for each population is calculated as the percentage of non-Unc worms in the complete brood. Some weakly fluorescent non-Unc worms (column marked with asterisk) progressed past the L3 larval stage and were further analyzed by PCR and dauer-exit assays.

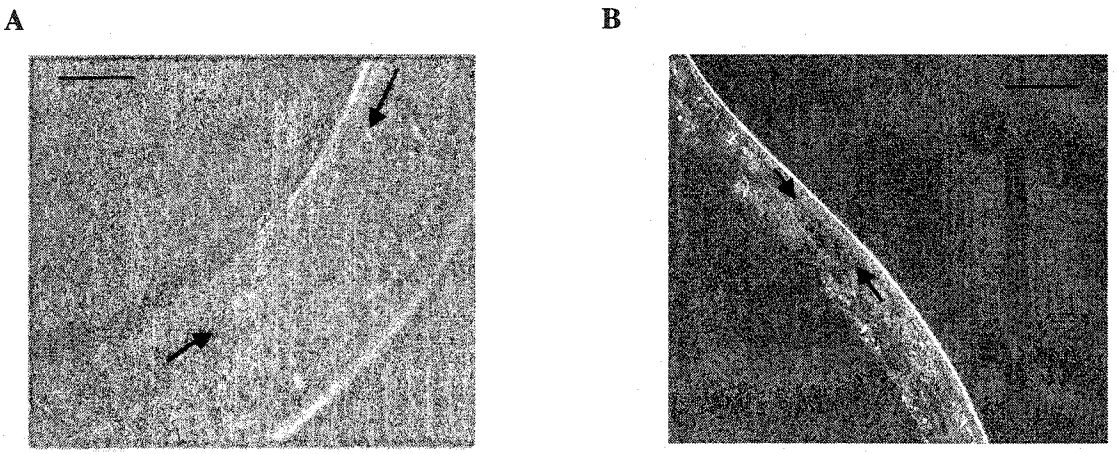

Figure III-8. Nomarski photographs showing gonad development in LB21B and LB77 *uaEx22* strains grown for 7d at 20 °C

Homozygous *nuo-1(ua1)* progeny from **A**, LB21B strain; **B**, LB77 *uaEx22* strain. Both worms are L3 arrested with L2-sized gonads. Arrows indicate the positions of the distal tip cells. Scale bars = 1.5 μm in A and 3 μm in B.

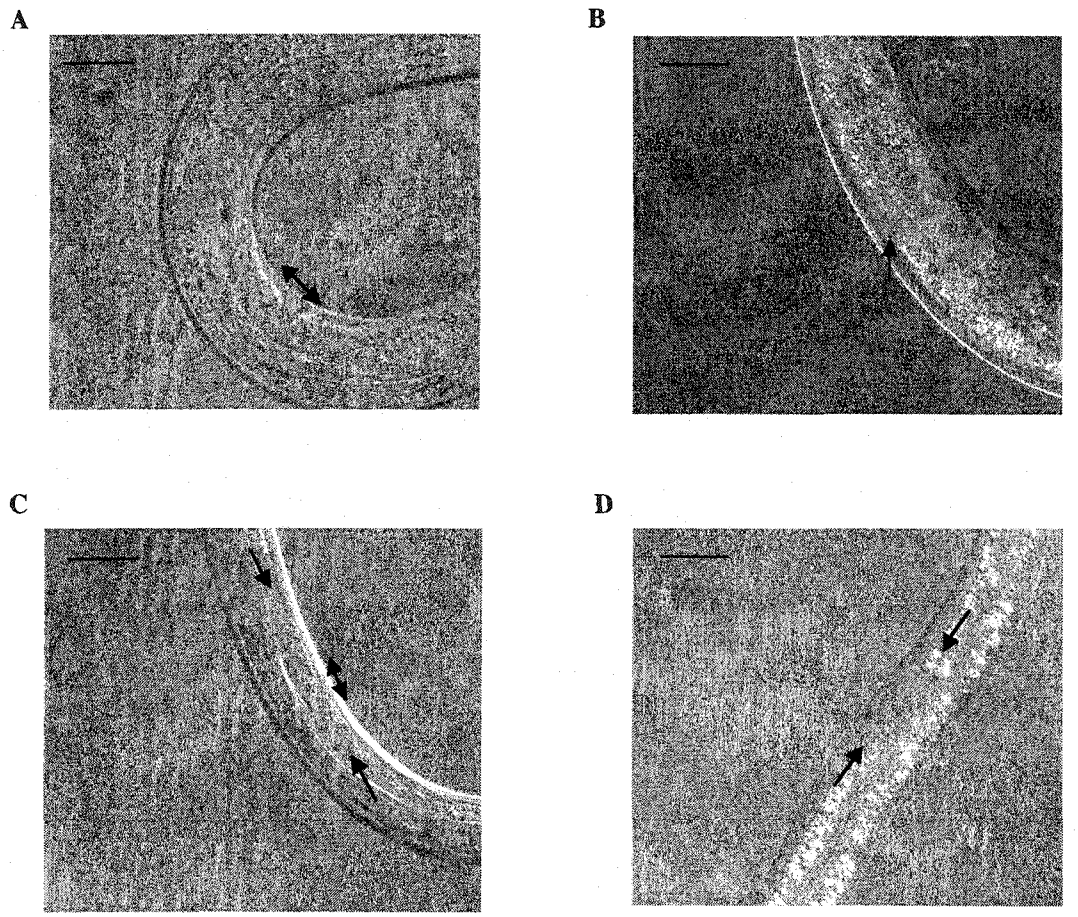

Figure III-9. Nomarski photographs showing gonad and vulval development in LB77 *uaEx21* and LB77 *uaEx19* strains grown for 7d at 20 °C

Homozygous *nuo-1(ua1)* progeny from LB77 *uaEx21* strain **A**, L4 worm showing triangular shaped vulval invagination; **B**, L4 worm showing reflexed gonad; **C**, L3-arrested worm showing L2-sized gonad and the first signs of vulval development. Homozygous mutant *nuo-1(ua1)* progeny from LB77 *uaEx19* **D**, L3-arrested worm showing L2-sized gonad. Arrows indicate the positions of the distal tip cells. Double arrows indicate the position of the vulva. Scale bars = 3 μm.

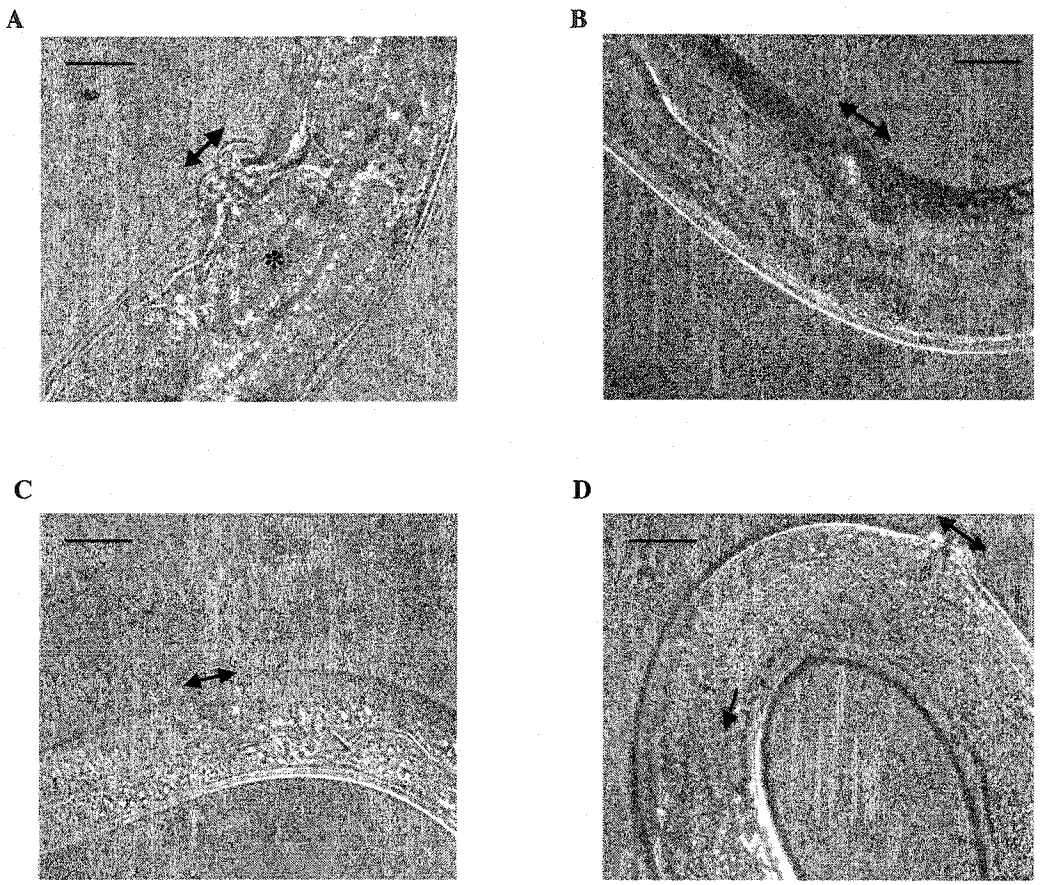

Figure III-10. Nomarski photographs showing gonad and vulval development in LB21B, LB77 *uaEx13*, and LB77 *uaEx17* strains grown for 7d at 20 °C

A, Gravid heterozygous *nuo-1(ual)*/+ worm from the LB21B strain showing adult vulva and developing embryos within gonad. Homozygous *nuo-1(ua1)* progeny from LB77 *uaEx13* strain **B**, sterile adult showing adult vulva. Homozygous mutant *nuo-1(ua1)* progeny from LB77 *uaEx17* strain **C**, L4 worm showing triangular shaped vulval invagination; **D**, sterile adult showing adult sized vulva and reflexed gonadal arm. Arrows indicate the positions of the distal tip cells. Double arrows indicate the position of the vulva. Asterisk indicates position of developing embryo. Scale bars = 3 μm.

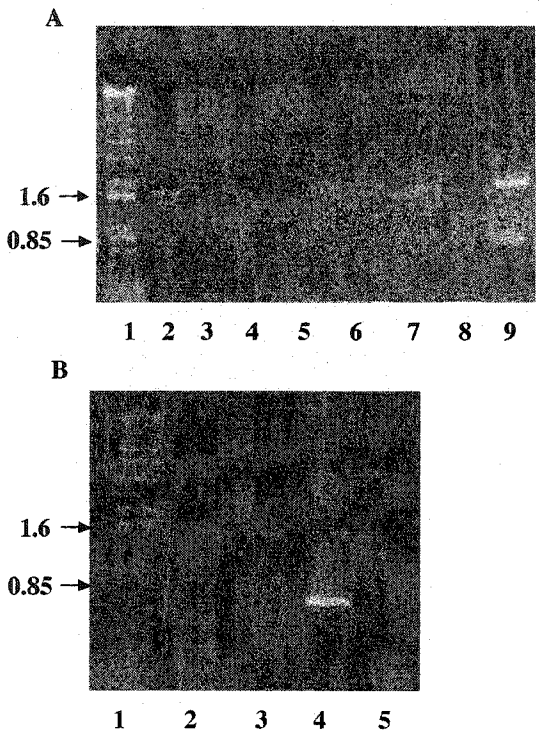

Figure III-11. Confirmation of the *nuo-1(ua1)/nuo-1(ua1)* genotype in LB77 *uaEx17* and LB77 *uaEx13* Transmitting Lines grown for 7d at 20 °C

Single worm lysates of L4-early adult worms from the LB77 *uaEx17* and LB77 *uaEx13* strains were used for PCR with the NFP2, NFP3, and NFP7 primers. An aliquot of the PCR reaction was run on a 1% agarose gel along with a 1-kb DNA ladder (lane1). **A**, Lanes 2 to 6 show the PCR products of 5 individual LB77 *uaEx17* sterile adult worms and lane 7 shows the PCR product for an individual LB77 *uaEx17* L4 worm. PCR using reaction buffer alone is shown as negative control in lane 8. Lane 9 shows the PCR products obtained using template DNA from a LB22 multiworm lysate as a control. **B**, Lanes 2 to 3 show the PCR products of 2 individual LB77 *uaEx13* adult worms. Lane 4 shows the PCR product obtained using template DNA from a LB22 multiworm lysate as a control. PCR using reaction buffer alone is shown as negative control in lane 5. A band at 1.7 kb corresponds to the *nuo-1(ua1)* allele, while a band at 0.85 kb corresponds to the *nuo-1(+)* allele.

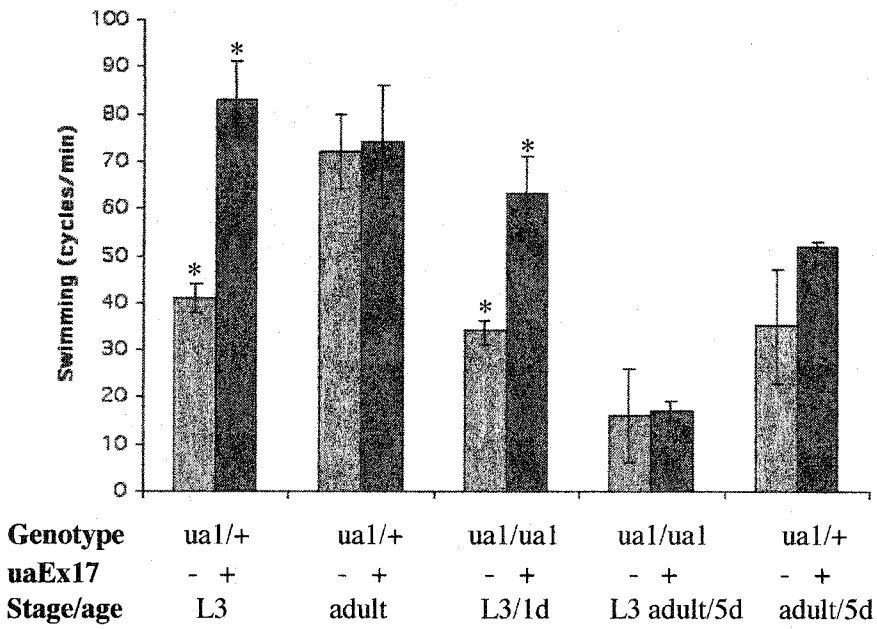

Figure III-12. Swimming assay comparing LB77 *uaEx17* and LB77 *uaEx22* strains of the same chronological age grown at 20 °C

Bar graphs compare heterozygous *nuo-1(ua1)*/+ and homozygous *nuo-1(ua1)*/ *nuo-1(ua1)* mutant worms at different stages of development. Values are means ± S.D. Asterisk indicates statistical significance based on a two-tailed Student's t test (p value < 0.001).

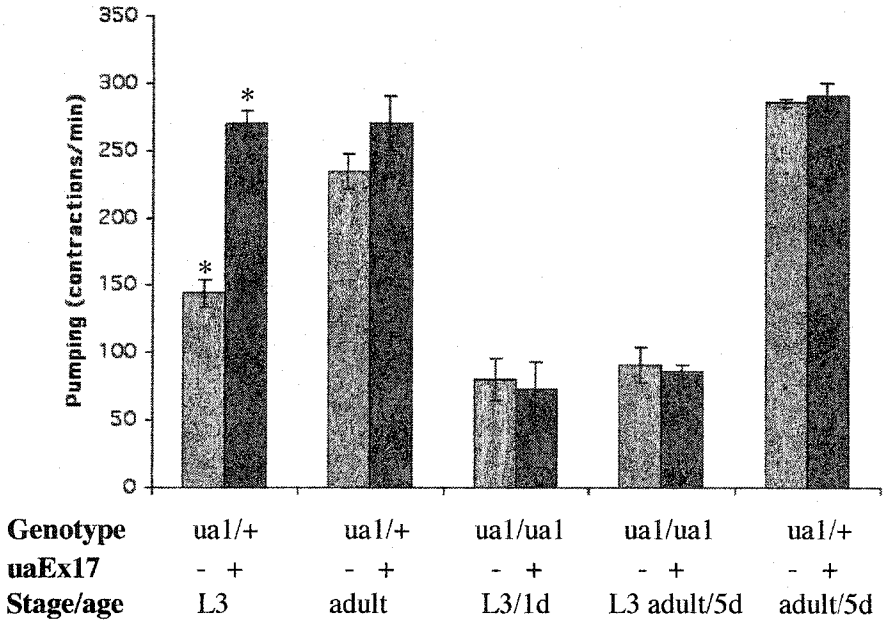

Figure III-13. Pharyngeal pumping assay comparing LB77 *uaEx17* and LB77 *uaEx22* strains of the same chronological age grown at 20 °C

Bar graphs compare heterozygous *nuo-1(ua1)*/+ and homozygous *nuo-1(ua1)/nuo-1(ua1)* mutant worms at different stages of development. Values are means ± S.D. Asterisk indicates statistical significance based on a two-tailed Student's t test (p value < 0.001).

BIBLIOGRAPHY:

Hodgkin, J. 1999. Conventional genetics, pp.245-270 in *C. elegans* A Practical Approach, edited by I.A. Hope. Oxford University Press Inc., NY.

Lewis, J.A., and J.T. Fleming. 1995. Basic culture methods. *Methods Cell Biol.* **48:**3-29.

Tissenbaum, H.A., J. Hawdon, M. Perregaux, P. Hotez, L. Guarente, and G. Ruvkun. 2000. A common muscarinic pathway for diapause recovery in the distantly related nematode species *Caenorhabditis elegans* and *Ancylostoma caninum. Proc. Natl. Acad. Sci. U.S.A.* **97:**460-465.

Tsang, W.Y., L.C. Sayles, L.I. Grad, D.B. Pilgrim, and B.D. Lemire. 2001. Mitochondrial Respiratory Chain Deficiency in *Caenorhabditis elegans* Results in Developmental Arrest and Increased Life Span. *J. Biol. Chem.* **276:**32240-32246.

IV. Discussion

IV-1. Discussion

The work presented in this thesis describes the effect of tissue-specific expression of the complex I nuclear-encoded gene, *nuo-1* (NADH-ubiquinone oxidoreductase) in homozygous *nuo-1(ua1)* mutants. The *nuo-1(ua1)* mutation is homozygous lethal and results in a characteristic L3 larval arrest. Homozygous *nuo-1(ua1)* animals exhibit impaired pharyngeal pumping and mobility and fail to exit the dauer pathway (Tsang *et al.*, 2001) We expressed the *nuo-1(+)* gene under the control of several tissue specific promoters and monitored the developmental and behavioral effects in several assays. We assessed gonad development, vulval development, mobility, pharyngeal pumping, and exit from the dauer stage. A transgenic strain containing the endogenous promoter driving *nuo-1(+)* expression has been previously generated by microinjection. Homozygous *nuo-1(ua1)* mutants worms carrying this transgene become fertile adults and have the ability to exit the dauer pathway. This strain was used as a positive control with which to compare results of the chimeric genes.

As judged by these assays, expression of *nuo-1(+)* under the control of the nervous system specific promoter, *unc-119*, was effective at partially complementing larval arrest and the sensory and neurological defects associated with *nuo-1(ua1)* mutants. The majority of worms expressing *nuo-1(+)* under the control of the *unc-119* promoter developed to the L4 or early adult stage, but were invariably sterile with L4-sized gonads. The majority of the worms displayed adult sized vulvas. Worms expressing *nuo-1(+)* in the nervous system were able to exit the dauer pathway suggesting that sensory function had been restored. Swimming and pumping assays

indicated enhanced muscular and neurological function at the L3 stage when compared with the *nuo-1(-)* control. Interestingly, a significant difference between the nervous system specific expression of *nuo-1(+)* and *nuo-1(-)* worms was observed in heterozygous *nuo-1(ua1)*/+ L3 worms in both swimming and pharyngeal pumping assays. The presence of the transgene improved the swimming and pumping rates, but the effect tapered off as animals developed to adulthood. Interestingly, the swimming rate in the absence of the array for *nuo-1(ua1)*/+ animals was almost the same as that for *nuo-1(ua1)/nuo-1(ua1)* animals, 41 ± 3 and 34 ± 3 respectively. There are at least two explanations for this result. The first explanation is that the haploid contribution from the wild-type allele is inadequate to elicit a normal phenotype (Cook *et al.*, 1998), suggesting haploinsufficiency in the *nuo-1(ua1)*/+ animals. The theory that the *ua1* allele is not completely recessive has not been previously reported for *nuo-1*. Previous work using wild-type N2 worms reported a swimming rate of 116 ± 7 at the L3 stage (Tsang *et al.*, 2001). These results suggest that the improvement of swimming rate at the L3 stage in the presence of *uaEx17* array of 83 ± 8 and 63 ± 8 for *nuo-1(ua1)*/+ and *nuo-1(ua1)/nuo-1(ua1)* animals respectively is not an artifact. The second explanation is that the *nuo-1* gene could normally be expressed in limited quantities at the L3 stage based solely on maternal inheritance. If transgenic DNA allows the protein expression of *nuo-1* to significantly increase at the L3 stage, this may explain a relatively improved swimming rate.

The pharyngeal muscle specific *myo-2* promoter was not as effective as *unc-119* in complementing developmental arrest. Worms only developed to the L4 stage and failed to exit the dauer pathway. The body-wall muscle specific *unc-54* promoter and the

germ-line specific *pie-1* promoter were both ineffective in complementing larval arrest. Similar to *nuo-1(-)* controls, worms expressing *nuo-1(+)* in body-wall muscle or in the germ-line remained arrested at the L3 stage and failed to exit the dauer stage. All worms exhibited L2-sized gonads and showed no signs of vulval development.

The *let-858* promoter for general *nuo-1(+)* expression only partially complemented the *nuo-1(ua1)* developmental arrest. All worms progressed to adulthood but displayed L4-sized gonads and were sterile. General *nuo-1(+)* expression also allowed worms to exit the dauer pathway faster than what was observed with *unc-119* promoter-driven nervous system specific *nuo-1(+)* expression. Therefore, we never observed complete complementation in any of our strains, even with ubiquitous *nuo-1(+)* expression.

Several theories may help explain these results. First, the nervous system may be the tissue that contributes all or a major component of the developmental signal that allows worms to proceed to adulthood. Complementary or additional signals or functions originating from other tissues such as muscle, hypodermis, intestine, and/or germ-line may also be required for the generation of fertile adults. Second, the degree of complementation may be affected by the strength of the promoter. Non-optimal levels of NUO-1 in the nervous system may prevent or interfere with one or more essential steps in development. Alternatively, expression of *nuo-1(+)* from a transgenic array may reduce the tissue specificity of expression of the *unc-119* promoter. Third, extrachromosomal inheritance may provoke gene silencing in certain tissues, a phenomenon that has been observed in other studies (Mello and Fire, 1995). Fourth, partial complementation may be the result of differences in developmental signals and/or regulatory mechanisms

between somatic and germ-line tissue. Finally, an energy sensor hypothesis may dictate that optimal development in the worm may only be achieved when sensors respond to multiple indicators of mitochondrial condition. Each of these theories will be examined in the following paragraphs.

Several behavioral and functional characteristics of homozygous *nuo-1(ua1)* worms are strongly indicative of the importance of the nervous system in the developmental signaling that allows worms to progress to adulthood. In the absence of food, wild-type L1 worms stop developing and stay in an arrested state until returned to plates containing a food supply. Similarly, *nuo-1(ua1)* L3-arrested animals appear to be impaired at feeding and are often located off the food supply. This is consistent with an impaired nervous system since it is the amphid neurons that sense the presence of food. Homozygous *nuo-1(ua1)* animals also exhibit impaired pharyngeal pumping, mobility, and defecation and do not exit the dauer stage (Tsang *et al.*, 2001). These observations are consistent with neurological defects associated with MRC dysfunction. A similar study to identify the tissues important in developmental signaling and energy metabolism looked at an insulin-like signaling pathway. Mutations in the *daf-2* insulin receptor-like gene or the downstream *age-1* phosphoinositide 3-kinase gene dramatically extend life-span (Kimura *et al.*, 1997; Kenyon *et al.*, 1993). Using the pan neuronal *unc-14* and *unc-119* promoters, *age(+)* or *daf-2(+)* expression in neurons was sufficient to restore wild-type life-span in both *age-1* and *daf-2* mutants (Wolkow *et al.*, 2000). However, results with promoters specific for muscle (*unc-54*), intestine (*ges-1*), and a small subset of neurons (*mec-7*) indicated muscle, intestine or the neural subset expression of *daf-2(+)* or *age(+)* were not sufficient to rescue the long life-span phenotype of *daf-2* or *age-1*

mutants (Wolkow *et al.*, 2000). The authors concluded that the nervous system plays a significant role in the insulin-like signaling pathway regulation of life-span (Wolkow *et al.*, 2000). They speculated that the loss of DAF-2 activity in neurons elicited diminished production of ROS by increasing expression levels of free radical scavenging enzymes under the transcriptional control of DAF-16, a downstream target in the *daf-2* signaling pathway (Wolkow *et al.*, 2000). Furthermore, the notion that neurons may be more sensitive to free radical damage during development is highlighted by the fact that overexpression of superoxide dismutase only in motorneurons can extend life-span in *Drosophila* by 48% (Parkes *et al.*, 1998).

While the nervous system may play a significant role in developmental signaling, complementary or additional signals originating from other tissues such as muscle may also be required for the generation of fertile adults. In addition to the techniques utilized in this study, the tissue-specificity of an MRC mutation may be studied using mosaic analysis (Yochem *et al.*, 2000). This technique makes use of rare mosaic animals that occur due to the spontaneous loss of a transgenic array from certain cell lineages during early development. A recent study using mosaic analysis for the *atp-2* mutation revealed that worms that endured a loss of the *atp-2* gene in the ABa cell lineage that gives rise to neuronal, pharyngeal, and hypodermal cells, and/or the E lineage that gives rise to intestinal cells, occasionally bypassed L3 arrest (Tsang and Lemire, 2003). Surprisingly, animals with a loss in any lineage that gives rise to body-wall muscle invariably arrested at the L3 stage (Tsang and Lemire, 2003). In contrast to the results presented in this thesis, mosaic analysis with the *atp-2* gene suggests that body-wall muscle may produce a

large fraction of the developmental signal allowing worms to proceed past the L3-larval stage (Tsang and Lemire, 2003).

The apparent discrepancy between the results reported in this thesis and results obtained by mosaic analysis is somewhat perplexing. However, a few different aspects of methodology must be taken into account. The results with *atp-2* mosaics involve loss of expression from cell lineages that give rise to a combination of tissue or cell types, including neuronal cells as well as body muscle. In the *atp-2* work, the native promoter was used to drive the expression. In this work, chimeric genes were used and the levels of expression may be inappropriate. For example, the *unc-54* promoter for body-wall muscle expression may not have produced a uniform or sufficient expression of NUO-1 in all body-wall muscles. Work with different body-wall muscle promoters such as *myo-3* driving *nuo-1* expression in combination with western blot analysis to monitor protein levels, would help address this concern. Although the vast majority of neurons in *C. elegans* are derived from the AB cell lineage, neuronal cells are not exclusively derived from one particular lineage. It is important to note that neuronal cells arise from all except one of the lineages (the D lineage, which gives rise exclusively to body muscle) that were sensitive to loss of *atp-2* (Tsang and Lemire, 2003). Interestingly, these results suggest that the subset of neuronal cells derived from the ABa lineage may be of less importance in developmental regulation than neurons of other lineages. The presence of the complementing array in all but one body muscle nucleus (that derived from the ABp lineage) was not sufficient to allow normal development to adulthood (Tsang and Lemire, 2003). Therefore, it is unlikely that body-wall muscle functions alone in developmental regulation.

The observation that nervous system specific expression of *nuo-1* elicited partial complementation of the L3 arrest may be related to the number of cells in which that promoter is active i.e. the *unc-119* promoter may restore *nuo-1(+)* activity to more cells than the other promoters. The adult hermaphrodite contains 302 neuronal cells in comparison to 95 body-wall muscle cells (Wood, 1988). If all cells contribute equally to a developmental signal, only the *unc-119* promoter may produce a sufficient level of that signal for development to proceed to the L4-early adult stage. Results with the *myo-2* promoter are consistent with this interpretation since this promoter is only active in a small subset of muscle tissue. Instead, it is more likely that the expression in the pharynx enhances the ability of *nuo-1(ua1)* mutants to feed and develop the energy levels needed to support the increased aerobic metabolism associated with the L4 stage. The pharyngeal nervous system would still be *nuo-1(-)* but pharyngeal pumping continues even after laser ablation of the pharyngeal nervous system (Avery and Horvitz, 1989). Pharyngeal pumping assays comparing worms with pharyngeal muscle specific expression of *nuo-1(+)* to *nuo-1*(-) worms would prove instrumental in confirming this hypothesis.

Is *nuo-1(+)* expression tissue-specific in our strains? One measure of specificity is that reporter gene fusions using *lacZ* or GFP with the *unc-119* or the *myo-2* promoters show specific expression in neurons or pharyngeal cells, respectively (Maduro and Pilgrim, 1995; Jantsch-Plunger and Fire, 1994; Gaudet and Mango, 2002). There is evidence of some non-neuronal expression with the *unc-119* promoter anterior to the pharyngeal bulb (Maduro and Pilgrim, 1995). This observation weakens the conclusion that the enhanced pharyngeal pumping ability of worms expressing *nuo-1(+)* under the

control of the *unc-119* promoter can be purely attributed to nervous system specific expression.

Relatively little is known about the expression of genes introduced by microparticle bombardment. There has been no systematic analysis of the relationship between the copy number of the transgenic DNA in extrachromosomal arrays and the levels of RNA and/or of protein products (Jin, 1999). One concern with low copy DNA transformants is that the gene of interest may not be intact after integration or array formation. This may account for results with the body-wall muscle and germ-line specific promoter constructs that failed to complement the L3-arrest phenotype. Developing multiple, independently-derived strains with these promoters addresses the concern that the lack of complementation was array specific. Furthermore, certain promoter constructs that are active in a subset of cells may display mosaicism. This mosaicism appears to be a function of a stochastic activation of gene expression in a subset of cells and silencing in others (Mello and Fire, 1995). Although the nervous system-specific strains and ubiquitously expressing strains were partially complemented, the gonad invariably remained underdeveloped, arresting at an L4 stage in adult sized worms. This result may be a function of poor germ-line expression of the array due to silencing. Thus, the predicted ubiquitous expression of *nuo-1(+)* in our *let-858* strains was not truly uniform. Additionally, Northern blot analysis suggests that while *let-858* is expressed at all stages, it is most abundant at the embryo and larval stages which could only allow for partial complementation in our strains. Obtaining integrated strains for each promoter construct would allow us to investigate the effects of transgene structure and copy number on expression levels and on complementation.

Differences in developmental signals and/or regulatory mechanisms have been proposed to exist between somatic and germ-line tissue. Mutations in the germ line proliferation gene, *glp-1*, result in an almost complete absence of germ line cells while somatic development is normal and animals progress to adulthood (Austin and Kimble, 1987). This indicates that germ-line development is not required for the L3 to L4 progression. Germ-line signals were observed to repress growth and longevity in favor of reproduction while the somatic gonad emitted signals that promote longevity (Patel *et al.*, 2002). Consistent with these results, the longevity of *clk-1* mutants is inhibited with the ablation of somatic gonad precursor cells (Dillin *et al.*, 2002), whereas germ-line laser ablation in *daf-2* results in life-span extension only when the somatic gonad is kept intact (Hsin and Kenyon, 1999). These results suggest that in addition to energy status, signals arising from somatic and germ-line cells act reciprocally to regulate life-span. One hypothesis is that germ-line signals act by modulating the activity of the insulin/IGF-1 pathway to link reproductive state with life-span (Hsin and Kenyon, 1999). The reciprocal control may be explained by the theory that somatic signals act on DAF-16, which extends life-span, and germ-line signals target DAF-2, which shortens life-span (Hsin and Kenyon, 1999). Therefore, the DAF-2/DAF-16 system may act to regulate the development of the reproductive system in response to internal signals such as metabolic status. Provocatively, mutations that disrupt sensory neuron function extend life-span via a nuclear accumulation of DAF-16 (Lin *et al.*, 2001). It is possible that metabolic signaling via the DAF-2/DAF-16 pathway may dictate whether or not the germ-line develops based on a certain energy threshold. Results with the *unc-119* and *let-858* promoter driven expression of *nuo-1(+)* suggest that full complementation of the larval

arrest may be possible if the metabolic status of the germ-line is adequate for full development.

Our results indicate that *nuo-1* exhibits cell non-autonomy. This suggests that development beyond the L3 stage is regulated by a global mechanism that that allows all cells to reach a consensus decision based on energy status on whether or not to continue with development. Some evidence exists that strengthens this hypothesis. In addition to *nuo-1*, mutations in multiple nuclear genes with distinct functions, including the *clk-1*, *coq-3*, and *atp-2* genes, also exhibit the L2-L3 arrest phenotype (Ewbank *et al.*, 1997; Hihi *et al.*, 2002; Jonassen *et al.*, 2001; Tsang et al., 2001). Furthermore, when mitochondrial protein synthesis is inhibited by chloramphenicol or doxycycline in wild-type worms, L3 larval arrest also occurs (Tsang et al., 2001). Therefore, the common larval arrest phenotype suggests a common energy-sensing checkpoint at which distinct functional pathways converge for developmental regulation. Participation in decision-making may involve one or more signaling mechanisms. The most intuitive theory is that potential "energy sensing molecules" could respond to one or more metabolites whose concentrations transmit information about energy status, including NAD^+/NADH ratios and ATP levels. The NAD^+/NADH ratio could also influence the expression of genes involved in development. In addition, the energy sensing mechanism could involve a phosphorylation cascade with second messengers acting as the "sensor molecules". Examples exist to support all these signaling mechanisms.

A few candidate proteins capable of sensing concentrations of metabolites that may reflect mitochondrial energy status have been identified. The carboxy-terminal binding protein (CtBP) is a transcriptional regulator containing an NAD^+/NADH binding

motif important for development and cell-cycle regulation (Zhang *et al.*, 2002). CtBP, in association with its partner proteins functions as a redox sensor by being remarkably sensitive to NADH levels (Zhang *et al.*, 2002). It is hypothesized that CtBP may serve as a redox sensor for transcription (Zhang *et al.*, 2002). The histone deacetylase activity of SIRT3, a conserved mitochondrial protein, is NAD^+ dependent, potentially linking SIRT3 protein activity with metabolic status and the redox state of a particular tissue or cell (Onyango *et al.*, 2002). A homolog of the silent information regulator two or SIR2, the exact targets of SIRT3 are still under investigation, but it is likely that the NAD^+-dependent protein deacetylase activity is involved in the regulation of genes involved in development, perhaps in cells that respond to DAF-2 signaling (Guarente, 2000; Tissenbaum and Guarente, 2001). Interestingly, a SIR2 homolog in *Salmonella enterica* was recently reported to control metabolism by deacetylating an enzyme required for energy metabolism (Starai *et al.*, 2002). The mammalian target of rapamycin (mTOR) is a phosphatidylinositol (PI)-related protein kinase that regulates cell growth by sensing the intracellular concentration of ATP (Dennis *et al.*, 2001). Fascinatingly, mutations in the *C. elegans* homologue of mTOR (ceTOR) result in arrest at the L3 stage (Long *et al.*, 2002). The authors attributed developmental arrest to the inhibition of global mRNA translation, making ceTOR a major upstream regulator of global mRNA translation in *C. elegans* (Long *et al.*, 2002). Indeed, this result strongly suggests that ceTOR may play a significant role as a developmental energy sensor in the L3 to L4 transitional checkpoint. In summary, these results suggest that a developmental checkpoint sensitive to levels of ATP and/or the ratio of NAD^+/NADH may be required for the L3 to L4 transition.

In addition to proteins, studies have suggested that other molecules may also have the ability to act as energy sensors. In addition to the previously mentioned antioxidant and redox cofactor properties of ubiquinone, it has also been shown to function as a signaling molecule. For example, ubiquinone in *E. coli* has been reported to act as a redox signal for the Arc regulatory system (Georgellis *et al.*, 2001). Normal respiratory rates with *C. elegans clk-1* and *coq-3* mutants also suggest that ubiquinone plays a non-mitochondrial role in animal development (Felkai *et al.*, 1999; Hihi *et al.*, 2002).

A phosphorylation cascade has also been proposed in complex I regulation indicating that second messengers may also act as energy sensors. When complex I is treated with a non-denaturing detergent, it dissociates into the Iα and Iβ subcomplexes (Heales *et al.*, 2002). The Iα subcomplex mostly consists of soluble peptides that reside in the matrix and retains biochemical activity (Heales *et al.*, 2002). The membrane domain with no biochemical activity makes up the Iβ subcomplex (Heales *et al.*, 1997). Interestingly, an 18-kDa subunit from the Iα subunit contains a cAMP-dependent kinase phosphorylation site motif (Sardanelli *et al.*, 1995) and phosphorylation of this subunit activates complex I. It is speculated to be an additional mechanism that regulates MRC activity (Papa *et al.*, 2001). These findings indicate that complex I activity is regulated by intracellular signal transduction pathways and that cAMP may act as a messenger to transmit metabolic information.

The entrance and exit from the dauer pathway are developmental responses to chemosensory signals of food availability (Troemel, 1999). As previously mentioned, the link between reproductive state and life-span (Wolkow *et al.*, 2000; Hsin and Kenyon, 1999) suggests that normal and dauer developmental pathways may have common

components that sense energy status and involve insulin-like signaling. In *C. elegans,* mutations that reduce the activity of *daf-2*, an insulin-like receptor or *age-1*, a phosphatidylinositol-3-OH kinase, favor entry into the dauer pathway by activating DAF-16, a transcription factor that promotes stress resistance and dauer formation (Tissenbaum and Guarente, 2001). We believe that mitochondrial energy metabolism is linked to the regulation of dauer formation. DAF-12 (dauer larva formation abnormal), a nuclear hormone receptor important in the decision to enter the dauer pathway has a steroid hormone ligand that is produced by DAF-9 (a cytochrome p450 enzyme) in response to environmental cues including food availability and temperature extremes (Gerisch *et al.*, 2001). DAF-12 may potentially link development with energy production. Provocatively, certain isoforms of DAF-12 are expressed in various tissues including the epidermis, somatic gonad, intestine, nervous- system, and muscle with stage- and tissue-specific dynamics (Antebi *et al.*, 2000). DAF-12 acts on different target tissues at appropriate stages in concert with its proposed roles in dauer formation, developmental age determination, and ageing (Antebi *et al.*, 2000). Interestingly, DAF-12 also has a role in the heterochronic gene pathway in the control of stage-specific cell fates, possibly required in the switch from L2 to L3 (Ambros, 1997). Hence, DAF-12 could function as a temporal regulator that is required for various L3-specific events including dauer larva formation and potentially development past an energy sensing checkpoint. Mutations in *daf-12* also affect gonad morphogenesis indicating that *daf-12* functions in multiple developmental pathways in addition to interaction with *lin-14* and *lin-28* in the heterochronic gene pathway. Therefore, DAF-12 may act by regulating developmental gene expression in response to multiple intercellular signals of energy status.

A picture of the endocrine axis that could regulate development is slowly emerging. Firstly, environmental cues may signal the release of insulin-like ligands for neuronal DAF-2 (Gems and Partridge, 2001). Interestingly, the highest DAF-2 abundance using antibodies for DAF-2 has also been shown to reside within the nerve ring (Wolkow *et al.*, 2000). Of the 37 known insulin-like peptides for DAF-2, most are expressed in neurons, but some are also found in intestine, muscle, epidermis and gonad (Tatar *et al.*, 2003). Binding of these ligands to DAF-2 in neuronal tissues could initate an insulin-like pathway phosphorylation cascade and the generation of a global signal (potentially a steroid hormone) speculated to regulate the developmental changes of other tissues through DAF-12 (Tatar *et al.*, 2003). This hypothesis indicates that insulin/IGF-1-like signaling that originates in neuronal tissue may converge on DAF-12 as a hormonal receptor in the regulation of the L3 to L4 developmental checkpoint.

The yeast *NDI1* (NADH dehydrogenase 1) gene that encodes a yeast NADH-ubiquinone oxidoreductase, can partially complement the L3-arrest phenotype of homozygous *nuo-1(ua1)* mutants (Sayles and Lemire, unpublished data). Yeast Ndi1p can oxidize NADH to NAD^+ but does not generate a proton gradient across the membrane. This result suggests that a cellular redox state is linked with the *nuo-1* induced L3 arrest. Interestingly, the *NDI1* gene has also been shown to complement complex I dysfunction in mammalian cells (Bai *et al.*, 2001), suggesting it as a possible candidate for gene therapy.

In summary, the most conclusive results favor the premise that the energy sensing checkpoint governing the L3 to L4 transition in *C. elegans* may be sensitive to the levels of ATP (as indicated by the ceTOR mutants) and/or the NAD^+/NADH ratio (as suggested

by *NDI1* complementation). One reason that may help explain why we never observed complete complementation in any of our strains, even with constitutive *nuo-1(+)* expression, is that optimal development in the worm might only be achieved when energy sensors respond to multiple indicators of mitochondrial condition. If these sensors detect early in development that the mitochondrial energy status is not optimal, development may be slowed down, or even halted in the case of gonadogenesis. This may help explain why worms exhibiting nervous system specific *nuo-1(+)* expression take significantly longer to develop to the L4 or early adult stage. Additional signals generated from the germ-line, perhaps in response to insulin-like signaling, may work in concert with these somatic sensors allowing the production of fertile adults only when there are sufficient metabolic reserves to support germ-line development. Figure IV-1 illustrates a developmental model to support the results and discussion presented in this thesis.

IV-2. Future Studies

In summary, partial complementation was only achieved with transgenic strains expressing *nuo-1(+)* in the nervous system or in the pharyngeal muscle. Several approaches can be taken to further characterize these strains and gain a deeper understanding of the potential molecular mechanisms involved. Biochemical analysis including measuring the enzymatic and bioenergetic activity of mitochondria is the next key step in analyzing our transgenic strains. Currently, biochemical analysis in *C. elegans* is hampered by the inability to obtain sufficient quantities of intact purified mitochondria. *C. elegans* mitochondria or submitochondrial membranes are the main source of assay material. Mitochondria are harvested by breaking open the worms with

glass beads in a BeadBeater followed by isolation by differential centrifugation (Murfitt *et al.*, 1976). Respiratory function in isolated mitochondria can be tested using a variety of respiratory substrates, cofactors, and inhibitors (Hofhaus *et al.*, 1996), and an enzymatic defect can be localized to a specific complex (Hofhaus and Attardi, 1993). However, some measures of mitochondrial function can be performed on live animals. ATP levels and oxygen consumption rates can be measured as global indicators of mitochondrial function. Measuring ATP levels would serve as an indicator of instantly available energy and can be measured by monitoring the level of light emitted when luciferin reacts with oxygen in the presence of luciferase (Braeckman *et al.*, 2002). Oxygen consumption would specify metabolic rate and would be performed on animals suspended in liquid using Clark type electrodes (Braeckman *et al.*, 2002). Measuring ATP biosynthesis and oxygen consumption in *nuo-1(ua1)* mutants would provide a platform by which to compare MRC function in our transgenic strains. Assays have been established to measure the activities of individual MRC complexes. It would be interesting to elucidate the threshold level of inhibition required to impair ATP synthesis and energy metabolism in *C. elegans*. Measuring the succinate- and the rotenone-sensitive NADH-decylubiquinone reductase activities of mitochondria will provide useful information about enzyme assembly and enzyme kinetics. It will also be interesting to see if different complexes can partially compensate for complex I dysfunction.

Past studies have also shown that impaired mitochondrial function has often been associated with an increase in the production of ROS. A lucigenin-mediated light emission assay using freeze-thawed worms has been developed to measure the amount of superoxide produced (Vanfleteren and De Vreese, 1996) and has been used to show the

increase of superoxide production with age. To assay the integrity of different MRC components, the mitochondrial lucigenin mediated luminescence assay can be used (Braeckman *et al.*, 2002). In conjunction with a life-span assay, this technique would be useful in determining whether the production of ROS is a factor in *nuo-1(ua1)* mutants and if the level of ROS production is altered in transgenic strains.

In partially complemented strains, DAPI staining could be used to analyze gonad development and to determine how many cells are mitotic and how many are meiotic in the trans zone (where nuclei undergo the transition from the mitotic cell cycle through early stages of meiotic prophase) (Mounsey *et al.*, 1999). This would provide evidence as to whether germ-line development in its earliest stages is occurring in these strains.

Once an antibody specific for NUO-1 is obtained, valuable information about protein levels and localization will help interpret the results presented in this thesis. An antibody to the ATP synthase is available because of the crossreactivity of the worm protein with the yeast anti-ATP2p antibody. The ATP2p antibody has been used to establish that levels of ATP-2 protein significantly increase in the L3 to L4 transition (Tsang and Lemire, unpublished data). In addition, the presence of maternally inherited ATP-2 in *atp-2* mutants has been detected (Tsang *et al.*, 2001). Antibodies to the other complexes could also indicate overexpression of a particular complex to compensate for complex I dysfunction, and the indication of protein assembly problems. Since only partial complementation was achieved with the constructs described in this thesis, problems may arise with western blot or immunolocalization analysis due to the inheritance of maternal NUO-1 in *nuo-1(ua1)* offspring of heterozygous *nuo-1(ua1)*/+

hermaphrodites. Levels of NUO-1 in a particular tissue would have to be significantly higher than that of maternally inherited NUO-1 for localization studies to be conclusive.

DNA microarrays have recently been developed to provide some clues as to the gene expression levels of *nuo-1* associated with different developmental stages (Jiang *et al.*, 2001). As expected, microarray data suggest that *nuo-1* expression constantly increases throughout development peaking at the L4 larval stage (Jiang *et al.*, 2001). Interestingly, germ-line gene expression levels fall after the L2 larval stage (Reinke *et al.*, 2000). Until an antibody to NUO-1 is generated, rtPCR could provide evidence of the localization of mRNA in the appropriate tissues, although maternally inherited *nuo-1* mRNA may interfere with this technique. Generating transgenic strains containing nuo-1::GFP fusions would also help to elucidate the normal expression pattern of *nuo-1*.

For a more complete tissue-specific analysis of *nuo-1* expression, we could try several different promoters in addition to the ones presented here. For example, promoters for body muscle (*myo-3*), nervous system (*unc-14*), intestinal (*F22B7.9*), hypodermal (*jam-1*), and smaller subsets of neuronal (*unc-129 and mec7*) genes could help identify tissues or subsets of tissues important in the L3 to L4 transition. Additionally, promoters for genes specifically involved in the dauer pathway, such as *daf-2* or *daf-12* should be considered to test the hypothesis that insulin-like signaling may be involved in the L3-L4 developmental checkpoint. Bombarding a combination of expression plasmids containing different tissue-specific promoters may identify combination(s) of tissues that are most crucial to developmental signaling. The generation of multiple transgenic strains exhibiting the *unc-119* nervous system specific

expression of NUO-1 would help confirm that the observed partial complementation is not array specific.

Another interesting approach to study the role of *nuo-1* in the development of different tissues would be to generate transgenic strains containing *nuo-1* promoter deletion derivatives (Boer *et al.*, 1998). This technique could potentially lead to the identification of putative tissue-specific elements (Boer *et al.*, 1998). In this way, the tissue-specific expression of *nuo-1(+)* could also be achieved. This tissue-specific knock out strategy could be useful in elucidating whether *nuo-1* plays a role in the reproductive maturation of the somatic gonad or of the germ-line.

We have proposed an energy sensor is required to bypass the L3 to L4 checkpoint. One way to identify an energy sensor would be to look for mutations that suppress the L3-arrest of homozygous *nuo-1(ua1)* mutants. Identification of a suppressor would be strong evidence for the existence of an energy sensor. The identity of a suppressor would also give insight into molecular components and regulatory pathways that underlie dysfunctional energy metabolism and developmental arrest. Concordantly, the creation of double mutations in proteins such as DAF-2 and DAF-16 would help elucidate the relationship between various components that may play a role in energy sensing and developmental control.

In conclusion, the results obtained with the *unc-119* promoter driving *nuo-1(+)* expression suggest the importance of the nervous system in energy metabolism and development. This result may help explain the pathogenesis of neurodegenerative disorders such as Leigh syndrome and Parkinson's disease that are often associated with complex I deficiency (Orth and Schapira, 2001). As more human mitochondrial

mutations are described, the nematode model system will continue to provide valuable insights into the complex molecular mechanisms that underlie these defects. This approach is promising in yielding new and specific avenues for therapy of the various mitochondrial diseases.

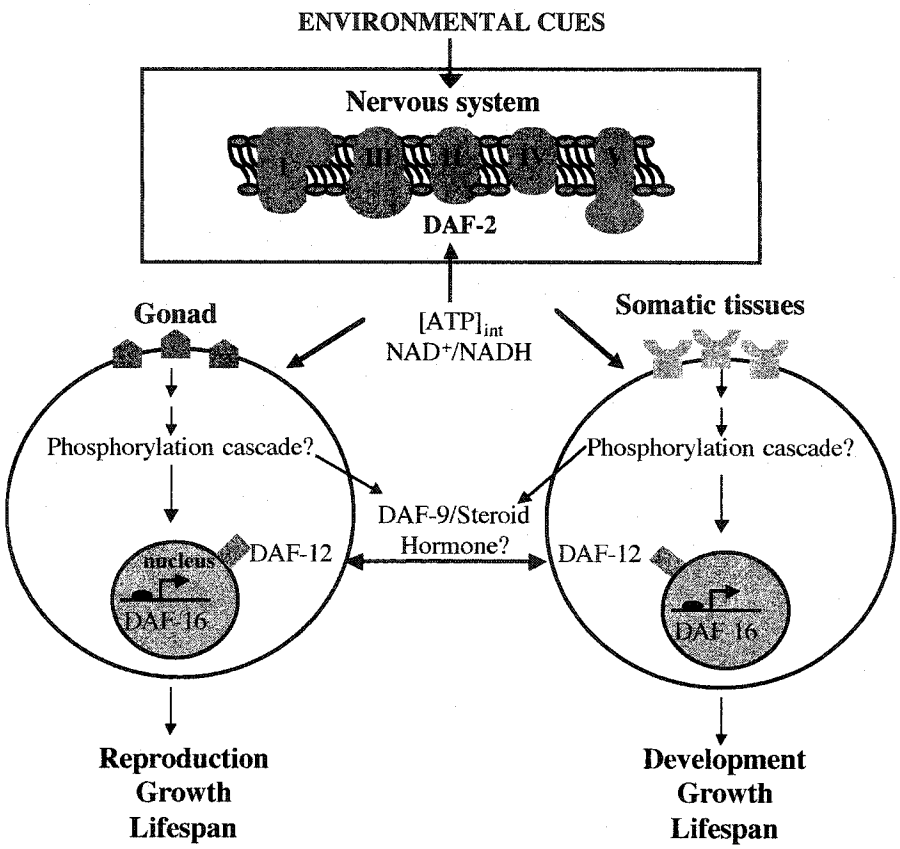

Figure IV-1. Developmental Model

An energy-sensing molecule primarily situated in the nervous system, potentially the DAF-2 receptor, may respond to one or more metabolites whose concentrations transmit information about energy status including NAD^+/NADH ratios and ATP levels. A nervous system specific signal could in turn initiate downstream signaling pathways involving phosphorylation cascades and the generation of a steroid hormone ligand via DAF-9. This steroid hormone ligand would interact with DAF-12, a nuclear hormone receptor, thereby acting as a global signal for transcriptional regulators such as DAF-16, CtBP, and SIRT3. The end result would be the regulation of genes involved in various processes including reproduction, lifespan, and development. Optimal development would be achieved when energy sensors respond to multiple indicators of mitochondrial condition including the crosstalk between different tissues via steroid hormone interaction with DAF-12, thereby regulating the expression of developmental genes. If these sensors detect early in development that mitochondrial status is not optimal, development would be stopped at a developmental checkpoint.

BIBLIOGRAPHY:

Ambros, V. 1997. Heterochronic Genes, pp. 501-518 in *C. elegans* Volume II, edited by D.L. Riddle, T. Blumenthal, B.J. Meyer, and J. Preiss. Cold Spring Harbor Laboratory, Cold Spring Harbor, NY.

Antebi, A., W.-H. Yeh, D. Tait., E.M. Hedgecock, D.L. Riddle. 2000. *daf-12* encodes a nuclear receptor that regulates the dauer diapause and developmental age in *C. elegans*. *Genes Dev.* **14:**1512-1527.

Ardizzi, J.P., and H.F. Epstein. 1987. Immunochemical localization of myosin heavy chain isoforms and paramyosin in developmentally and structurally diverse muscle cell types of *C. elegans*. *J. Cell Biol.* **105:**2763-2770.

Austin, J., and J. Kimble. 1987. *glp-1* Is Required in the Germ Line for Regulation of the Decision between Mitosis and Meiosis in *C. elegans*. *Cell* **51:**589-599.

Avery, L., and H.R. Horvitz. 1989. Pharyngeal Pumping Continues after Laser Killing of the Pharyngeal Nervous System of *C. elegans*. *Neuron* **3:**473-485.

Bai, Y., P. Hajek, A. Chomyn, E. Chan, B.B. Seo, A. Matsuno-Yagi, and G. Attardi. 2001. Lack of complex I activity in human cells carrying a mutation in mtDNA-encoded ND4 subunit is corrected by the *Saccharomyces cerevisiae* NADH-quinone oxidoreductase (*NDI1*) gene. *J. Biol. Chem.* **276:**38808-38813.

Braeckman, B.P., K. Houthoofd, A. De Vreese, J.R. Vanfleteren. 2002. Assaying metabolic activity in ageing *Caenorhabditis elegans*. *Mech. Ageing Dev.* **123:**105-119.

Boer, B.G.W. den, S. Sookhareea, P. Dufourcq, and M. Labouesse. 1998. A tissue-specific knock-out strategy reveals that *lin-26* is required for the formation of the somatic gonad epithelium in *Caenorhabditis elegans*. *Dev.* **125:**3213-3224.

Cook, D.L., A.N. Gerber, and S.J. Tapscott. 1998. Modeling stochastic gene expression: Implications for haploinsufficiency. *Proc. Natl. Acad. Sci. USA* **95:**15641-15646.

Dennis, P.B., A. Jaeschke, M. Saitoh, B. Fowler, S.C. Kozma, and G. Thomas. 2001. Mammalian TOR: a homeostatic ATP sensor. *Science* **294:**1102-1105.

Ewbank, J.J., T.M. Barnes, B. Lakowski, M. Lussier, H. Bussey, and S. Hekimi. 1997. Structural and functional conservation of the *Caenorhabditis elegans* timing gene *clk-1*. *Science* **275:**980-983.

Felkai, S., J.J. Ewbank, J. Lemieux, J.C. Labbe, G.G. Brown, and S. Hekimi. 1999. CLK-1 controls respiration, behavior and aging in the nematode *Caenorhabditis elegans*. *EMBO J.* **18:**1783-1792.

Gaudet, J., and S.E. Mango. 2002. Regulation of organogenesis by the *Caenorhabditis elegans* FoxA protein PHA-4. *Science* **295:**821-825.

Gems, D., and L. Partridge. 2001. Insulin/IGF signalling and ageing: seeing the bigger picture. *Curr. Opinion Genet. Dev.* **11:**287-292.

Georgellis, D., O. Kwon, and E.C. Lin. 2001. Quinones as the redox signal for the arc two-component system of bacteria. *Science* **292:**2314-2316.

Gerisch, B., C. Weitzel, C. Kober-Eisermann, V. Rottiers, and A. Antebi. 2001. A hormonal signaling pathway influencing *C. elegans* metabolism, reproductive development, and life span. *Dev. Cell* **1:**841-851.

Guarente, L. 2000. Sir2 links chromatin silencing, metabolism, and aging. *Genes Dev.* **14:**1021-1026.

Heales, S.J.R., M.E. Gegg, and J.B. Clark. 2002. Oxidative Phosphorylation: Structure, function, and intermediary metabolism. *Int. Rev. Neurobiol.* **53:**25-56.

Hihi, A.K., Y. Gao, and S. Hekimi. 2002. Ubiquinone is necessary for *Caenorhabditis elegans* development at mitochondrial and non-mitochondrial sites. *J. Biol. Chem.* **277:**2202-2206.

Hofhaus, G., and G. Attardi. 1993. Lack of assembly of mitochondrial DNA-encoded subunits of respiratory NADH dehydrogenase and loss of enzyme activity in a human cell mutant lacking the mitochondrial *ND4* gene product. *EMBO J.* **12:**3043-3048.

Hofhaus, G., R.M. Shakeley, and G. Attardi. 1996. Use of polarography to detect respiration defects in cell cultures. *Methods Enzymol.* **264:**476-483.

Hsin, H., and C. Kenyon. 1999. Signals from the reproductive system regulate the lifespan of *C. elegans*. *Nature* **399:**362-366.

Jantsch-Plunger, V., and A. Fire. 1994. Combinatorial structure of a body muscle-specific transcriptional enhancer in *Caenorhabditis elegans*. *J. Biol. Chem.* **269:**27021-27028.

Jiang, M., J. Ryu, M. Kiraly, K. Duke, V. Reinke, and S.K. Kim. 2001. Genome-wide analysis of developmental and sex-regulated gene expression profiles in *Caenorhabditis elegans*. *Proc. Natl. Acad. Sci. USA* **98:**218-223.

Jin, Y. 1999. Transformation, pp. 69-96 in *C. elegans* A Practical Approach, edited by I.A. Hope. Oxford University Press Inc., NY.

Jonassen, T., P.L. Larsen, and C.F. Clarke. 2001. A dietary source of coenzyme Q is essential for growth of long-lived *Caenorhabditis elegans clk-1* mutants. *Proc. Natl. Acad. Sci. USA* **98:**421-426.

Kelly, W.G., S.Q. Xu, M.K. Montgomery, and A. Fire. 1997. Distinct requirements for somatic and germline expression of a generally expressed *Caenorhabditis elegans* gene. *Genetics* **146:**227-238.

Kenyon, C., J. Chang, E. Gensch, A. Rudner, R. Tabtiang. 1993. A *C. elegans* mutant that lives twice as long as wild type. *Nature* **366:**461-464.

Kimura, K.D., H.A. Tissenbaum, Y. Liu, G. Ruvkun. 1997. *daf-2*, an insulin receptor-like gene that regulates longevity and diapause in *Caenorhabditis elegans*. *Science* **277:**942-946.

Lin, K., H. Hsin, N. Libina, and C. Kenyon. 2001. Regulation of the *Caenorhabditis elegans* longevity protein DAF-16 by insulin/IGF-1 and germline signaling. *Nature Genet.* **28:**139-145.

Long, X., C. Spycher, Z.S. Han, A.M. Rose, F. Müller, and J. Avruch. 2002. TOR Deficiency in *C. elegans* Causes Developmental Arrest and Intestinal Atrophy by Inhibition of mRNA Translation. *Curr. Biol.* **12:**1448-1461.

Mello, C., and A. Fire. 1995. DNA transformation. *Methods Cell Biol.* **48:**451-482.

Mounsey, A., L. Molin, and I.A. Hope. 1999. Gene expression patterns, pp. 181-1999 in *C. elegans* A Practical Approach, edited by I.A. Hope. Oxford University Press Inc., NY.

Murfitt, R.R., K. Vogel, and D.R. Sanadi. 1976. Characterization of the mitochondria of the free living nematode, *Caenorhabditis elegans*. *Comp. Biochem. Physiol.* **53B:**423-430.

Onyango, P., I. Celic, J.M. McCaffery, J.D. Boeke, and A.P. Feinberg. 2002. SIRT3, a human SIR2 homologue, is an NAD-dependent deacetylase localized to mitochondria. *Proc. Natl. Acad. Sci. USA* **99:**13653-13658.

Orth, M., and A.H.V. Schapira. 2001. Mitochondria and Degenerative Disorders. *Am. J. Med. Genet.* **106:**27-36.

Papa, S., S. Scacco, A.M. Sardanelli, R. Vergari, F. Papa, S. Buddle, L. Van den Heuvel, and J. Smeitink. 2001. Mutations in the *NDUFS4* gene of complex I abolishes cAMP dependent activation of the complex in a child with fatal neurological syndrome. *FEBS Lett.* **489:**259-262.

Parkes, T.L., A.J. Elia, D. Dickinson, A.J. Hilliker, J.P. Phillips, and G.L. Boulianne. 1998. Extension of *Drosophila* lifespan by overexpression of human SOD1 in motorneurons. *Nature Genet.* **19:**171-174.

Patel, M.N., C.G. Knight, C. Karageorgi, and A.M. Leroi. 2002. Evolution of germ-line signals that regulate growth and aging in nematodes. *Proc. Natl. Acad. Sci. USA* **99:**769-774.

Reinke, V., H.E. Smith, J. Nance, J. Wang, C.V. Doren, R. Begley, S.J.M. Jones, E.B. Davis, S. Scherer, S. Ward, and S.K. Kim. 2000. A global profile of germline gene expression in *C. elegans*. *Mol. Cell* **6:**605-616.

Sardanelli, A.M., Z. Technikova-Dobrova, S.C. Scacco, F. Speranza, and S. Papa. 1995. Characterization of proteins phosphorylated by the cAMP-dependent protein kinase of bovine heart mitochondria. *FEBS Lett.* **377:**470-474.

Starai, V.J., I. Celic, R.N. Cole, J.D. Boeke, and J.C. Escalante-Semerena. 2002. Sir2-dependent activation of acetyl-CoA synthetase by deacetylation of active lysine. *Science* **298:**2390-2392.

Tatar, M., A. Bartke, and A. Antebi. 2003. The Endocrine Regulation of Aging by Insulin-like Signals. *Science* **299:**1346-1351,

Tissenbaum, H.A., and L. Guarente. 2001. Increased dosage of a *sir-2* gene extends lifespan in *Caenorhabditis elegans*. *Nature* **410:**227-230.

Troemel, E.R. 1999. Chemosensory signaling in *C. elegans*. *Bioessays* **21:**1011-1020.

Tsang, W.Y., L.C. Sayles, L.I. Grad, D.B. Pilgrim, and B.D. Lemire. 2001. Mitochondrial Respiratory Chain Deficiency in *Caenorhabditis elegans* Results in Developmental Arrest and Increased Life Span. *J. Biol. Chem.* **276:**32240-32246.

Tsang, W.Y., and B.D. Lemire. 2003. Mitochondrial ATP synthase controls larval development cell nonautomously in *Caenorhabditis elegans*. *Dev. Dyn.* **226:**719-726.

Vanfleteren, J.R. and A. De Vreese. 1996. Rate of aerobic metabolism and superoxide production rate potential in the nematode *Caenorhabditis elegans*. *J. Exp. Zool.* **274:**93-100.

Wolkow, C.A., K.D. Kimura, M.-S. Lee, and G. Ruvkun. 2000. Regulation of *C. elegans* Life-span by Insulinlike Signaling in the Nervous System. *Science* **290:**147-150.

Wood, W.B. 1988. Introduction to *C. elegans* Biology, pp.1-16 in The Nematode *Caenorhabditis elegans*, edited by W.B. Wood. Cold Spring Harbor Laboratory, Cold Spring Harbor, NY.

Yochem, J., M. Sundaram, and E.A. Bucher. 2000. Mosaic analysis in *Caenorhabditis elegans*. *Methods Mol. Biol.* **135:**447-462.

Zhang, Q., D.W. Piston, and R.H. Goodman. 2002. Regulation of Corepressor Function by Nuclear NADH. *Science* **295:**1895-1897.